

Design Analysis Cover Sheet

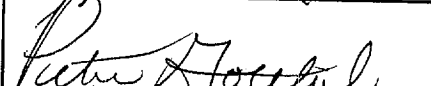
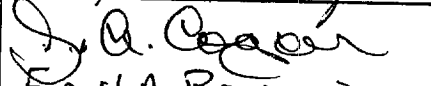
Complete only applicable items.

1.

QA: L

| Page: 1 Of: 52

SCPB:NJA

2. DESIGN ANALYSIS TITLE Initial Waste Package Probabilistic Criticality Analysis: Uncanistered Fuel (TBV)			
3. DOCUMENT IDENTIFIER (Including Rev. No.) B00000000-01717-2200-00079 REV 01		4. REV. NO. 01	5. TOTAL PAGES 52
6. TOTAL ATTACHMENTS 1		7. ATTACHMENT NUMBERS - NO. OF PAGES IN EACH I-45 pages	8. SYSTEM ELEMENT MGDS System Element
9. Originator	Print Name John R. Massari	Signature 	Date 10/5/95
10. Checker	Print Name Lewie E. Booth	Signature 	Date 10/5/95
11. Lead Design Engineer	Print Name Peter Gottlieb	Signature 	Date 10/5/95
12. QA Manager	Print Name D. J. Gilstrap	Signature 	Date 10/5/95
13. Department Manager	Print Name Hugh A. Benton	Signature 	Date 10/6/95
14. REMARKS MOL.19960422.0336			

Design Analysis Revision Record

Complete only applicable items.

1.

QA: L

Page: 2 Of: 52

2. DESIGN ANALYSIS TITLE

Initial Waste Package Probabilistic Criticality Analysis: Uncanistered Fuel (TBV)

3. DOCUMENT IDENTIFIER (Including Rev. No.)

B0000000-01717-2200-00079 REV 01

4. REVISION NO.

01

5. Revision No.	6. Total Pages	7. Description of Revision
00	61 + 3 Attachments 67 Total Pages	Original Issue
01	52 + 1 Attachment 97 Total Pages	Revised to provide increased detail of calculations performed. Mathcad+ v5 used in place of Lotus123. Minor changes to input parameters. No changes to calculation method, scope, or assumptions.

**INITIAL WASTE PACKAGE
PROBABILISTIC CRITICALITY
ANALYSIS: UNCANISTERED FUEL
SCPB#: N/A
(TBV)**

October 5, 1995

Table of Contents:

<u>Item</u>	<u>Page</u>
1. Purpose	5
2. Quality Assurance	5
3. Method	6
4. Design Inputs	7
4.1 Design Parameters	7
4.2 Criteria	7
4.3 Assumptions	8
4.4 Codes and Standards	8
5. References	8
6. Use of Computer Software	11
7. Design Analysis	11
7.1 System Description	11
7.2 Failure Modes and Effects Analysis	14
7.3 Development of Fault Tree Logic	18
7.4 Development of Probabilities and Probability Density Functions (pdf) ..	21
7.4.1 <u>Flow Defining Events</u>	21
7.4.2 <u>Concentration of flow on individual waste package</u>	24
7.4.3 <u>Corrosion Events</u>	26
7.4.4 <u>Probability of sufficient fissile material in a package</u>	37
7.4.5 <u>Evaluations of two-fold convolutions of pdf's</u>	38
7.4.6 <u>Probability of sufficient moderator</u>	39
7.4.7 <u>Probability that Fuel Assemblies Maintain Geometry Required For Criticality (geometry)</u>	39
7.5 Fault Tree Analysis	48
8. Conclusions	51
9. Attachments	52

1. Purpose

This analysis is prepared by the Mined Geologic Disposal System (MGDS) Waste Package Development Department (WPDD) to provide an assessment of the present waste package design from a criticality risk standpoint. The specific objectives of this initial analysis are to:

1. Establish a process for determining the probability of waste package criticality as a function of time (in terms of a cumulative distribution function, probability distribution function, or expected number of criticalities in a specified time interval) for various waste package concepts;
2. Demonstrate the established process by estimating the probability of criticality as a function of time since emplacement for an intact uncanistered fuel waste package (UCF-WP) configuration;
3. Identify the dominant sequences leading to waste package criticality for subsequent detailed analysis.

The purpose of this analysis is to document and demonstrate the developed process as it has been applied to the UCF-WP. This revision is performed to correct deficiencies in the previous revision and provide further detail on the calculations performed.

Due to the current lack of knowledge in a number of areas, every attempt has been made to ensure that the all calculations and assumptions were conservative. This analysis is preliminary in nature, and is intended to be superseded by at least two more versions prior to license application. The information and assumptions used to generate this analysis are unverified and have been globally assigned TBV identifier TBV-059-WPD. Future versions of this analysis will update these results, possibly replacing the global TBV with a small number of TBV's on individual items, with the goal of removing all TBV designations by license application submittal. The final output of this document, the probability of UCF-WP criticality as a function of time, is therefore also TBV.

This document is intended to deal only with the risk of internal criticality with unaltered fuel configurations. The risk of altered fuel configuration, or external, criticalities will be evaluated as part of our ongoing criticality risk analyses. The results will be contained in interim reports, and collected into the next version of the Waste Package Probabilistic Criticality Analysis (1996).

2. Quality Assurance

This activity entails the use of risk assessment techniques to assess the probability of a UCF-WP criticality event. This activity will also provide input for the Total System Performance Assessment (TSPA) which will be included in the License Application Design (LAD) phase and may be used to set design requirements and material

specifications. Therefore, it has the potential to affect the design and fabrication requirements of the Waste Package/Engineered Barrier Segment. This activity can impact the proper functioning of the MGDS waste package; the waste package has been identified as an MGDS Q-List item important to safety^(5.1). The QA Program applies to this analysis. The WPDD QAP-2-0 Work Control evaluation^(5.2) determined that "Perform Probabilistic Waste Package Design Analysis," within which this analysis is prepared, is subject to QARD requirements^(5.3). Applicable procedural controls are listed in the evaluation. The information and results presented in this analysis are preliminary and, at this time, are yet to be verified (TBV-059-WPD). Any additional notation of TBV will be omitted since the TBV qualification applies universally to the contents of this analysis.

3. Method

A quantitative estimate of the probability of a UCF-WP criticality event, and the dominant sequences leading to this event, will be determined using the method of fault tree analysis. In the first step, a qualitative Failure Modes and Effects Analysis (FMEA) will be performed to determine the credible initiating events, and UCF-WP failure modes which could lead to criticality. This process is similar to that used for failure mode analysis of complex systems, such as those in a nuclear power plant. In the present case the system is the engineered barrier (whose components include the barriers and basket of the waste package). Failure modes for components within the defined system are evaluated for their impact on other components and the system as a whole.

The FMEA will be conducted within the framework of a fault tree analysis. The analysis method includes the following steps:

1. Definition of the system to be analyzed and its boundaries;
2. Performance of a qualitative Failure Modes and Effects Analysis (FMEA) to determine the credible initiating events and subsequent individual component failure modes (basic events) which could lead to criticality;
3. Development of the fault tree logic structure indicating the sequences of events which could lead to waste package criticality (the top event);
4. Description of discrete events and those which take place continuously over time;
5. Estimation of probabilities of discrete events and probability density functions (probabilities per unit time) based on the current understanding of their likelihood of occurrence;
6. Quantification of the fault tree to determine the probability of occurrence of the top event (waste package criticality).

Initiating and basic event probabilities used in the fault tree will be determined by

statistical analysis of experimental information on UCF-WP material degradation, with the assistance of empirical, mathematical models of underlying physical mechanisms and forecasts of the environmental conditions and hazards which make up the initiating events.

4. Design Inputs

4.1 Design Parameters

Waste Package

UCF-WP Basket Inner Length:	4580 mm, Reference 5.32
Length from Basket to Inner Lid	5 mm, Reference 5.32
Outer Barrier Material:	ASTM A 516 Carbon Steel, Key 042, Reference 5.5
Outer Barrier Thickness:	100 mm, Reference 5.7
Inner Barrier Material:	Incoloy Alloy 825, Key 042, Reference 5.5
Inner Barrier Thickness:	20 mm, Reference 5.7
Basket Absorber Material:	Borated Type 316 Stainless Steel Reference 5.7
Filler Material:	Inert Gas, Reference 5.7

Emplacement Drift and Near-field Environment

Thermal Loading:	24.2 MTU/acre Reference 5.11
Backfill:	None, Key 046, Reference 5.5
Drift Diameter:	4.27 m (14 ft), Reference 5.11
TSw2 Volumetric Fracture Freq.:	19.64 fractures/m ³ Reference 5.24

Materials Corrosion Data

All materials corrosion data used as input to develop distributions is provided in Table 7.6 and Attachment I.

WP Criticality Data

Figure 6.8.3-5, Time Effects on Criticality Potential - 21PWR Metallic Multi-Barrier WP Design (No Additional Neutron Absorbers Added), Reference 5.7.

Table 2, Percentiles of Burnup and Criticality, Reference 5.25.

4.2 Criteria

The analysis addresses the probability of criticality events. Such work is a partial response to the following requirements:

The Engineered Barrier Segment design organization shall establish and execute a reliability, availability, and maintainability program to support Integrated Logistics Support and the general engineering program for the Engineered Barrier Segment.

Reliability shall be addressed as an element of design reviews. [EBDRD 3.2.5.1.1]^(5.4)

The Engineered Barrier Segment shall be designed to ensure that a nuclear criticality accident is not possible unless at least two unlikely, independent, and concurrent or sequential changes have occurred in the conditions essential to nuclear criticality safety. Each system shall be designed for criticality safety under normal and accident conditions. The calculated effective multiplication factor must be sufficiently below unity to show at least a five percent margin, after allowance for the bias in the method of calculation and the uncertainty in the experiments used to validate the method of calculation. [EBDRD 3.2.2.6.A]^(5.4)

4.3 Assumptions

Assumptions and their bases are given in Section 7, in connection with the individual events. They have been italicized for easy identification and generally contain a form of the word "assume" (note: single words and titles which may be italicized are not assumptions). The assumptions are generally conservative, so that they involve larger probabilities of the events in the sequences leading to criticality. The only exception is for the corrosion events, for which we have attempted to be as realistic as possible, within the context of presently available experimental and theoretical understanding.

4.4 Codes and Standards

The following document was used as a standard for the construction and evaluation of fault tree models:

Fault Tree Handbook, NUREG-0492, U.S. Nuclear Regulatory Commission, Washington, D.C., January 1981^{5.6}

5. References

- 5.1 "Yucca Mountain Site Characterization Project Q-List," YMP/90-55Q, REV 3, December 1994
- 5.2 "Perform Probabilistic Waste Package Design Analyses SCPB:N/A," DI# BB0000000-01717-2200-00030 ~~REV 01, August 30, 1995~~ *REV 02, Sept. 29* *JM 10/6/95*
- 5.3 "Quality Assurance Requirements and Description," DOE/RW-0333P, REV 4, August 4, 1995
- 5.4 "Engineered Barrier Design Requirements Document," YMP/CM-0024 REV 0, ICN 1, September 21, 1994
- 5.5 "Controlled Design Assumptions Document," DI# B00000000-01717-4600-00032

REV 01, April 28, 1995

- 5.6 "Fault Tree Handbook," NUREG-0492, U.S. Nuclear Regulatory Commission, Washington D.C., January 1981
- 5.7 "Initial Summary Report for Repository/Waste Package Advanced Conceptual Design," DI# B00000000-01717-5705-00015 REV 00, August 29, 1994
- 5.8 Modarres, M., "What Every Engineer Should Know About Reliability And Risk Analysis," Marcel Dekker, Inc., New York, NY, 1993
- 5.9 McCoy, J.K., "Updated Report on RIP/YMIM Analysis of Designs," DI# BBA000000-01717-5705-00002 REV 02, July 13, 1995
- 5.10 Stahl, David, "Waste Package Corrosion Inputs," IOC LV.WP.DS.06/93.107, June 21, 1993
- 5.11 Bahney III, R.H., "Thermal Evaluations of Waste Package Emplacement," DI# BBA000000-01717-4200-00008 REV 00, July 21, 1994
- 5.12 Buscheck, T.A., Nitao, J.J, Saterilie, S.F., "Evaluation of Thermo-Hydrological Performance in Support of the Thermal Loading Systems Study," in *High Level Radioactive Waste Management: Proceedings of the Fifth International Conference*, (American Nuclear Society, La Grange Park, IL, and American Society of Civil engineers, New York, 1994), pp. 592-610
- 5.13 Sandia National Laboratories, "Total-System Performance Assessment for Yucca Mountain - SNL Second Iteration" (TSPA-1993) (SAND93-2674), April 1994
- 5.14 Knief, R.A., "Nuclear Criticality Safety - Theory and Practice," American Nuclear Society, La Grange Park, IL, 1993
- 5.15 "Initial Demonstration of the NRC's Capability to Conduct a Performance Assessment for a High-Level Waste Repository," NUREG-1327, May 1992
- 5.16 Gdowski, G.E., Bullen, D.B., "Survey of Degradation Modes of Candidate Materials for High-Level Radioactive- Waste Disposal Containers," UCID-21362 Vol. 2, August 1988
- 5.17 "Immersion Studies On Candidate Container Alloys For The Tuff Repository," NUREG/CR-5598, May 1991
- 5.18 "CRC Handbook Of Chemistry and Physics," 66th Edition, CRC Press, Inc., Boca Raton, FL, 1985

- 5.19 "Swedish Nuclear Fuel and Nuclear Waste Management Co, Site Characterization and Validation - Final Report," STRIPA PROJECT 92-22 (April 1992)
- 5.20 "ASM Handbook, Volume 13 - Corrosion," ASM International, December 1992
- 5.21 McCright, R.D., Halsey, W.G., Van Konynenburg, R.A., "Progress Report On The Results Of Testing Advanced Conceptual Design Metal Barrier Materials Under Relevant Environmental Conditions For A Tuff Repository," UCID-21044, December 1987
- 5.22 Jones, D.A., Howryla, R.S., "Electrochemical Sensor to Monitor Atmospheric Corrosion in Repository Environments," presented at Waste Package Workshop, Las Vegas, Nevada, September 21-23, 1993
- 5.23 "Pitting, Galvanic, and Long-Term Corrosion Studies on Candidate Container Alloys for the Tuff Repository," NUREG/CR-5709, January 1992
- 5.24 Bauer, S.J., Hardy, M.P., Lin M., "Fracture Analysis and Rock Quality Designation Estimation for the Yucca Mountain Site Characterization Project," SAND92-0449, February 1993
- 5.25 Gottlieb, P., "Waste Package Design Basis Fuel Analysis", DI# BBA0000000-01717-0200-00121 REV 00, February 22, 1994
- 5.26 Cerne, S.P., Hermann, O.W., and Westfall, R.M., "Reactivity and Isotopic Composition of Spent PWR Fuel as a Function of Initial Enrichment, Burnup, and Cooling Time", Oak Ridge National Laboratory, 1987 (ORNL/CSD/TM-244)
- 5.27 National Research Council, "Ground Water at Yucca Mountain, How High Can it Rise", National Academy Press, Washington, D.C., 1992
- 5.28 Andrews, R., Dale, T., and McNeish, J., "Total System Performance Assessment-1993: An Evaluation of the Potential Yucca Mountain Repository", DI# B00000000-01717-2200-00099 REV 01, 1994.
- 5.29 Flint, A.L., Flint, L.E., "Spatial Distribution of Potential Near Surface Moisture Flux at Yucca Mountain", Proceedings of the Fifth Annual International Conference on High Level Radioactive Waste Management, pp. 2352-2358, American Society of Civil Engineers, 1994
- 5.30 Anna, L. O., USGS, Private communication
- 5.31 Wheatfall, W.L., "Metal Corrosion in Deep-Ocean Environments," Naval Engineers Journal, NNA.890919.0280, August 1967.

- 5.32 Wallin, W.E., "Waste Package Sizing Spreadsheet ACD Sizing, Masses and Costing," IOC LV.WP.WEW.7/95-229, July 14, 1995.

6. Use of Computer Software

Microsoft Excel version 4.0 spreadsheet software was used to plot certain graphs, and as a general calculational aid. Plotting of the fault tree diagrams was performed using CAFTA version 2.3. Evaluation of McCoy's corrosion model utilized a simple C code provided by McCoy. Mathcad+ version 5.0 was used to perform the convolutions of the various distributions, the quantification of the fault tree, and to perform some additional calculations and plots. All software used meets the QAP-SI-0 definition of Computational Support Software. All software inputs, user defined formulas, algorithms, and outputs are contained in Attachment I.

7. Design Analysis

7.1 System Description

The first step in performing any risk analysis is to provide a clear and concise description of the boundaries of the system to be analyzed. The system boundary for this analysis includes the waste package and the local drift environment into which it has been emplaced (see Figure 7.1). These are collectively referred to as the engineered barrier system in the context of this analysis. Events which may affect the local drift environment but are not part of the system defined here, such as changes in water infiltration rate or climate, are considered external events (which are usually initiating events).

The waste package concept to be evaluated in this analysis is the 21 Pressurized Water Reactor (PWR) fuel assembly Uncanistered Fuel Waste Package (UCF-WP) described in section 6.2.3 of Reference 5.7. Criticality risk for the emplacement package containing the Multi-Purpose Canister (MPC) is evaluated in a companion document to this. Other spent fuel configurations will be included with the update of this analysis planned for April 1996. In the UCF-WP, spent nuclear fuel (SNF) assemblies are isolated from the external environment by a container consisting of two layers or barriers. The outer barrier consists of 100 mm of A 516 carbon steel corrosion allowance material. The inner barrier is fabricated from 20 mm of Incoloy Alloy 825 corrosion resistant material. Two designs have been proposed for the internal basket structure; an interlocking plate basket (ILB) design, and a bundled tube basket design. The ILB design provides criticality control by fabricating all plates separating fuel assemblies from neutron absorbing material. This material consists of 10 mm of borated Type 316 stainless steel. The tube design achieves criticality control by placing each assembly in neutron absorbing Type 316 borated stainless steel tubes that are 5 mm thick (resulting in 10 mm of borated stainless steel between adjacent assemblies). *For the current analysis, both designs will be treated identically as a single 10 mm thickness of stainless steel. The remainder of the interior of the UCF-WP is assumed to contain only an inert gas and no filler material^(5.7).* The

UCF-WP design is assumed to have an inner cavity length of 4.585 m^(5.32).

The local emplacement environment to be used in this evaluation is consistent with the horizontal in-drift emplacement concept using a low-thermal loading (24.2 MTU/acre) strategy and 4.27 m (14 ft) drifts. *It is also assumed that backfilling of the emplacement drifts has not been performed.* With a low thermal loading, the near-field temperatures fall below the boiling point of water within 200 years following last emplacement^(5.11). The lower temperatures result in reduced rock stresses, providing more stable and longer lived emplacement drift openings. However, the relatively quick drop below the boiling point of water (as opposed to that for a high thermal loading) greatly reduces the time before liquid water can come into contact with the waste package. The presence of water would result in more rapid corrosion of the waste package barriers and enhance the subsequent leaching of the neutron absorber material from the basket structure. It also allows for the possibility that the waste package interior could fill with water (which is the most efficient moderator available in the natural environment) immediately following breach of the outer and inner barriers, thus creating an environment for neutron moderation. Therefore, within the present understanding of the Yucca Mountain hydro-thermal processes, evaluating the UCF-WP with a low thermal load is a conservative assumption with respect to criticality. It should be noted that the recent CRWMS/M&O TSPA-93^(5.28) has shown the intermediate thermal loading (57 kW/acre) to be more stressing with respect to radionuclide release. If that alternative is under active consideration at the time of the next revision of this document (1996) then it will be included.

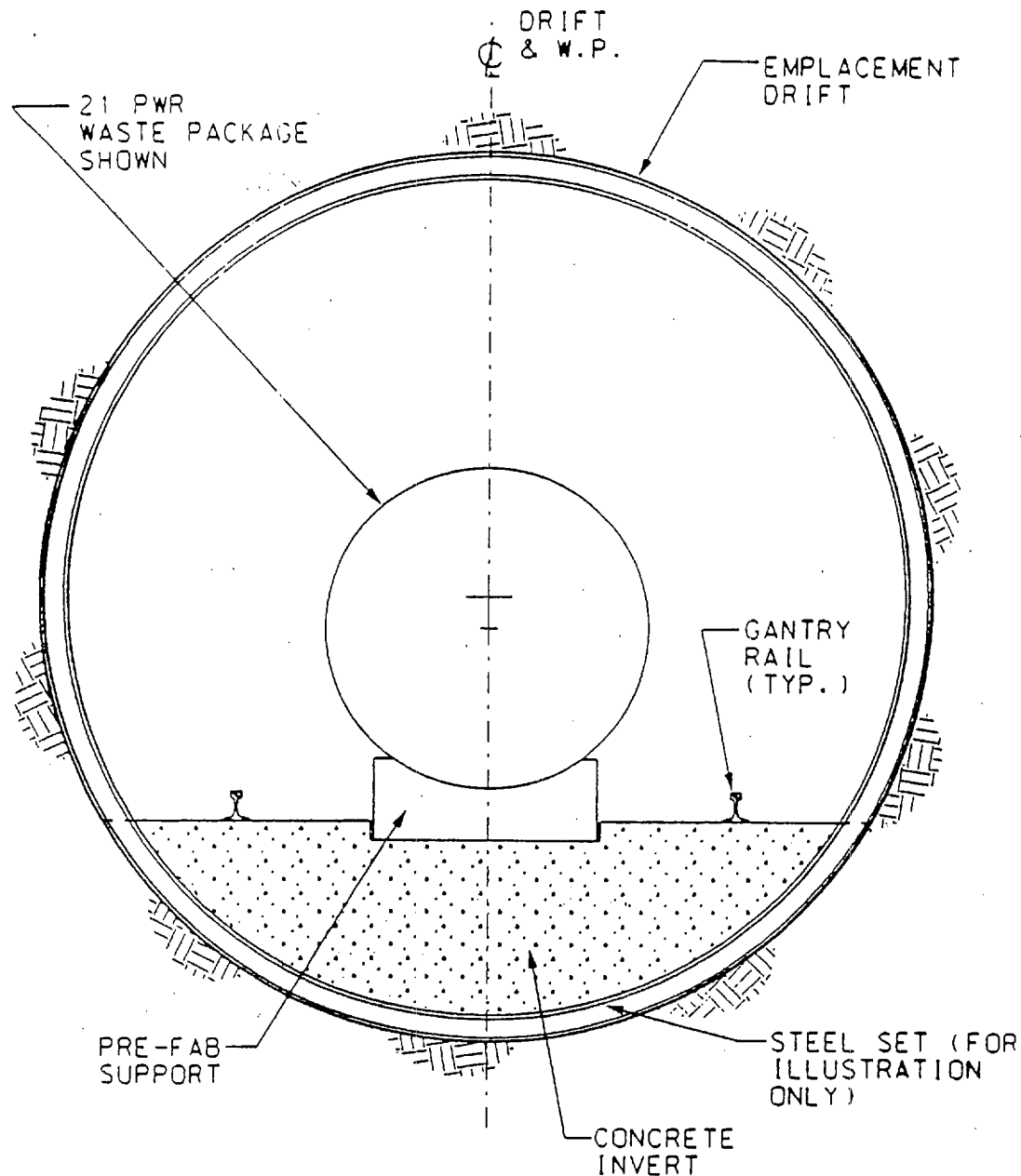


Figure 7.1. Waste Package and Local Drift Environment

7.2 Failure Modes and Effects Analysis

To assist in the development of the fault tree logic diagram, the technique of failure modes and effects analysis (FMEA) has been applied to the system of the waste package and its local drift environment. The FMEA process is qualitative in nature and is useful in determining sequences of events which can cause the defined system to fail to perform its intended function. The mission of the engineered barrier system being evaluated by this analysis is to safely contain fissile material and other radionuclides and isolate them from the accessible environment. In accomplishing the above mission, one of the functions performed by the system is to maintain the waste package in a subcritical condition. This is the function to be evaluated by this analysis, and the failure of the waste package to remain subcritical will represent the top event of the fault tree to be developed in Section 7.3. For the events in the more probable (but still unlikely) sequences leading to criticality, the probability of discrete events and probability density functions (pdf) for the events continuous in time will be developed in Section 7.4. These events can also be interpreted as engineered barrier system component failure modes, with their relationships provided in Table 7.1.

Event sequences leading to criticality

This analysis considers only water moderated criticality internal to the waste package. It has been shown that unmoderated criticality is impossible for intact light water reactor fuel with fissile content less than 5%^(5,14). Water is the only moderator present in the waste package environment which can enter the waste package. External criticality, which could involve moderation by silica, will be considered in the 1996 version of this analysis.

While a large list of event sequences (scenarios) involving extensive water intrusion has been proposed for performance analyses of radionuclide containment^(5,15) (i.e., magmatic intrusion, excavation by future drilling, etc.), most of these could not result in criticality. Only two basic scenarios are capable of introducing water into the local drift environment in a manner which could create the conditions necessary for a criticality event. These involve 1) the possible concentration of the episodic infiltration flux by a fracture directly over a waste package (hereafter referred to as the "concentration" scenario), and 2) the possible flooding of a drift due to an external event producing a significant rise in the water table (for which the principal mechanisms are changing of the climate to wetter conditions or a severe tectonic event) or high infiltration combined with poor drift drainage. These event sequences (scenarios) can be described in terms of the following specific events:

1. Concentration of the flow so as to directly impinge upon the waste package (e.g., flowing fractures in the drift directly above the waste package, or flooding of the entire drift). A fracture configuration leading to such concentration is assumed to be stable with respect to minor geologic changes over thousands of years, but not

- necessarily with respect to events on a 100,000 year time scale which could produce major geologic changes,
- 2. Increased water flow or flooding,
 - 3. Breach of the waste package to permit moderator entry (primarily by corrosion),
 - 4. Leach of the neutron absorber from the containing matrix,
 - 5. Ponding of water in the waste package to serve as a stable moderator (which is a direct consequence if the alternative flooding is used in steps 1 or 2 above), and
 - 6. All of the above events act on a package which has enough fissile material to go critical (SNF with high enough enrichment and low enough burnup).

The above water intrusion scenarios are conditional on the temperature of the rock in the local drift environment being below 100°C. The initiating events for this analysis are therefore defined as infiltration flow (nominal and high rates), flooding due to climate change, and flooding due to severe tectonic activity.

Component Failure Modes

Of the 6 events (or conditions) listed above as being essential ingredients of a criticality sequence (scenario), the third and fourth can be viewed as failure modes of individual components of the waste package: the barriers (inner and outer) component and the basket component.

Failure Modes of the Immediate Rock Environment

The repository is based on the assumption that the rock environment (including available moisture) will severely limit infiltrating water and prevent its coming into contact with the waste package. The presence of concentration fractures in the drift ceiling above a waste package which could direct infiltrating water onto a waste package represents one mode of failure of this environment. Another possible mode of failure is the collapse of a drift opening in such a way that a local dam is created, causing flooding of the drift if sufficient infiltration flow is available to the drift by the fractures described above. However, as mentioned previously, drift flooding can also occur in the absence a drift failure mode due to an initiating event which causes a rise in the water table to the repository horizon.

There are also several possible rock failure modes which could directly affect the integrity of the waste package. These include events which could impose a severe mechanical stress on the waste package, such as the impact of a falling rock or shearing by the movement of a new or unidentified fault. However, subsequent flooding of the drift and leaching of the neutron absorber would be required before a criticality event could occur. Further information on the frequency of a rockfall striking the package, and the variation in the structural response of the WP as it degrades, will be required before such sequences can be represented in the fault tree diagram. As this information is still under development, these sequences will be specifically included in future analyses.

Table 7.1. Summary of Engineered Barrier System Failure Modes and Criticality Effects

Component	Function	Failure Modes	Mechanisms	Effects	Comments
Immediate rock environment. (Surrounding the emplacement drift)	Provide an environment which ensures long waste package life by limiting contact with water and other hazards	Fails to prevent infiltrating water from contacting waste package	Hydraulically conductive ceiling fracture concentrates infiltrating water onto waste package	Eventual corrosion of barriers, and possible filling of WP, and leaching of neutron absorber.	Requires infiltration of surface water to initiate sequence. Requires proper corrosion hole configuration to fill WP.
			Drift collapse forms a dam, preventing drainage of infiltrating water from drift.	Eventual flooding of drift and immersion of one or more WPs. Eventual corrosion of barriers, filling of WP, and leaching of absorber.	Requires infiltration of surface water to initiate sequence. However, flooding may occur in the absence of drift failure modes due to other initiating events.
		Fails to prevent mechanical damage to waste package.	Rock fall or faulting incident on waste package, which may be partially degraded by corrosion.	Possible breach of WP barriers depending on amount of applied stress and degree of barrier degradation.	Sequence not included in current fault tree.

Table 7.1. Summary of Engineered Barrier System Failure Modes and Criticality Effects

Component	Function	Failure Modes	Mechanisms	Effects	Comments
Waste Package Barriers	Isolate SNF from environment and prevent intrusion of water to interior.	Waste package barriers breached, allowing moderator entry and neutron absorber removal.	Corrosion of barriers by intruding water.	WP eventually breached. Immediate filling under flooded conditions. Specific corrosion hole configuration required for filling by overhead dripping.	Rate of corrosion varies according to drift conditions. Rates of sufficient magnitude to cause breach in the time frame of this analysis are conditional on water intrusion.
			Pre-existing through-wall defect in both barriers	WP barriers breached. Immediate filling if flooded conditions occur.	Sequence not included in current fault tree.
Waste Package Basket	Maintain SNF in a subcritical condition	Insufficient neutron absorber available to maintain sub-criticality under moderated conditions	Sufficient neutron absorber leached from basket material by intruding water	Waste package criticality if fuel assemblies maintain appropriate geometry and basket filled with water.	Leaching is conditional on waste package breach and intrusion of water.
			Basket material doped with insufficient absorber during fabrication	WP criticality if fuel assemblies maintain proper geometry and basket filled with water.	Sequence not included in current fault tree.

7.3 Development of Fault Tree Logic

The fault tree approach is a deductive process whereby an undesirable event, called the top event, is postulated, and the possible means for this event to occur are systematically deduced. In this analysis, the undesired event is waste package criticality. In the previous section, the deductive FMEA process was performed to determine the basic criticality scenarios, initiating events, and engineered barrier system failure modes that could lead to a waste package criticality event. In this section, the results of the FMEA will be used to develop the fault tree logic diagram.

The fault tree diagram is a graphical representation of the various parallel and sequential combinations of faults that lead to the occurrence of the top event. The methodology and symbols used in the construction of the fault tree diagram are given in the Fault Tree Handbook^(5,6). Figure 7.2 is provided as a reference for the symbols utilized in this analysis. The fault tree developed from the engineered barrier system FMEA is shown in Figure 7.3. The fault tree was plotted using CAFTA version 2.3 fault tree analysis software. In addition to a one line description, each intermediate gate, basic event, and conditional event, is uniquely identified with an acronym. These acronyms will be used as identifiers for each gate and event in the quantification of the fault tree that is performed in Section 7.5. These acronyms are individually identified with the complete event descriptions in the headings of the subsections of Section 7.4, where we have also given the derivation of the associated probabilities and probability density functions.

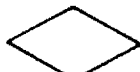
PRIMARY EVENT SYMBOLS



BASIC EVENT – A basic initiating fault requiring no further development



CONDITIONING EVENT – Specific conditions or restrictions that apply to any logic gate (used primarily with PRIORITY AND and INHIBIT gates)



UNDEVELOPED EVENT – An event which is not further developed either because it is of insufficient consequence or because information is unavailable



EXTERNAL EVENT – An event which is normally expected to occur

INTERMEDIATE EVENT SYMBOLS



INTERMEDIATE EVENT – A fault event that occurs because of one or more antecedent causes acting through logic gates

GATE SYMBOLS



AND – Output fault occurs if all of the input faults occur



OR – Output fault occurs if at least one of the input faults occurs



INHIBIT – Output fault occurs if the (single) input fault occurs in the presence of an enabling condition (the enabling condition is represented by a CONDITIONING EVENT drawn to the right of the gate)

Figure 7.2. Definitions of Event and Gate Symbols Used in Analysis

Waste Package Development

Design Analysis

Title: Initial Waste Package Probabilistic Criticality Analysis: Uncanistered Fuel (TBW)
 Document Identifier: B0000000-01717-2200-00079 REV 01, 10/5/95

QA: I
 Page 20 of 52

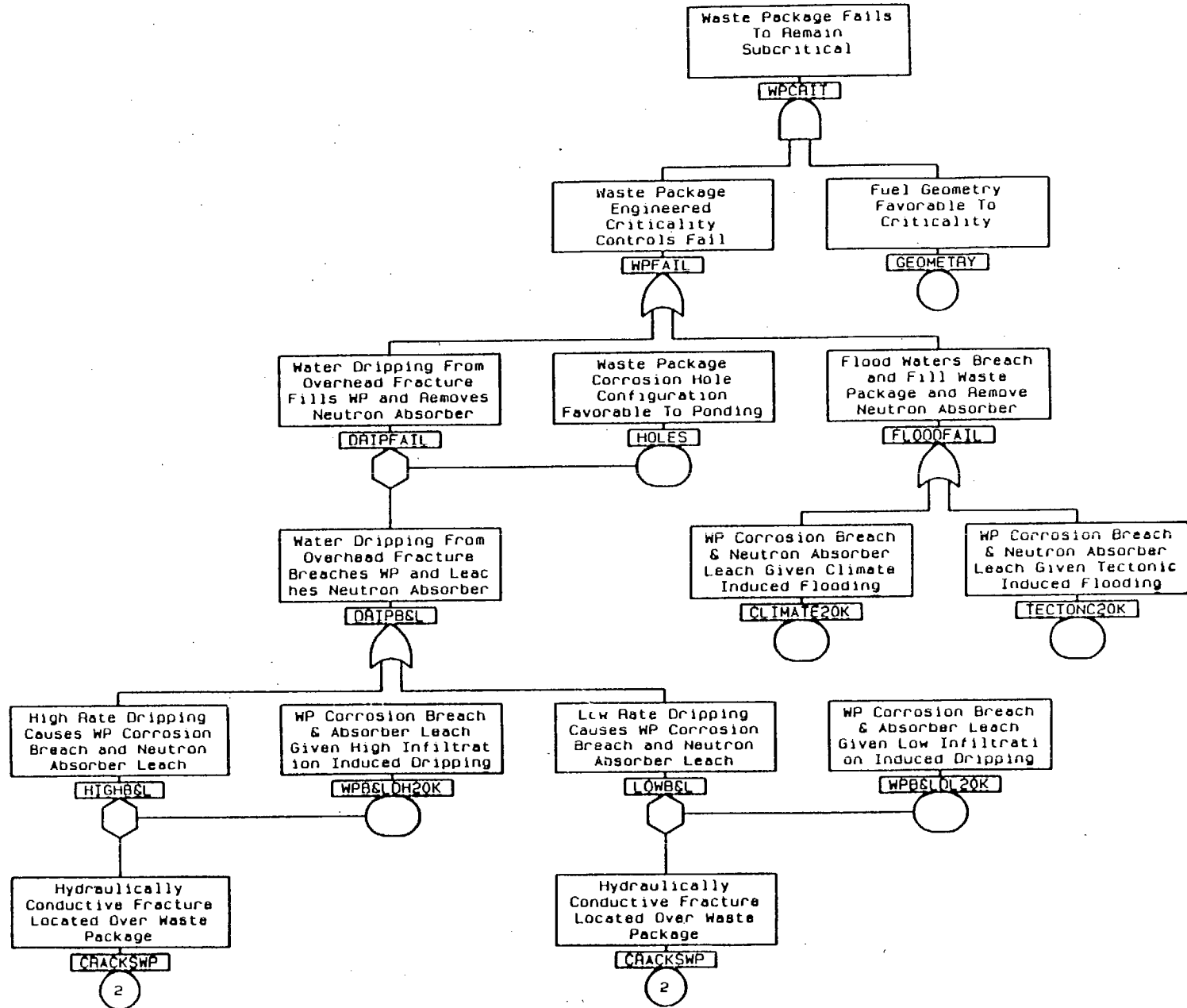


Figure 7.3. Initial Post-Closure Waste Package Criticality Fault Tree

Originator: J.R. Massari

Checker: L.E. Booth

7.4 Development of Probabilities and Probability Density Functions (pdf)

The following sections provide a detailed description of the estimation of the probabilities of discrete events and the probability density function of events which are continuous in time. All basic, conditional, and initiating events in the fault tree diagram for the system defined in Section 7.1. Event identifiers used to abbreviate the full description in the analysis of the fault tree are given in parentheses. Event probabilities and pdf's have been summarized in Table 7.7. Copies of the actual calculations performed in this section are contained in Attachment I.

The three events involving water: (1) flow defining events (increased flow or repository flooding), (2) breach of the waste package by aqueous corrosion, (3) leach of the absorber by dissolution of the basket, will be represented by pdf's which will be convolved together to incorporate the fact that they must occur in the sequence indicated. In other words, the pdf for the occurrence of all three events, with the last event occurring at time t , requires that event 1 take place at some time, $0 < t_1 < t$, followed by event 2 at some time $t_1 + t_2$, such that $0 < t_1 + t_2 < t$, which is followed by event 3 occurring at time t . The pdf for t is then found from the two-fold convolution

$$f(t) = \int_0^t f_1(t_1) dt_1 \int_0^{t-t_1} f_2(t_2) f_3(t-t_1-t_2) dt_2 \quad (1)$$

7.4.1 Flow Defining Events

These are the initiating events; all are characterized by a pdf, denoted by $f_1(t)$. All describe a state of flow or flooding; *it is assumed that this state continues indefinitely once initiated*. In other words, we use a pdf to define the probability of occurrence within a small interval of time centered about a specific time and assume that the occurred condition will continue indefinitely. This is a very conservative assumption, since it is possible that any increased state of flow or flood will eventually revert to something like the original state before the enhanced corrosion rate has completed the corrosion of the waste package component (barrier or basket). These pdf's are all in expressed in units of per-year.

It should be noted that the description of alternative flow defining events is intended to be qualitative only, without specifying the actual water accumulation (net of infiltration and outflow). The effects of these flows are treated more quantitatively in section 7.4.3 (Corrosion Events) below.

The events, or event scenarios, described below reflect alternative forecasts of climatological or tectonic change. As such they should be mutually exclusive. However, this would be an oversimplification. The actual environmental changes over the next 1,000,000 years would be a mixture of these four alternatives at different points in time. An analysis based on comparison of the large number of combinations possible would be confusing

and difficult to interpret, and, considering the uncertainty in the forecast process itself, would not be very meaningful. For these reasons we have calculated the pdf's as if each event were certain to occur, given enough time. The question of how to combine these probabilities does not arise until we have convolved them with the corrosion breach and leach pdf's and with the discrete probabilities for sufficient fissile material and sufficient moderator (sections 7.4.4 and 7.4.6, below).

Pdf for Surface water infiltration of repository horizon at a low rate (f_1 for wpb&ldl)

This is the probability that a corrosively significant stream will pass through the waste emplacement areas. Such a stream would have to accumulate sufficient volume to fill a waste package to a depth of at least 1 meter. Over a period of 10,000 years, this would require a flow rate of 0.1 mm/yr, which just happens to be the middle of the flow rate range presently estimated for the repository area^(5.29). However, in addition to ponding in the package, there must be enough flow to leach out the boron absorber from the basket; *we conservatively assume that at least a factor of 10 increase would be required for such a process*, for a total infiltration rate of 1 mm/yr. [Note: This estimation of required flow rate is only to define this low infiltration category. The actual rate of basket leach is estimated in section 7.4.3.2 (Corrosive leach of absorber/basket) below.] For such an increased flow rate to be maintained over many years, there would have to be a significant climate change (one as significant as an ice age). *We very conservatively assume that such an event is certain to occur within 10,000 years (and that such an enhanced flow rate would be maintained thereafter)*. It should also be more likely at the end of this period than at the beginning, since such a changed climate would take thousands of years to develop. Nevertheless, we chose a conservative probability model, the uniform distribution between 1,000 and 10,000 years, which can be expressed in units of per year as

$$f_1(t) = 1/9000 \quad 1000 < t < 10000 \quad (2)$$

This pdf is shown in Figure 7.4, together with the resulting cdf.

Pdf for surface water infiltration of repository horizon at a high rate (f_1 for wpb&ldh)

This would be an infiltration flow rate of greater than 10 mm/year, which is 10 times the low infiltration flow rate given above, and would be expected to give a correspondingly increased corrosion rate (on the waste package) and leach rate (for the boron). [It may be that 10 mm/yr is still so low as to not significantly disturb the corrosion passivating film, so that the conditional corrosion rate is not significantly higher than for low infiltration, but the boron leach rate would still be higher.] *Such a high infiltration rate would require a very significant climate change, which we assume to be likely sometime between 2,000 years and 100,000 years (which would be likely to encompass several ice ages, and their aftermaths, which could result in increased atmospheric precipitation)*. As with the low infiltration case, we use the conservative uniform distribution, again expressed in units of per year

$$f_1(t) = 1/98000$$

$$2000 < t < 100000$$

(3)

This pdf, together with the associated cdf, is shown in Figure 7.5.

Change to a very wet climate raises water table to repository horizon (f_1 for climate)

The present tectonic trends are moving the climate in a dryer direction. For example, one major cause of the shift from a moist climate to a dry one over the past several million years has been the rise of the Sierra Nevada, which prevent the moist Pacific air from reaching Nevada. Flooding of the repository would require a substantial increase in rainfall, sustained over a long time period, since the proposed repository horizon is approximately 300 meters above the current water table. The National Research Council has examined the possibility of water table rise to the level of the repository^(5,27). They reported that even a 100% increase in rainfall (and a corresponding 15 fold increase in recharge) would produce an insufficient rise (raising the level only 150 meters). Their report also indicated that the last ice age saw only a 40% increase in precipitation (p. 6), and that as far back as 50,000 years ago the water table in the recharge area north of Yucca Mountain was no more than 100 meters above its present level (p. 78).

Therefore, we assume the probability of flooding due to climate change in the next 10,000 years to be zero. The probability of flooding thereafter is conservatively estimated from available geologic information. The National Research Council report cited above suggests that the return period for simple flooding to be greater than 10^6 years, and that the probability of flooding during the early part of this period is much less than later. This inequality is so small that we can conservatively assume an asymmetric triangular distribution with the upper limit at 10,000,000 years, which would be

$$f_1(t) = 2 \times 10^{-14} t \quad 10,000 < t < 10,000,000 \quad (4)$$

where t is expressed in years, and f_1 is expressed in units of per year. For simplicity, we have normalized this pdf as if the lower limit were 0, instead of 10,000. This normalization approximation is valid to six significant figures, which is certainly adequate for this analysis. This pdf, together with the associated cdf, is shown in Figure 7.6.

A flood of the magnitude described above would affect all packages in the repository equally. This situation is commonly referred to as a non-lethal shock common cause failure in component reliability analysis^(5,8). Given a repository wide non-lethal shock, such as flooding and immersion of all waste packages, each waste package will fail independently with a conditional probability of p (to be defined later; see section 7.4.3.1). Therefore, the above flooding event frequency may be applied to any given package. This is appropriate since the fault tree top event will be in terms of a frequency of criticality per package which can then be multiplied by the number of packages to get the expected number of criticalities in the repository.

Pdf for severe tectonic activity raising water table to repository horizon (f, for tectonic)

Flooding can also be caused by hydrothermal or volcanic activity raising the water table from below. This would require a tectonic change comparable to the major volcanic activity which produced Yucca Mountain in the first place. The geologic record indicates that this has not happened for the last 10^7 years. *The time scale for occurrence of this severe tectonic activity is, therefore, similar to that which applies to climate change induced flood, so the pdf for this event will be assumed to be the same as that given in Figure 7.6.*

This reasoning is more conservative than the authoritative finding that the possibility of a dike intrusion close to the repository is less than 10^{-8} per year and would cause only a 10-15 meter rise in the water table anyway (5.27, p. 7). One possible type of seismo-tectonic event which has been advanced as a possible initiator of repository flooding is a rupture in the low permeability zone imputed to be the source of the steep hydraulic gradient north of the site. An authoritative analysis has shown that should such a barrier exist, its removal would cause no more than a 40 meter rise in the water table at the repository site (5.27, p. 70).

The conditions that occur as a result of tectonically induced flooding are similar in nature to those of the climatologically induced flooding. Therefore, this event can also be thought of in terms of a non-lethal shock leading to common cause failure of waste packages, and can be applied on an individual package basis as well.

A seismo-tectonic event could release perched water if it were present in any volume, but any subsequent flooding of the repository would be transient only, unless all possible avenues of repository drainage were blocked, a very unlikely event.

7.4.2 Concentration of flow on individual waste package

In order to be effective in corroding a hole in the package, the nominal infiltration flow must be concentrated over some localized position on the package (typically by the location of a flowing fracture). This localized flow serves both to generate the corrosion hole and to channel the water into that hole, from where it can fill the lower half of the package and leach the neutron absorber. This section estimates the probability that a rock fracture capable of concentrating the infiltrating water exists over the waste package and directs the flow onto the waste package (crackswp). *This probability is assumed to be a property of the repository which remains constant over at least 100,000 years during which we are concerned about corrosion from leaking of fractures on a waste package.* It has been suggested that fractures may be a dynamic occurrence over the time periods of interest, and that they may even increase with time. The mechanisms which have been proposed include (1) changing stress patterns (e.g., those caused by the time and/or spatial variations of the repository thermal load, including the local stresses from individual waste packages), and/or (2) diversion to alternate fractures from flowing fractures which

might get plugged by some silica redistribution mechanism. However, there is no evidence that new, or alternate, fractures would possess the necessary connectivity to provide flow enhancement. Furthermore, there is no model of the hypothesized time dependent behavior, so a constant value intended to have a safety margin large enough to accommodate any increase with time of the number flowing fractures will be used. This probability will be expressed in units of per-package.

The first step in developing a probability that a waste package is located under a dripping fracture is to determine the frequency of these fractures per unit length of drift ceiling. We have started with an estimate of the non-directional volumetric fracture frequency for the TSw2 unit of approximately 19.64 fractures per m³, from available borehole sample data^(5,24). The present, simple, model does not account for more detailed parameters, such as distribution of aperture sizes or fracture surface conditions; such information will be incorporated into future models when it becomes available.

For the purposes of this analysis, the most appropriate form is a linear ceiling fracture frequency, which can be developed from the volumetric frequency. To do this, the above volumetric frequency was used to determine the number of fractures in a cylindrical volume of rock equivalent to a 1 m long section of a 4.27 m (14 ft) diameter emplacement drift (281 fractures). *It was then assumed that only 50% of the fractures would intersect the surface of the volume (evenly distributed) and that the drift ceiling constituted approximately 8% of the surface area of that volume (top 90° arc of drift).* This resulted in an estimate of approximate 11.28 fractures per meter of drift ceiling.

With the linear ceiling fracture frequency estimated, the next step is to determine the percentage of fractures capable of conducting and concentrating the infiltration flow. A study performed in the STRIPA validation drift found that 14% of the tunnel surface area accounted for nearly all the flowing fractures^(5,19, p. 139). The high flowing 14% actually had a three times higher fracture density, suggesting that such areas could be easily detected and avoided. Without more data on the variable density of fractures in the repository horizon, and some possible correlation of such data with any flowing water, we take a somewhat different approach.

We assume that there will be some density of undetected flowing fractures. We estimate such a density by starting with the STRIPA 14% and applying it on a fracture basis rather than an area basis. This may not seem conservative since the STRIPA flowing area has a higher density of fractures than the rest of the drift, but is conservative since we take no credit for detecting any of these high flow zones before emplacement. Since the tuff at the repository horizon is unsaturated, and infiltrating water will be preferentially absorbed in the rock pores rather than flowing through fractures, we assume that this flowing fraction of all fractures should be reduced by a factor of 100 for a drift in the TSw2 rock unit. [Note: This is the most significant of the assumptions to be verified by the time of the next revision of this document.] With this assumption, the linear frequency of flowing/dripping ceiling fractures is estimated to be of 0.0157 fractures per

meter of drift ceiling or 1 flowing fracture every 64 meters. This frequency will have to be verified by actual observation in the Exploratory Studies Facility.

Lacking precise characteristics of the fracture flows in the repository horizon, this model is necessarily somewhat arbitrary. It will be revised in the next version of this document, according to ESF measurements expected by that time. In the meantime we can have some confidence in the model because it is consistent with the flowing fracture density in the "weeps model" developed by Sandia^(5,13, Ch.15). Furthermore, this result is somewhat consistent with the interim results of fracture mapping in the starter tunnel, which indicates 1 fracture per meter of drift, without restriction to ceiling, but only reduces that fraction slightly in order to specify connected fractures^(5,30). This strong connectivity is expected to be reduced as the tunnel reaches further under the surface, and there should be some additional reduction in order to specify flowing fractures.

With the above estimate of the linear flowing fracture frequency, the probability that a certain number of flowing fractures, n , will be located in a given length of drift can be determined using a Poisson distribution,

$$Pr(n) = \frac{(\lambda x)^n \exp(-\lambda x)}{n!} \quad \text{for } x\lambda > 0, n=0,1,2,\dots \quad (5)$$

where λ represents the frequency of flowing fractures per unit drift length, x is the length along the drift in question. Given the above flowing fracture frequency, and a WP inner cavity length of 4.585 m, the probability that a waste package does not have a flowing fracture over it, $Pr(0)$, is 0.931. Therefore, the probability that a waste package has at least one flowing fracture over it is $1-Pr(0)$, or 0.069.

7.4.3 Corrosion Events

In this analysis, criticality cannot occur until the waste package barriers have been breached by corrosion and the basket material containing the neutron absorber has been leached. These corrosion processes will be represented by the pdf's f_2 and f_3 in the two-fold convolution given in section 7.4.5. This section describes the methodology for obtaining these pdf's.

At the present time there is a great range in the corrosion rates derived from the accepted experimental data. There is no definitive model to explain even a major portion of this data. For this reason, we have developed a probabilistic model which reflects the wide variation of observations with probability distributions for failure times of the individual components being corroded. In the present state of uncertainty regarding corrosion models, we have chosen to be realistic rather than conservative. *To compensate for this lack of conservatism we have provided a complete alternative calculation under the worst case barrier corrosion assumption: that the outer and inner barriers are penetrated by pitting corrosion in no time at all following occurrence of the initiating event.* This

approach does not resolve the conflict between pitting and bulk corrosion interpretations of some of the data, but it does present the range of possible consequences.

It is well known that rate of corrosion depends on many properties of the aqueous environment, particularly pH, which is incorporated into corrosion models more sophisticated than the model used here. However, most of the data comes from tests which were not controlled for these parameters, so we have chosen to use the experimental data in a model which reflects the worst case parameter values likely to be encountered in the aqueous environment. We have also simplified the analysis by neglecting dry oxidation since, (1) if water is present for any significant fraction of the time, dry oxidation will have a small effect by comparison, and (2) if water is never present we can't have an internal criticality.

For this analysis, *it has been assumed that the primary variables influencing the rate of corrosion in the postulated environments are the surface temperature of the waste packages and the chemistry of the intruding water. However, the latter will be postulated to be constant for a given environment unless otherwise stated.* The variations in waste package surface temperature with respect to time and location in the repository, provides the basis for the use of a pdf to represent time to breach of a given barrier.

Stahl^(5,10) has summarized diversity of measurements and analytic models with the following time and temperature dependent equation as a heuristic representation of the penetration of certain metals by aqueous corrosion,

$$P = At^c \exp\left(-\frac{B}{T}\right), \quad (6)$$

where P is corrosion penetration depth, t is time (years), T is temperature (K), and A , B , and c are constants. This equation is representative of experimental data for moderate temperatures (up to about 350K). At higher temperatures the equation is expected to be conservative because it does not account for the decreasing solubility of oxygen. The value of c describes the degree of protection afforded the base metal surface by the corrosion products. For $c = 1$, the corrosion rate is independent of time if temperature and humidity are constant; this is appropriate if the products of corrosion are entirely unprotective. For $c = 0.5$, corrosion has the parabolic dependence on time that is typical for a layer of corrosion products that act as a diffusional barrier to corrosive species. Intermediate values of c can be used to describe varying degrees of protectiveness.

Stahl's formula is adequate for predicting aqueous corrosion penetration of a material that is held at constant temperature. However, because waste package surface temperatures will be time and location dependent, it becomes necessary to put Stahl's model into a form that gives the rate of corrosion. Since the definition of zero time is arbitrary, it is also desirable to have an expression for the corrosion rate that does not have an explicit time dependence. McCoy^(5,9) has proposed the following expression for corrosion rate, in which all time dependence is implicit:

$$\frac{dP}{dt} = cP^{(c-1)/c} A^{1/c} \exp[kh/c - B/(cT)] \quad (7)$$

Here h is a complement to the relative humidity H , and given by the expression $h = H(\text{in \%}) - 100$, and the remaining constants are equivalent to those used in Stahl's equation. Equation 7 provides an expression for the corrosion rate that depends only on the amount of corrosion product present and the environmental conditions. The equation generalizes Stahl's equation in two ways: it is applicable to time-dependent environmental conditions, and it postulates a humidity dependence. To determine the corrosion penetration during a given interval of time, Equation 7 may be reduced to a problem of integration:

$$P_f^{1/c} = P_i^{1/c} + A^{1/c} \int_{t_i}^{t_f} \exp[kh/c - B/(cT)] dt, \quad (8)$$

where the subscripts i and f indicate initial and final values, respectively. A C program provided by McCoy was used to perform the above integration for this analysis to determine the times at which both barriers would be penetrated for six WP positions in section 7.4.3.1. A copy of the source code is included in Attachment I.

McCoy^(5.9) obtained a value of k of 0.1908 for a static environment from measurements by Jones^(5.22) of corrosion current as a function of humidity. *Since McCoy's model is being used here to develop a failure distribution for a waste package in a flooded drift, the relative humidity will be assumed to be 100% for all times when T<100°C* (the expression kh/c in the above formula will go to zero). This will simulate wetting of the waste packages as soon as physically possible after emplacement in a low thermally-loaded repository. This is a conservative assumption because (1) the repository temperatures (and thus the corrosion rates) may be substantially lower by the time an initiating event actually occurs, and (2) the actual boiling point of water at the repository horizon is $\approx 96^\circ\text{C}$. *For times when T≥100°C the environment is taken to be a mixture of superheated steam and air at atmospheric pressure.*

For early years the waste package surface temperature depends primarily on its own internal heat and is best determined by a drift-scale calculation; for later years it depends on the average heat from all the packages and is best determined by a repository scale calculation. For the low thermal loading case, the dividing point is approximately 100 years after emplacement. For times less than 100 years the results of a waste package model developed by Bahney^(5.11) were used. Bahney created a three-dimensional finite element ANSYS model of near field and surface temperatures for a single waste package, with the remainder of the repository represented as an infinite grid of waste packages with 16 m along the drift between waste packages and 95 m between drifts. For times greater than 100 years, modified versions of the repository scale results of Buscheck^(5.12) were used. Buscheck calculated repository horizon temperatures for a disk-shaped repository with a smeared heat source. In similar calculations that were reported previously^(5.9), the

difference in temperature between the waste package surface and the drift wall was taken to be

$$T_{wp} - T_{dr} = q/h \quad (9)$$

Here T_{wp} and T_{dr} are the temperatures of the waste package and drift wall, respectively, h is a heat transfer coefficient, and q is the heat output of the waste package. The heat transfer coefficient is given by the equation

$$h = (98.36543 + 0.8127311 T_{mn} + 0.005341355 T_{mn}^2) \text{ watts/K} \quad (10)$$

where $T_{mn} = [(T_{wp} + T_{dr}) / (2 \text{ K})] - 273.15$, that is T_{mn} is a dimensionless quantity that is numerically equal to the mean temperature, expressed in degrees Celsius, of the waste package and drift. The heat output of the waste package is taken to be

$$q = \exp(11.49766 - 0.7238801 \ln[t/(1 \text{ yr})]) \text{ watts} \quad (11)$$

where t is the age of the fuel, measuring from the time of discharge. This heat output is suitable for fuel with an initial enrichment of 3.92% and a burnup of 42.4 GWd/MTU.

Since the temperature drop $T_{wp} - T_{dr}$ predicted from Equation 9 is only that from the waste package to the drift wall, it is smaller than that from the waste package to the repository horizon. The total temperature from the waste package to the repository horizon was taken to be $F(T_{wp} - T_{dr})$, where F is a constant that depends on the position of the waste package within the repository. F was chosen so that the temperature of the waste package would be continuous at 100 years after emplacement. The required values of F were as follows:

Position	F
12%	2.56
50%	2.56
75%	2.56
90%	2.59
97%	2.81
99%	3.00

The resulting blended temperature history is shown in Figure 7.7. The various curves represent time-temperature profiles at different locations in the repository; percentages give the fraction of waste packages that are closer to the center of the repository than the package in question (0% is at the center, 25% is halfway from center to edge, and 100%

is the edge).

For the functional form of the pdf for corrosion (f_2 or f_3) the three parameter Weibull distribution will be used. This distribution is often used in reliability analysis to model corrosion resistance^(5,8). The pdf of the Weibull distribution is given by,

$$f(t) = \frac{\beta}{\alpha} \left(\frac{t-\theta}{\alpha}\right)^{\beta-1} \exp\left[-\left(\frac{t-\theta}{\alpha}\right)^\beta\right] \quad (12)$$

where α , β , and θ represent the scale, shape, and location parameters respectively (all > 0) and $t \geq \theta$. The associated Weibull cdf is given by,

$$F(t) = 1 - \exp\left[-\left(\frac{t-\theta}{\alpha}\right)^\beta\right] \quad (13)$$

for $t \geq \theta$. For values of $t < \theta$, both $f(t)$ and $F(t)$ equal zero. The values for α , β , and θ are typically chosen such that the shape of the resulting distribution closely matches the distribution of observed time to failure data of a sample of components.

7.4.3.1 Corrosive breach of waste package barriers

Parameter Development for McCoy Model

The first step in developing breach distributions was to determine values for the parameters required by McCoy's model. For aqueous general corrosion of carbon steel Stahl^(5,10) recommends $A=2525$ mm/yr, $B= 2850$ K and $c=0.47$. Stahl indicates that these values are based on corrosion tests of cast steel and iron in seawater. The ASM Handbook^(5,20) also presents the results of a 9 week corrosion testing program performed for carbon steel in tuff groundwater at temperatures ranging from 50 to 100°C. Pitting corrosion rates were found to be approximately 1 mm/yr for most temperatures in the above range. Using Stahl's values for A and B , and assuming a c of 0.75, produces an average corrosion rate at 9 weeks time similar to that reported in the ASM Handbook. *Therefore, this analysis will assume a c of 0.75 for carbon steel.* This modification of c is considered appropriate, as the oxide layer formed during corrosion of carbon steel (i.e., rust) is typically regarded as providing very little protection against a corrosive environment. The above parameters from Stahl, and the c determined here, will be used for modeling carbon steel corrosion in harsh, or continuously wetted, environments.

The ASM Handbook^(5,20), also provided general corrosion rates for immersion in tuff groundwater at temperatures ranging from 50 to 100°C. These corrosion rates were found to be 0.3-0.5 mm/yr for the temperatures in the above range. Using the corrosion rate at the middle of this range, Stahl's value for B , and a c of 0.75, produces an A of ≈ 1000 mm/year. Therefore, this A will be used with the previously defined values of B and c to define the corrosion performance of carbon steel in mild, or intermittently wetted, environments.

The parameters for Alloy 825 were developed from available corrosion data for representative environments and assumptions about the time and temperature dependence of the material. *The temperature dependance parameter, B, was assumed to have a value of 5000°K*, which is almost twice the value used for carbon steel. This assumption was considered appropriate for a corrosion resistant material such as Alloy 825, as it typically maintains this resistance over a larger temperature range than carbon steel. *The protectiveness of the corrosion product layer was conservatively assumed to be similar to that of carbon steel, and thus, a c of 0.75 was chosen.* One source of corrosion data^(5,16) indicated that Alloy 825 experienced a corrosion rate 1.01 $\mu\text{m}/\text{yr}$ during 1.06 years of exposure to seawater at the ocean surface at 17.2°C^(5,31). Using the values of B and c as given above, this gives an A of 31,512 mm/yr. These parameters will be used to define the corrosion performance of Alloy 825 in the continuous wetting environment.

Another study sponsored by the Nuclear Regulatory Commission^(5,23) tested the corrosion behavior of Alloy 825 immersed in a sample of J-13 well water that was specifically modified to present an aggressive pitting environment (called Solution No. 20), including the addition of up to 4800 ppm peroxide to simulate radiolysis. This test, which was performed at 90°C for 2784 hours found a pitting corrosion rate of 9.17 $\mu\text{m}/\text{yr}$. Using the same assumptions for B and c as above, this results in an A of 6602 mm/yr. Since this environment is less aggressive than the seawater immersion case above, these parameters will be used to define the corrosion performance of Alloy 825 in the intermittent wetting environment.

Table 7.2. Summary of McCoy Model Parameters for WP Barrier Materials

Material	Continuous Wetting			Intermittent Wetting		
	A (mm/yr)	B (K)	c	A (mm/yr)	B (K)	c
Carbon Steel	2525	2850	0.75	1000	2850	0.75
Alloy 825	31512	5000	0.75	6602	5000	0.75

Evaluation of McCoy Model and Development of Weibull pdfs

Using the corrosion parameters identified above for carbon steel and Alloy 825, each of the six temperature histories shown in Figure 7.7 were evaluated using McCoy's model to predict waste package breach times for different locations in the repository. This evaluation was performed on the WP HP9000 computer Opus using the compiled C code and batch files contained in Attachment I. The time to penetrate the 120 mm thick dual-barrier waste package was determined by using the parameters for carbon steel until the penetration depth was equal to 100 mm (the thickness of the outer barrier), and then switching to the Alloy 825 parameters for the remaining 20 mm. *Also, for the Alloy 825 barrier, c was assumed to be 0.75 for the first 5000 years of inner barrier exposure, and*

1.0 thereafter. This is equivalent to assuming the corrosion product layer becomes unprotective after 5000 years and adds an extra degree of conservatism to the estimate of inner barrier lifetimes. The results of the evaluation are given in Table 7.3 for both the continuous and intermittent wetting cases.

Table 7.3. WP Time To Breach Predicted By McCoy's Model

Repository Location	Intermittent Wetting		Continuous Wetting	
	Outer Barrier Breached (years)	Inner Barrier Breached (years)	Outer Barrier Breached (years)	Inner Barrier Breached (years)
12.5%	3150.1	34807.3	680.9	8188.9
50%	3198.2	33364.5	681.1	8250.1
75%	3496.4	34850	688.4	8594.4
90%	4402.6	38286.2	762.0	9348.2
97%	5279.5	40843.4	876.6	9960.1
99%	5579.7	41665.6	923.9	10174.8

To determine the Weibull parameters for the waste package breach distributions, f_2 , a least-squares fit of the data produced by McCoy's model was performed using a Microsoft Excel version 4 spreadsheet. An alternate check of the spreadsheet was performed by plotting the data for one case on Weibull probability paper. Both the spreadsheet (with all formulas identified) and the Weibull paper plot are included in Attachment I. For both methods, a value for θ was manually selected to produce the best fit of the data. The Weibull breach distribution, f_2 , parameters for the two basic environmental conditions, intermittent and continuous wetting of the WP barrier are summarized in Table 7.4. below. The continuous and intermittent wetting distributions described by these parameters are shown in Figures 7.8 and 7.9, respectively.

Inspection of the intermittent wetting data in Table 7.3 reveals that the packages nearest the center of the repository (12.5% range) breach later than those part-way out (50% range). It is evident that this is a direct result of the lower waste package surface temperatures predicted by Buscheck's model for the center-most group after the 10,000 year mark (see Figure 7.4). As the center-most packages have the longest time to breach in the 50% range, the time to waste package breach reported for the 12.5% location was entered into the Excel spreadsheet at the 50% failure point; the time to breach at the 50% location was then entered as the 37.5% failure point. The remaining points were plotted according to their location on the temperature history as before.

Table 7.4. Summary of Weibull Parameters for WP Barrier Corrosion PDFs

Condition	α	β	θ
Intermittent Wetting	5030.3	1.737	30,000
Continuous Wetting	425.4	0.93	8100

Conservative Approach to Pitting Corrosion (discounting waste package barriers)

Certain experimental and theoretical studies have concluded that Alloy 825 is subject to pitting corrosion which can rapidly penetrate the barrier in localized areas without having much metal weight loss overall so that the conventional experimental studies, summarized in the previous paragraph, fail to detect this potentially harmful process. For this reason the Sandia TSPA-93^(5,13) estimates a rapid corrosion process for Alloy 825 wherever it is contacted by a significant amount of water. For a Yucca Mountain repository environment, TSPA-93 predicts penetration of an Alloy 825 barrier in only a few hundred years. Since at least one study has found that Alloy 825 exhibits only broad shallow pits^(5,23), or none at all, in water of similar chemistry as that expected at the repository horizon, it may be concluded that further testing will either disprove the rapid pitting theory or will identify modified versions of Alloy 825 (such as high molybdenum) which are immune to rapid pitting. By the time of the next version of this document, we expect this issue may be resolved. In the meantime, as an alternative, we are presenting a conservative approach that has no barrier at all, since a corrosion time of a few hundred years is approximately zero on the time scale of tens of thousands of years considered here. These alternative, no-barrier, distributions will be further discussed in section 7.4.4.

It should also be noted that this analysis is independent of the density of corrosion pits per unit area of exposed metal. *The assumption has been made that (1) if a single pit can penetrate the package surface, the package can be considered breached, and (2) the expected pit density is at least 1 per surface area of an individual package barrier.*

Pdf for Flood breach (f_2 for climate & tectonic)

Sequences involving flooding of the emplacement drift would result in the WP being continuously wetted. Therefore, the Weibull pdf for continuous wetting developed above will be used as the waste package breach distribution, f_2 , for the flooding sequences.

Pdf for low infiltration breach (f_2 for wpb&ldl)

It is assumed that a fracture dripping at a low rate onto a waste package would be incapable of maintaining the surface of the package in a continuously wetted condition due to evaporation. This assumed intermittent wetting suggests that there will be a higher likelihood of starting corrosion pits at new locations, than continuing to extend their

depth. Since there is no information on the corrosion behavior of the barrier materials under conditions of intermittent wetting *it was assumed that the above behavior could be equally represented by general corrosion data from continuously immersed samples*. Thus, the intermittent wetting pdf developed above will be used as the waste package breach distribution, f_2 , for low infiltration sequences.

Pdf for Corrosion breach at high infiltration (f_2 for wpb&ldh)

It is assumed that high infiltration will cause the flow rate to be sufficient to ensure that the surface of the waste package below a dripping fracture is continuously covered with a film of water. Therefore, the continuous wetting pdf developed above will be used as the waste package breach distribution, f_2 , for high infiltration sequences.

7.4.3.2 Corrosive leach of absorber/basket

To determine f_3 for the condition of a flooded environment, *it is first assumed that the boron and the surrounding stainless steel matrix will leach/dissolve together*. The fastest possible rate for this process was conservatively taken to be the same as the general corrosion rate of Type 316 stainless steel immersed for 16 years in seawater at the Panama Canal, which was found to have experienced a corrosion rate of $1.25 \mu\text{m/yr}^{(5,16)}$. Since the basket can be attacked on both sides this rate is doubled to get a minimum time to corrode 10 mm of Type 316 stainless steel of 4,000 years. The fraction of basket corrosion which can be tolerated depends on the actual SNF characteristics. The basket will have sufficient boron that 20% of the basket can be lost before any of the commercial fuel can exceed the 5% sub-critical safety margin with bias and uncertainty. *The conservative assumption has been made that a loss of 60% of the basket would permit no more than 50% of the expected fuel to exceed the safety margin.* A more precise analysis based the expected characteristics of the commercial fuel discharges is given in section 7.4.4 below, and shows this assumption to be very conservative. This 60%, or 6 mm thickness of basket material, would be removed in no less than 2,400 years of exposure to seawater. This time has been conservatively taken to be the lower limit (θ) of the Weibull distribution for f_3 for the continuous wetting case.

A literature search was performed to locate general corrosion data for Type 316 stainless steel in aqueous environments similar to that which may result on a WP that is continuously wetted by infiltrating water. Information on the corrosion behavior of Type 304 stainless steels was also included because more extensive testing has been performed for Type 304 than 316, and because Types 304 and 316 were found to have relatively similar corrosion rates in tests which included both alloys. The corrosion rate information that was located is shown in Table 7.6, along with the estimated time at each rate to uniformly corrode 6 mm of material from both sides. The mean-time-to-corrode 6 mm of stainless steel in tuff groundwater, J-13 well water, and Solution No. 20 (bottom 7 rows in table) was found to be 19,823 years, with a standard deviation of 8,724 years (calculated using the AVERAGE and STDEVP functions in Microsoft Excel v4.0). Using

this mean-time-to-failure (MTTF), standard deviation, and the value of θ determined in the preceding paragraph, the remaining parameters of the Weibull distribution were determined using the expressions,

$$MTTF = \theta + \alpha \Gamma(1 + 1/\beta) \quad (14)$$

and,

$$\sigma = \alpha \sqrt{\Gamma(1 + 2/\beta) - [\Gamma(1 + 1/\beta)]^2} \quad (15)$$

where $\Gamma(n)$ is the gamma function evaluated at n . The parameters, α and β , were found to be 19,671 and 2.098, respectively, by solving the above system of two equations and two unknowns using Mathcad+ v5.0. The calculation is presented in its entirety in Attachment I. These parameters were used to define the Weibull distribution for time to 60% absorber leach from continuously wetted basket material.

The 60% neutron absorber leach pdf for the intermittent wetting case was developed by modification of the above lower limit, mean-time-to-corrode, and standard deviation developed for continuously wetted stainless steel. As before, this modification was based on the results of general corrosion test data for Types 304 and 316 stainless steel, and a further search of the available literature was performed to locate corrosion tests of intermittently wetted samples. *This test condition was assumed to be more applicable to overhead dripping than that of the continuous immersion tests used for flooding, because the level of water in the basket of a breached WP may change with time due to fluctuations in the drip rate, evaporation rate, or the formation of drainage holes.* One study of Type 316 stainless steel placed at the mean tide level of the Panama Canal (seawater) for 16 years was found to have experienced a corrosion rate of $0.16 \mu\text{m}/\text{yr}$ ^(5,16). Another test that was performed for 304L stainless steel in aerated simulated J-13 well water at 90°C for 1.5 years determined general corrosion rate to be $<0.005 \mu\text{m}/\text{yr}$ through measurements of weight loss^(5,23). In this test, the solution was allowed to evaporate, and new solution was added on a weekly basis. Comparison of the above test results with the immersion data in Table 7.6 reveals that the intermittently wetted corrosion rates may be an order of magnitude lower than those for complete immersion under the same conditions. *Therefore, it is assumed that doubling of the flooding leach lower limit, MTTF, and standard deviation should result in a conservative distribution of the time to corrode 6 mm of material (thus leaching 60% of the boron).* Doubling of the above mentioned parameters results in a θ of 4800 years, a MTTF of 39,646 years, and a standard deviation of 17,448. Using the Weibull expressions for MTTF and standard deviation presented in the flooding breach and leach discussion, α and β were determined to have values of 39343 and 2.098, respectively, using Mathcad+ v5.0. This calculation is also presented in its entirety in Attachment I.

The Weibull leach distribution, f_3 , parameters for the two basic environmental conditions, intermittent and continuous wetting of the basket are summarized in Table 7.5 below.

The continuous and intermittent wetting distributions described by these parameters are shown in Figures 7.10 and 7.11, respectively.

Table 7.5. Summary of Weibull Parameters for Absorber Leach PDFs

Condition	α	β	θ
Intermittent Wetting	39343	2.098	4800
Continuous Wetting	19671	2.098	2400

Although the deterministic component of general corrosion is evident, the following aspects of the random component of the process should be noted in justification of the use of a probability distribution:

1. Wide distribution of corrosion rates in the literature, even for seemingly similar water chemistry.
2. Experimental observations typically show corrosion rates which decrease with time on any given sample due to passivation. Random convective mixing within the filled package may remove this passive layer from some areas, leaving fresh surface for more rapid corrosion.
3. Temperature variations from one package to another will lead to different convection rates, which cause variations in corrosion rates according to the previous item. Package to package variations in convection rate will also cause variations in boron concentration remaining near the leaching basket material, where it can still be an effective, criticality suppressing, neutron absorber.
4. There will be local differences in water chemistry from one waste package interior to another, due to differences in travel paths through the partly corroded containers.
5. There are many tests in freshwater (lake and river) which show no measurable corrosion of Type 316 stainless steel for exposure times up to 16 years, suggesting that there is a significant tail on the high side of the distribution.
6. In order to permit criticality, the leached boron must be removed from the interior volume of the waste package, either by water flow out large holes, or by plating on the inner package walls as the water seeps through some slowly flowing leak. Both of these are random processes.

Pdf for flood leach of absorber/basket (f_3 for climate & tectonic)

Sequences involving flooding of the emplacement drift would result in the flooding of the interior of a breached WP, thus continuously wetting the basket material. Therefore, the Weibull pdf for continuous wetting developed above will be used as the waste package leach distribution, f_3 , for the flooding sequences.

Pdf for low infiltration leach of absorber/basket (f_3 for wpb&ldl)

Sequences involving water dripping onto a breached WP, as a result of low infiltration, would not be expected to immediately fill the interior of the package. Many factors, including the rate of water flow into the WP and the interior temperature, will control the internal water level. *For this reason, it is assumed that the basket material will not be continuously wetted.* Therefore, the Weibull pdf for intermittent wetting developed above will be used as the waste package leach distribution, f_3 , for the low infiltration sequences.

Pdf for high infiltration leach of absorber/basket

Sequences involving water dripping onto a breached WP, as a result of high infiltration, would not be expected to immediately fill the interior of the package. Many factors, including the rate of water flow into the WP and the interior temperature, will control the internal water level. *For this reason, it is assumed that the basket material will not be continuously wetted.* Therefore, the Weibull pdf for intermittent wetting developed above will be used as the waste package leach distribution, f_3 , for the high infiltration sequences.

7.4.4 Probability of sufficient fissile material in a package

After all the hazard events that are necessary for a criticality event (WP breach, absorber leach, and internal flooding) have occurred, there is still one fundamental requirement for each scenario: the SNF must have the right combination of high enough fissile material and low enough burnup to become critical. The criticality capability is determined by k_{eff} . Deterministic neutronics calculations of k_{eff} for a range of values for age, for specific burnup and initial enrichment indicate that after emplacement, most assemblies will have a peak in criticality potential at approximately 10,000 years. In particular, 21 PWR assemblies having 3% initial enrichment and 20 GWd/MTU burnup (waste package criticality design basis fuel) in a waste package design with stainless steel basket, will have a peak $k_{eff}=0.965$ at 10,000 years which is followed by a slow decline to $k_{eff}=0.932$ at 200,000 years (Ref. 5.7, Figure 6.8.3-5). The physical requirement to avoid criticality is $k_{eff} < 1.0$. For licensing calculations it is usually required that $k_{eff} \leq 0.95$, which provides a 5% safety factor. In addition, there is usually an additional amount (typically up to 0.06) to be subtracted for bias and error. For this analysis the dividing line for determining criticality is $k_{eff}=0.95$. This provides a conservative probabilistic estimate of what will actually happen, but not, necessarily conservative enough to license a waste package with respect to a deterministic estimate of worst case performance.

To determine the fraction of the packages which will have $k_{\text{eff}} \geq 0.95$, we use the Design Basis Fuel Analysis^(5.25) which tabulated SNF statistics with respect to k_{∞} using a parameterization of k_{∞} developed by ORNL^(5.26) for PWR fuel using 210 SCALE runs that covered a representative range of values of age, burnup, and initial enrichment. In this tabulation an age of 5 yrs was used. The correspondence between k_{∞} and k_{eff} is then determined by calculating k_{∞} from the formula given by ORNL^(5.26) for the design basis fuel (age=5 yrs, burnup=20 GWd/MTU, initial enrichment=3%), with the result $k_{\infty}=1.138$. An MCNP calculation showed this criticality design basis fuel to have a k_{eff} approximately equal to 0.98, so the difference between k_{∞} and k_{eff} is 0.158. We now interpret Ref. 5.7, Figure 6.8.3-5, as follows: (1) for times of interest (2,000 to 200,000 years) determine the difference between 0.95 and k_{eff} , (2) add that difference to 1.138 to determine the k_{∞} which would correspond to a $k_{\text{eff}}=0.95$, (3) consult the tabulation of k_{∞} percentiles in Ref. 5.25 to determine the percentage of SNF which would have a higher k_{∞} . The results are given in Figure 7.12. This curve is fitted to an 8th order log polynomial in the Mathcad worksheet and used as a multiplier on each of the three conditional breach and leach pdf's produced in section 7.4.5, to determine the corresponding breached, leached, and capable of criticality cdf.

An external criticality event would be expected to require a longer time (more waste package barrier corrosion, and extensive breaching of the fuel element cladding) than the internal criticality event sequences discussed thus far. Hence the probability of occurrence is correspondingly smaller, and has not been extensively studied thus far. Nevertheless, since this is an important topic, the final draft of this document will contain an estimate of the probability of the fuel being reconfigured into a flat plate mixture with moderator (water), and the k_{eff} which could result.

7.4.5 Evaluations of two-fold convolutions of pdf's

The pdf for the combined flow, breach and leach events was obtained from the convolution of f_1 , f_2 and f_3 . This convolution was computed by a Monte-Carlo numerical integration, performed in a Mathcad+ v5.0 worksheet, to randomly sample the cdf for each distribution and sum the times to reach the defined flow (or flood) condition, to breach the waste package and to leach 60% of the boron. The resulting pdf was then multiplied by the criticality capable curve defined in section 7.4.4 to determine the probability that a package will be breached, leached and capable of criticality at a given time. 250,000 trials were performed for each Monte-Carlo run. The fluctuations in the pdf are due to the random nature of the Monte-Carlo process. The conditional probability that a WP has breached, leached and is criticality capable by a given time for a given initiating event is obtained by numerically integrating the pdf. Five runs were performed to account for the Monte-Carlo fluctuation in the pdfs and the results were averaged to obtain better statistical estimates of the conditional probabilities. Probabilities of occurrence for each of the three conditional breach, leach, and criticality capable event sequences at 10,000, 20,000, 40,000, and 80,000 years, are summarized in Table 7.7, and in Attachment I for the five runs that were performed. The conditional probabilities

associated with sequences initiated by flooding, are represented by the acronyms *climate* and *tectonic*. Conditional probabilities for sequences initiated by low and high infiltration are represented by the acronyms *wpb&ldl* and *wpd&ldh*, respectively.

As discussed previously, due to apparently conflicting theories on the pitting corrosion behavior of Alloy 825, it was also decided to investigate a worst-case scenario in which the waste package barriers were penetrated in a relatively short period of time compared to the other events in the sequence. This was performed for each of the three event sequences by simply eliminating f_2 from the convolution, effectively producing conditional breach and leach distributions which consider the barrier to be instantly breached upon the occurrence of the initiating event. The convolutions were performed using the Mathcad worksheet in the same manner as above, and are also contained in Attachment I. The conditional probabilities for this no-barrier credit case are also given in Table 7.7.

7.4.6 Probability of sufficient moderator (holes)

For the overhead dripping scenarios, there must be holes around the middle of the package, but not the lower part. The most likely location is on the upper surface which is most exposed to dripping water. *The conditional probability of such a hole configuration, given that there is sufficient corrosion to produce the holes in the first place, is assumed to be the product of the conditional probability of holes around the middle (0.1) and the conditional probability of no holes in the lower half, given that there are holes around the middle (0.1).* This latter probability is actually quite conservative, since half of the weld around the lid will be in the lower, submerged, half of the horizontal package, and this weld is more likely to corrode and leave a hole to prevent ponding. On the other hand, there is a possibility that the leached/corroded material could plug up such holes, so that subsequent ponding could be supported even if the initial hole configuration were not favorable to ponding. This analysis will be refined in the next few years; by the time of license application it will include:

- More precise modeling of corrosion from dripping, particularly in welds.
- Fluid dynamic modeling of leach and ponding processes, including the effects of alternative hole configurations.
- Deterministic evaluation of criticality for likely flooding and assembly geometry configurations.

7.4.7 Probability that Fuel Assemblies Maintain Geometry Required For Criticality (geometry)

Since criticality of SNF assemblies will require nearly full moderation, there can be no criticality if the basket and assembly hardware fail in such a way that the fuel rods can collapse into a consolidated configuration which does not permit sufficient water between the rods. Such a collapse would generally require the corrosion of the fuel cladding or grid spacers in each assembly. *It is conservatively assumed that the fuel assemblies will*

always maintain a geometry which supports optimal moderation for the time frame covered by the current analysis. Therefore, this event has a probability of 1.0. This analysis will be refined in the next few years; by the time of license application it will include:

- More precise modeling of the fuel assembly structural failure distribution following loss of the inert environment;
- Deterministic evaluation of the criticality potential of other possible geometries which could be formed prior to complete degradation of the waste package structure.

Table 7.6. General Corrosion Data For Types 304 & 316 Stainless Steel

Stainless Steel Type	Test Environment	Test Temp (C)	Test Duration (years)	Corrosion Rate ($\mu\text{m}/\text{yr}$)	Time To Corrode 6mm (y)	Ref.
316	Seawater Immersion	≈27	16	1.25	2,400	5.16
316	Seawater Immersion	≈27	1	14.99	200	5.16
316	Seawater Mean Tide	≈27	16	0.16	18,750	5.16
316L	J-13 Immersion	50	1.3	0.154	19,481	5.21
304L	J-13 Immersion	50	1.3	0.133	22,556	5.21
304L	J-13 & 6E5 rads/hr	28	1	0.0811	36,991	5.21
304L wld	J-13 & 6E5 rads/hr	28	1	0.123	24,390	5.21
304L	J-13 Immersion	90	0.22	0.29	10,344	5.17
304L	Sol. 20 Immersion	90	0.33	0.2	15,000	5.17
304L	Tuff Groundwater at 3E5 & 6E5 rads/hr	?	0.15	0.3	10,000	5.20

Table 7.7. Summary of Fault Tree Event Probabilities For Various Times Since Emplacement

Time Emplaced (years)	Basic and Conditional Event Probabilities					
	holes	crackswp	geometry	climate & tectonc	wpb&ldl	wpb&ldh
<i>WP Barriers Provide Temporary Protection Against Moderator Entry</i>						
10,000	1.00x10 ⁻²	6.95x10 ⁻²	1.00	0	0	0
20,000	1.00x10 ⁻²	6.95x10 ⁻²	1.00	0	0	1.16x10 ⁻⁵
40,000	1.00x10 ⁻²	6.95x10 ⁻²	1.00	7.89x10 ⁻⁸	6.90x10 ⁻⁶	1.43x10 ⁻³
80,000	1.00x10 ⁻²	6.95x10 ⁻²	1.00	1.20x10 ⁻⁶	2.48x10 ⁻²	1.44x10 ⁻²
<i>WP Barriers Given No Credit For Preventing Moderator Entry</i>						
10,000	1.00x10 ⁻²	6.95x10 ⁻²	1.00	0	9.00x10 ⁻⁵	3.68x10 ⁻⁶
20,000	1.00x10 ⁻²	6.95x10 ⁻²	1.00	0	3.13x10 ⁻³	2.45x10 ⁻⁴
40,000	1.00x10 ⁻²	6.95x10 ⁻²	1.00	1.62x10 ⁻⁷	2.22x10 ⁻²	3.29x10 ⁻³
80,000	1.00x10 ⁻²	6.95x10 ⁻²	1.00	1.55x10 ⁻⁶	4.71x10 ⁻²	1.85x10 ⁻²

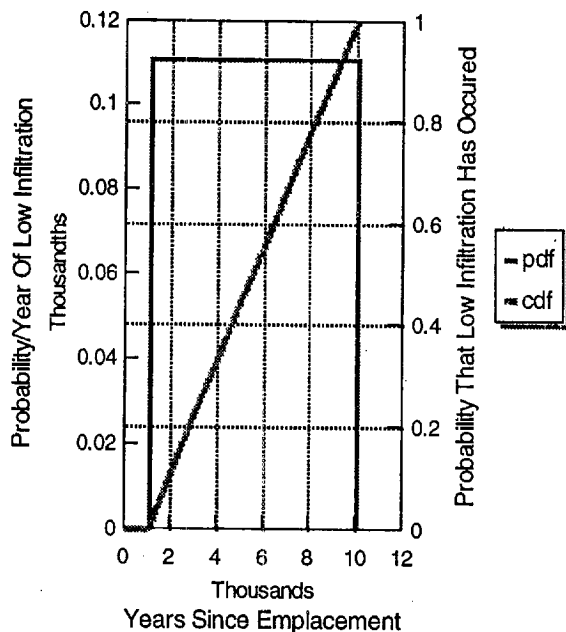


Figure 7.4. Distribution of time-to-occurrence of the low infiltration initiating event

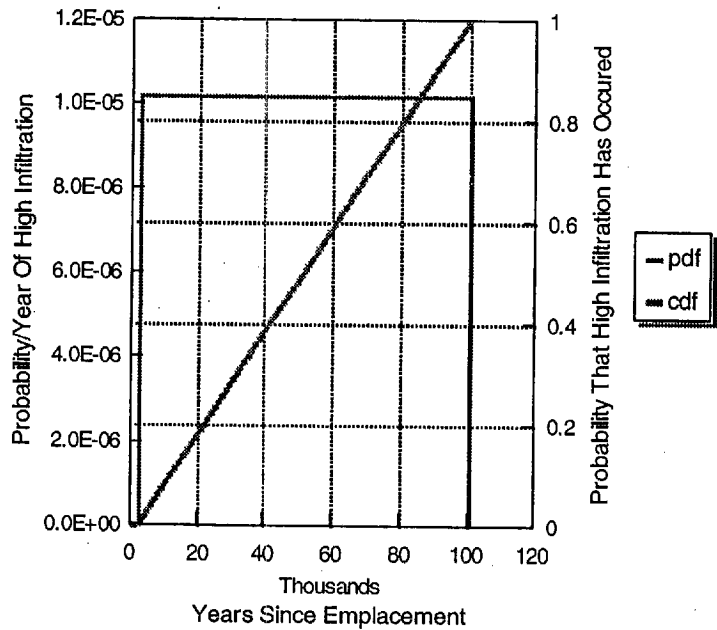


Figure 7.5. Distribution of time-to-occurrence of the high infiltration initiating event

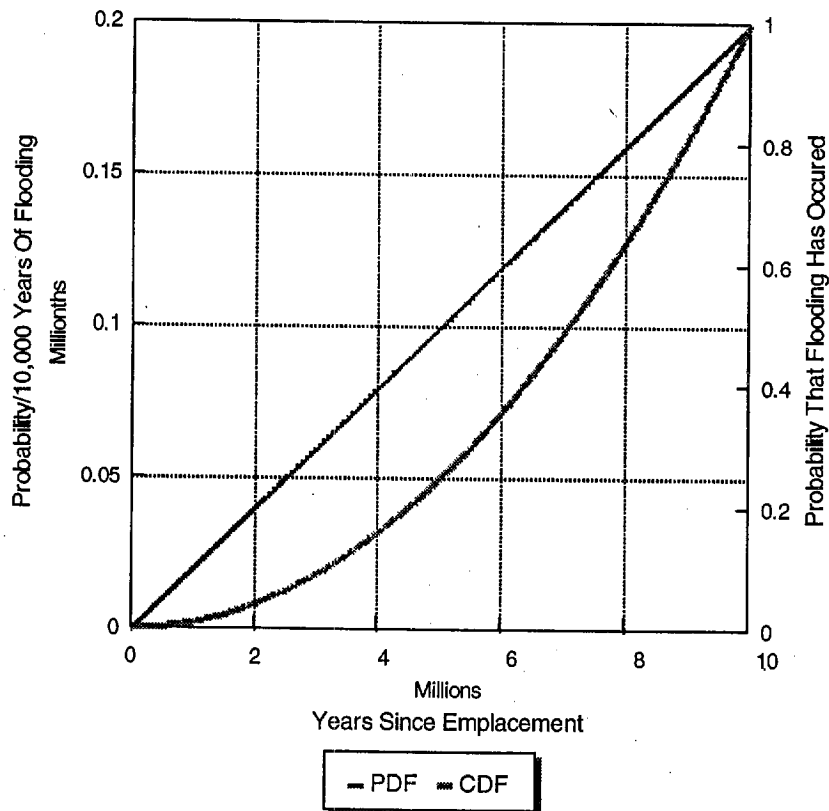


Figure 7.6. Distribution of time-to-occurrence of repository flooding

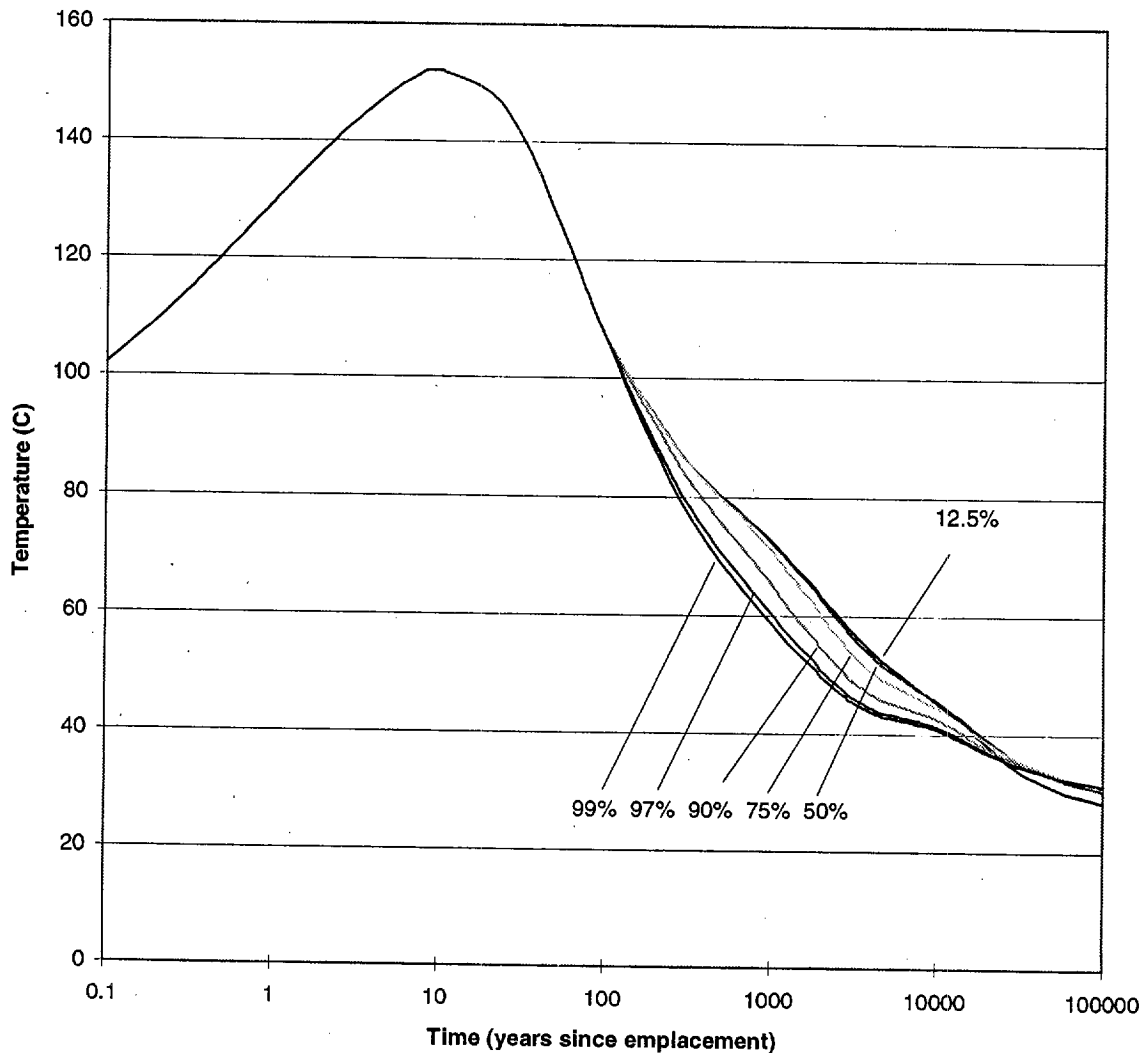


Figure 7.7. Waste Package surface temperature as a function of time for a mass loading of 6.0 kg U/m² (approximately 24 MTU/acre), curves are for different locations in the repository (0% - center, 25% - mid-way from center to edge, 100% - edge)

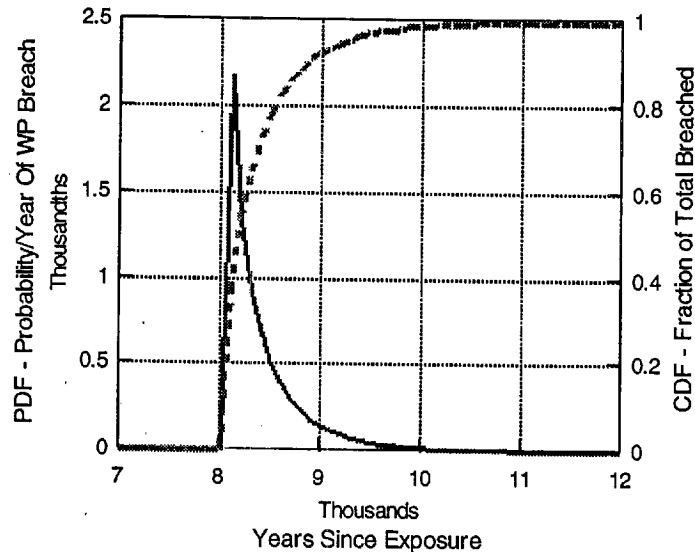


Figure 7.8. Distribution of WP breach failures developed using McCoy's model and parameters for continuous wetting

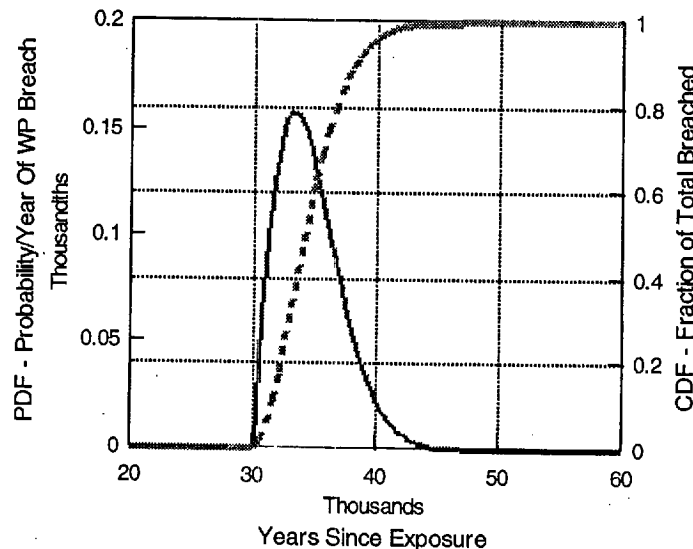


Figure 7.9. Distribution of WP breach failures developed using McCoy's model and parameters for intermittent wetting

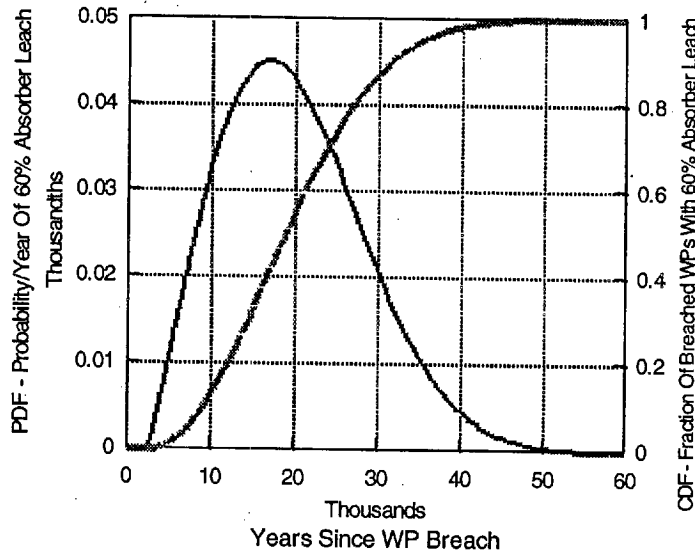


Figure 7.10. Distribution of time to leach 60% of neutron absorbing material from UCF-WP basket structure for continuously wetted conditions.

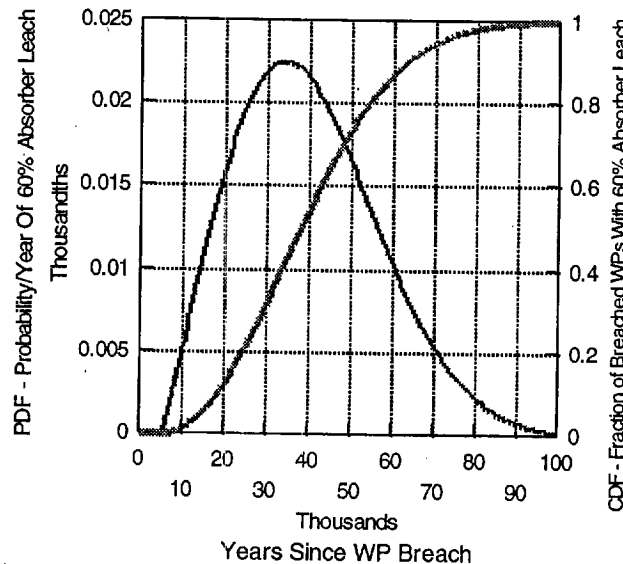


Figure 7.11. Distribution of time to leach 60% of neutron absorbing material from UCF-WP basket structure exposed to intermittent wetting conditions.

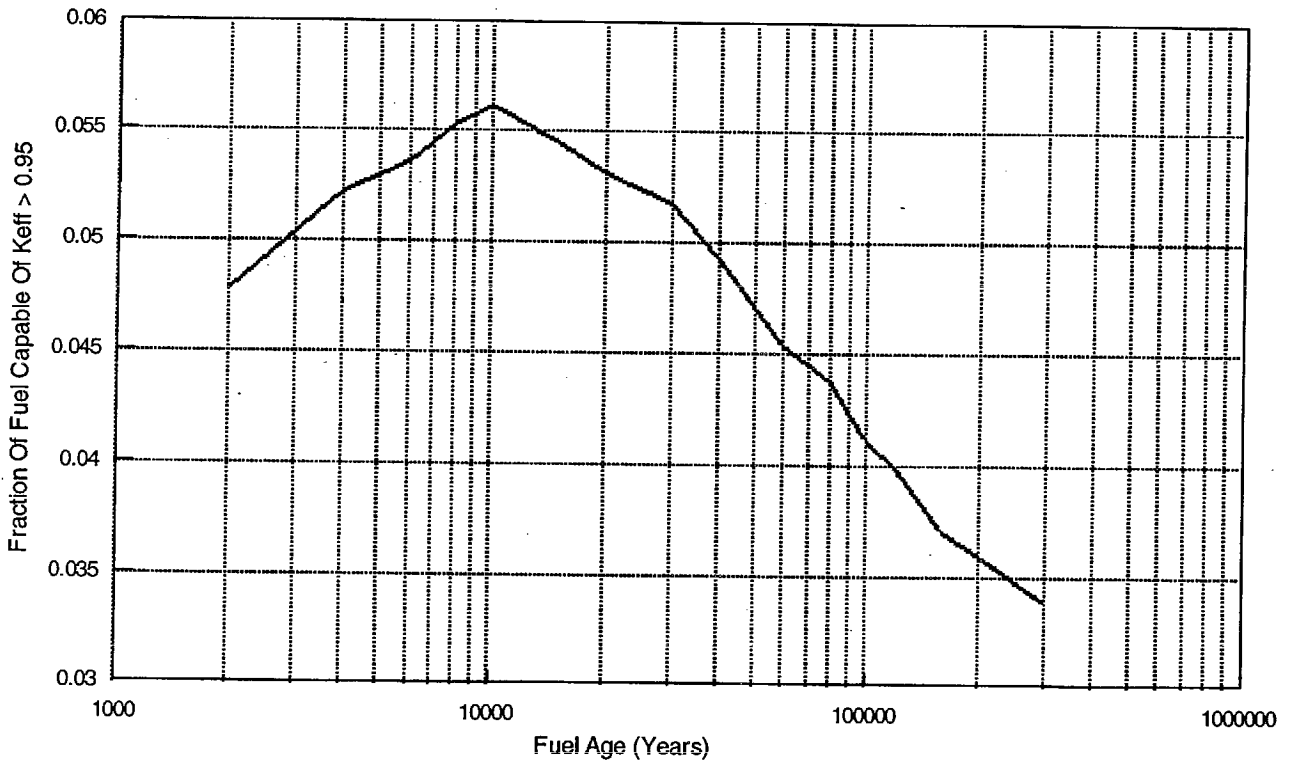


Figure 7.12. Fraction of design basis fuel (3% initial enrichment, 20 GWd/MTU Burnup) as a function of time capable of achieving $k_{eff} > 0.95$ in an UCF-WP geometry with no neutron absorber in the basket structure

7.5 Fault Tree Analysis

In this section, the basic and time dependent conditional event probabilities developed in Section 7.4 are input into the fault tree developed in Section 7.3. The fault tree was evaluated at the times after emplacement for which conditional event probabilities were quoted in Table 7.7. Since all basic event probabilities are on a per package basis, and all conditional probabilities are dimensionless, the fault tree top event will also be in terms of a criticality probability per package at a given point in time. This differs from the typical top event units for a fault tree of an active system of components, (such as a nuclear power plant safety system) which is usually expressed as a system failure rate or a probability of system failure in a given mission time. This is appropriate when the failure rates of the system components can be treated as constants and the mission time is relatively short when compared to the mean-time-to-failure of the components. However, when the majority of events are conditional on other events and have time dependent failure rates, as is the case in the current analysis, it is more useful to express the top event as a cumulative probability of occurrence at specific points in time. Evaluating the fault tree at various times will then produce a cumulative distribution for the occurrence of the top event (i.e., waste package criticality).

The fault tree cutset (sequences of events) probabilities were determined using Excel v4.0 and the top event was quantified by summing the cutset probabilities. Results of the quantification of the fault tree top event at each of the previously selected timesteps is given in Table 7.8. The individual cutsets which make up the top event probability, and their contribution to the top event is also shown. Table 7.8 also provides the results of the quantifications performed for the alternate "no-barrier" scenarios, which are intended to provide an upper bound criticality probability to address the uncertainty in barrier performance which currently exists. Figure 7.13 displays the cumulative per-package criticality probability as a function of time for both the barrier and no-barrier scenarios (TBV). The number of waste package criticalities expected to occur by a given time can be approximated from this plot simply by multiplying the cumulative probability at that time by the number of packages.

Table 7.8. Summary of Top Event Probabilities and Cutsets for UCF WP

Time (Years)	Top Event Probability	Cutset Probabilities and Event Sequences			
		(with Barrier Credit)			
10,000	0	All sequences are estimated to have an infinitesimally small (zero) probability of occurrence.			
20,000	8.07E-09	8.07E-09	CRACKSWP	GEOMETRY	HOLES WPB&LDH20K
40,000	1.15E-06	9.92E-07	CRACKSWP	GEOMETRY	HOLES WPB&LDH40K
		4.80E-09	CRACKSWP	GEOMETRY	HOLES WPB&LDL40K
		7.89E-08	TECTONC40K	GEOMETRY	
		7.89E-08	CLIMATE40K	GEOMETRY	
80,000	2.96E-05	1.72E-05	CRACKSWP	GEOMETRY	HOLES WPB&LDL80K
		1.00E-05	CRACKSWP	GEOMETRY	HOLES WPB&LDH80K
		1.20E-06	TECTONC80K	GEOMETRY	
		1.20E-06	CLIMATE80K	GEOMETRY	
(without Barrier Credit)					
10,000	6.51E-08	6.26E-08	CRACKSWP	GEOMETRY	HOLES WPB&LDL10K
		2.56E-09	CRACKSWP	GEOMETRY	HOLES WPB&LDH10K
20,000	2.34E-06	2.17E-06	CRACKSWP	GEOMETRY	HOLES WPB&LDL20K
		1.70E-07	CRACKSWP	GEOMETRY	HOLES WPB&LDH20K
40,000	1.80E-05	1.54E-05	CRACKSWP	GEOMETRY	HOLES WPB&LDL40K
		2.28E-06	CRACKSWP	GEOMETRY	HOLES WPB&LDH40K
		1.62E-07	TECTONC40K	GEOMETRY	
		1.62E-07	CLIMATE40K	GEOMETRY	
80,000	4.86E-05	3.27E-05	CRACKSWP	GEOMETRY	HOLES WPB&LDL80K
		1.28E-05	CRACKSWP	GEOMETRY	HOLES WPB&LDH80K
		1.55E-06	TECTONC80K	GEOMETRY	
		1.55E-06	CLIMATE80K	GEOMETRY	

Originator: J.R. Massari

Checker: L.E. Booth

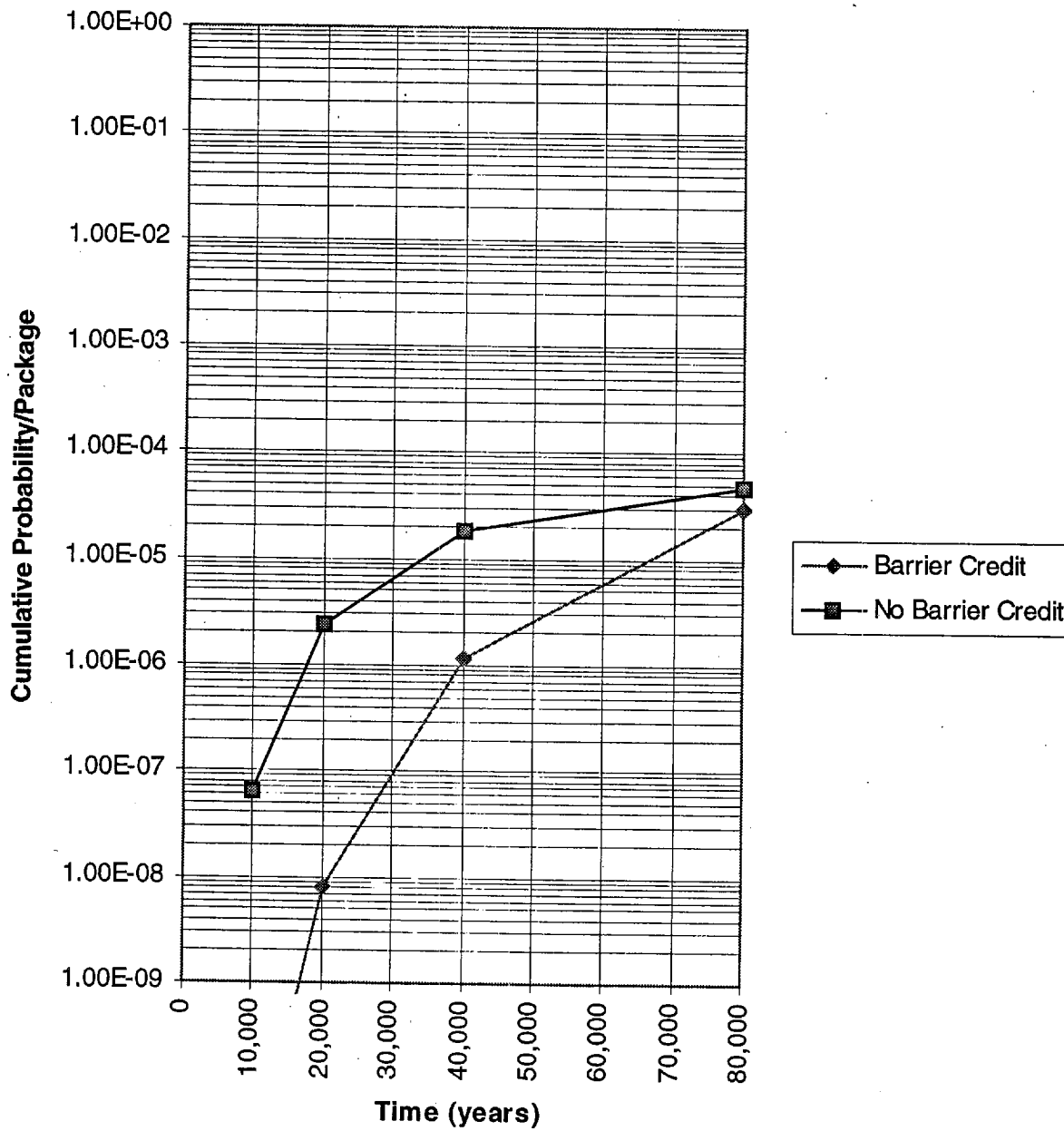


Figure 7.13. Cumulative per-package criticality probability for various times since emplacement with and without credit for the WP barriers (TBV).

8. Conclusions

This design analysis has demonstrated a process for estimating the probability of waste package criticality as a function of time, which is described in Section 7. In particular, Section 7.4 describes a methodology for estimating the probabilities and pdf's of the events which are essential to the production of a criticality. We have used the established process to estimate the probability of criticality as a function of time since emplacement for the uncanistered fuel waste package (UCF-WP); the results are summarized in the cdf's shown in Figure 7.13. The cutsets presented in Table 7.8 identify the dominant sequences leading to waste package criticality.

It is obvious from a review of the cutsets presented in Table 7.8 that the dominant sequences contributing to the rise in the probability of criticality during the first 80,000 years are those involving water dripping on a waste package from an overhead fracture. As mentioned previously in the discussion on fracture frequency in section 7.4, information from the STRIPA validation drift suggests that flowing fractures primarily occurred in regions of high fracture density. Actions taken to identify and avoid placement of waste packages in such areas would significantly reduce the probability that a waste package would be located under such a fracture, and thus reduce the rate and degree to which the overall waste package criticality probability rises in the first 80,000 years. These conclusions however, are subject to validation and/or refinement of the assumptions made in the analysis regarding flowing fracture frequency.

It is also evident from the cdf's shown in Figure 7.13 that the rate at which the barrier is assumed to be breached has a significant effect on the rate at which the criticality probability rises over the first 80,000 years, but little effect thereafter. The effect in the early years is primarily due to the uncertainty in the time-to-breach of the waste packages located below flowing fractures. However, in the later years, further increases in the probability of waste package criticality are primarily governed by the occurrence of events which produce repository flooding. As the time frame for occurrence of these events is on the order of several million years, and the range uncertainty in barrier performance spans at most only a few thousand years, there is little effect on the overall probability of criticality due to sequences initiated by flooding. It should be noted that the probability of criticality continues to slowly rise beyond 80,000 years, reflecting the increasing probability of repository flooding and the assumption that the fuel assembly geometry always remains intact. Future analyses which include external and altered fuel configuration criticality sequences may affect the results for later years.

Finally, the current analysis treated both UCF-WP basket designs identically, by assuming that there was a single 10 mm thickness of borated stainless steel absorber material between assemblies. In section 7.4.3.2, it was assumed that the boron would be leached out of the stainless steel matrix as it corroded from both sides by the process of general corrosion. This assumption is valid for the ILB UCF-WP design, but may be slightly unconservative for the tube basket UCF-WP design. Due to the fact that this design

employs 5 mm thick tubes, it would present four surfaces where corrosion of the stainless steel (and thus boron removal) could occur. This would have the effect of reducing the MTTF for the absorber leach distributions by a factor of two, thus slightly raising the probability of criticality at a given time. However, as the outside surface of one tube will be very close to the outside surface of the adjacent tube, there may be no credible mechanism for removal of the boron from the tight space, in which case, the above assumption would still remain valid. Also, the corrosion products may eventually plug the gap, preventing water entry and further corrosion between adjacent tubes. Regardless of which of the above scenario's is true, the tube design still remains bounded by the "no-barrier" case presented in section 7.

While this document does not deal with the consequences of the criticality, it should be noted that, all numerical calculations of such processes published to date indicate that the energy release would be limited to boiling of water at atmospheric pressure, similar to the natural reactor which occurred at Oklo several billion years ago. Such a low grade criticality could continue for thousands of years, but simple calculations show that at an expected number of criticalities less than 1, the inventory of radionuclides accumulated by the criticality at any time during such a criticality would be an insignificant fraction of the nuclides already present in the spent fuel inventory of the entire repository.

9. Attachments

Attachment I - Calculation Details

ATTACHMENT I**CALCULATION DETAILS**

CALCULATION OF CORROSION PARAMETERS FOR SECTION 7.4.3.1

Input

Start with Stahl Model detailed in IOC LV.WP.DS.06/93.107 "Waste Package Corrosion Inputs," 6/21/93

$$P = A \cdot t^c \cdot \exp\left(-\frac{B}{T}\right)$$

where P is corrosion penetration depth

t is time in years

T is temperature in K

A is a rate constant with units of mm/yr. IOC recommends 2525 mm/yr for carbon steel.

B is the activation energy (Q) over the gas constant (R). B is in units of K and is indicated to be 2850K for carbon steel.

c is a constant describing protectiveness of passive film. IOC indicates that it typically ranges from 0.5 to 0.8 for Carbon Steel. It specifically details tests in lake water which produced a c of 0.47.

Use of Stahl's model is appropriate for determining parameters as all corrosion data was collected at constant temperature.

Carbon steel

ASM Handbook page 977 Table 22 summary of 1020 carbon steel corrosion in tuff groundwater

Temperature (C)	General Corrosion Rate ($\mu\text{m/yr}$)	Pitting Corrosion Rate ($\mu\text{m/yr}$)
50	401	380
70	505	1018
80	531	465
90	414	1046
100	320	1018

Alloy 825

UCID-21362 volume 2 page 21 "Survey of Degradation Modes of Candidate Materials for High-Level Radioactive Waste Disposal Containers" and NNA.890919.0280 "Metal Corrosion in Deep Ocean Environments"

Temp: 17.2C Corrosion Rate: 1.01 $\mu\text{m/yr}$ Test Duration: 1.06 years
 Environment: Ocean Surface Immersion

NUREG/CR-5598 Table 5.5 "Immersion Studies on Candidate Container Alloys for the Tuff Repository"

Temp: 90C Corrosion Rate: 9.17 $\mu\text{m/yr}$ Test Duration: 2784 hours
 Environment: J-13 Well Water with 4800 ppm H_2O_2

Carbon Steel - Continuous Wetting (Harsh)

ASM Handbook (p. 977 Table 22) gives pitting rates for carbon steel in tuff ground water of approximately 1mm/year for 50-100C range (two low anomalies at 50 & 80C ignored). Test duration was 9 weeks.

Using values for A & B from above IOC of

$$A := 2525 \text{ mm/yr} \quad B := 2850 \text{ K},$$

$$\text{info from ASM Handbook of } t := \frac{9}{52} \text{ yrs.} \quad P := 1 \cdot t \text{ mm,}$$

$$T := 70 + 273 \quad K \quad (\text{midrange})$$

and solving Stahl's equation for c gives,

$$c := \frac{\ln\left(\frac{P}{A \cdot \exp\left(\frac{-B}{T}\right)}\right)}{\ln(t)} \quad c = 0.729$$

Based on this calculation, a c of 0.75 will be assumed for carbon steel for the remaining calculations. This rounding up is conservative because a c of 1 implies a constant corrosion rate and a c of .5 implies a corrosion rate which decreases parabolically with time.

Carbon Steel - Intermittent Wetting (Mild)

The same table in the ASM Handbook also details 9 week general corrosion rates for carbon steel in tuff groundwater of approximately 0.4 to 0.5 mm/yr for temperatures ranging from 50 to 100 C. Using a B of 2850K, the c determined above, and solving Stahl's equation for A gives,

$$c := 0.75 \quad P := .4 \cdot t$$

$$A := \frac{P}{\left[(t^c) \cdot \exp\left(\frac{-B}{T}\right) \right]} \quad A = 1.048 \cdot 10^3$$

Based on this calculation, A will be assumed to be 1000 mm/yr for the intermittent wetting case, in which the dominant mechanism is assumed to be general corrosion.

Alloy 825 - Continuous Wetting (Harsh)

Stahl's equation is essentially an Arrhenius corrosion model and should be applicable to Alloy 825 if the appropriate values can be determined for A, B, and c. However, due to a general lack of information on these values for Alloy 825 in the available literature, the following assumptions will be made:

$B := 5000 \text{ K}$ Since B is an indicator of corrosion resistance across a wide range of temperatures, and higher values imply increased resistance, a value approximately twice that of carbon steel for Alloy 825 is appropriate for a material that is expected to be much more corrosion resistant.

$c := 0.75$ As corrosion resistant materials such as Alloy 825 form very protective passive films, it is expected that this choice for c will be conservative. To add a further degree of conservatism due to the current uncertainty over the pitting corrosion performance of Alloy 825, c will be changed to 1 after 5000 years of exposure.

To determine A, UCID -21362 Volume 2 page 21 indicates that Alloy 825 displayed a corrosion rate of $1.01 \mu\text{m}/\text{year}$ during a 1.06 year test at the ocean surface, and that the corrosion took the form of pitting. This document did not give the temperature of the test, however, the original source document for the test data, NNA.890919.0280 "Metal Corrosion in Deep Ocean Environments," does give the temperature of the test as 17.2 C. Using this information, the above assumptions for B and c, and solving Stahl's equation for A gives,

$$t := 1.06 \quad P := 1.01 \cdot 10^{-3} \cdot t \quad T := 17 + 273$$

$$A := \frac{P}{\left[(t^c) \cdot \exp\left(\frac{-B}{T}\right) \right]} \quad A = 3.15126 \cdot 10^4$$

Since this data was obtained from seawater immersion, it would be expected to represent a conservatively harsh enough environment for the continuous wetting condition.

Alloy 825 - Intermittent Wetting (Mild)

For the intermittent wetting case, corrosion data from a milder environment was desired that could still be considered representative of potential repository conditions. NUREG/CR-5598 reported the results of corrosion testing of Alloy 825 immersed in J-13 well water with 4800 ppm H_2O_2 added to simulate radiolysis. This test, which was performed at 90C for 2784 hours found a pitting corrosion rate of $9.17 \mu\text{m}/\text{year}$. Using this information, the above assumptions for B and c, and solving Stahl's equation for A gives,

$$t := .317 \quad P := 9.17 \cdot 10^{-3} \cdot t \quad T := 90 + 273$$

$$A := \frac{P}{\left[(t^c) \cdot \exp\left(\frac{-B}{T}\right) \right]} \quad A = 6.60164 \cdot 10^3$$

Parameter Summary

The following parameters will be used in McCoy's model to develop time to WP Barrier breach PDFs

	Continuous Wetting			Intermittent Wetting		
	A	B	c	A	B	c
Carbon Steel	2525mm/yr	2850K	0.75	1000mm/yr	2850K	0.75
Alloy 825	31512mm/yr	5000K	0.75	6602mm/yr	5000K	0.75

McCoy model runs on WP HP9000 Opus

Set parameter values in C source code files provided by McCoy

CORRSTEAM for 100 mm Carbon Steel barrier

CORR825 (c = 0.75) and CORR825X (c = 1) for 20 mm Alloy 825 barrier

Compile all source code and use batch file ZOUTER to run CORRSTEAM executable. Follow instructions given by batch file for recording and entering data. Then use batch file ZSC to run CORR825 and CORR825X executables. Copies of source code, batch files, and runs attached for Continuous Wetting case.

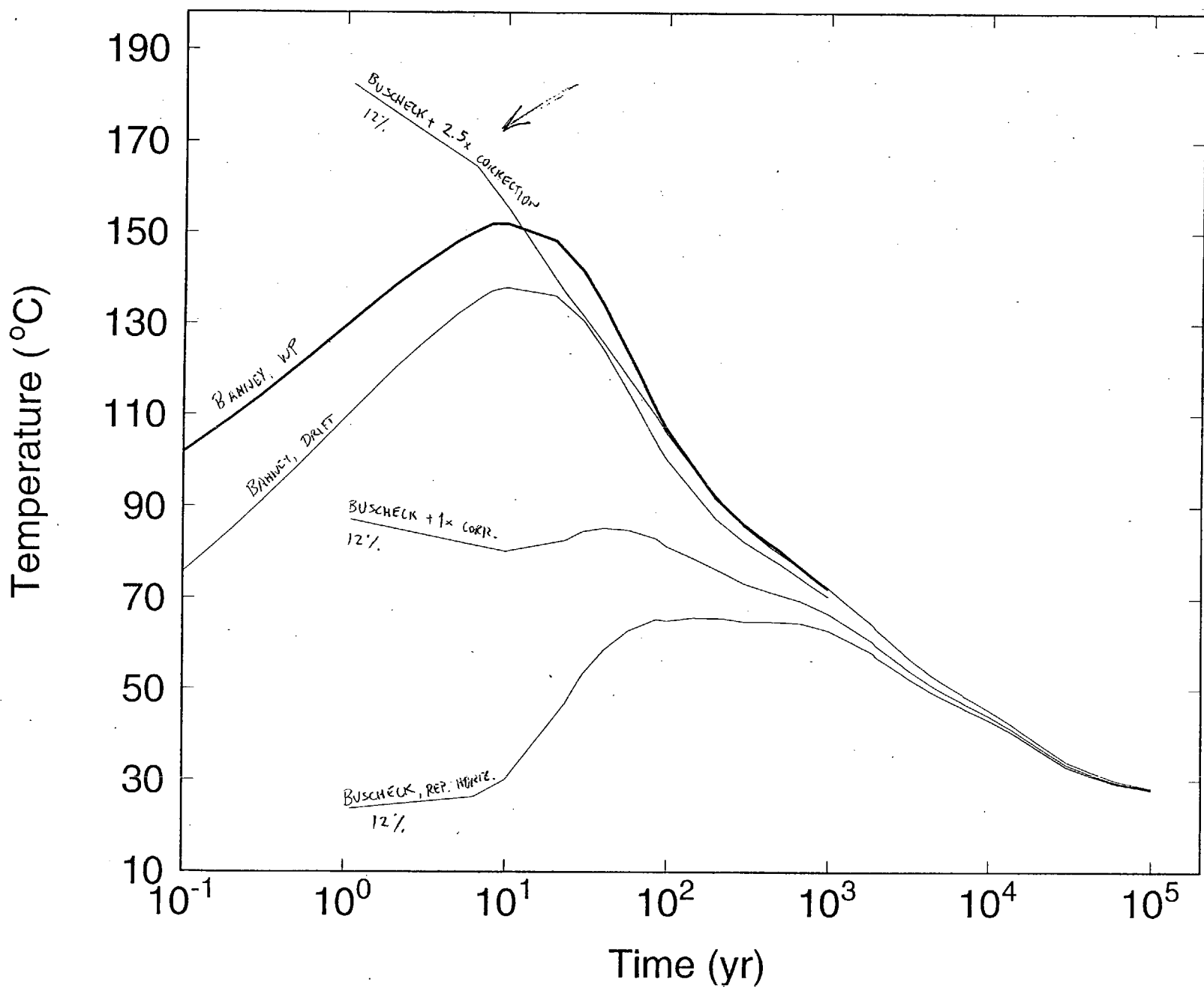
Blended Buscheck/Bahney curves also attached with correction factor to match Buscheck's curves with Bahney's at 100 years indicated by an arrow on each graph.

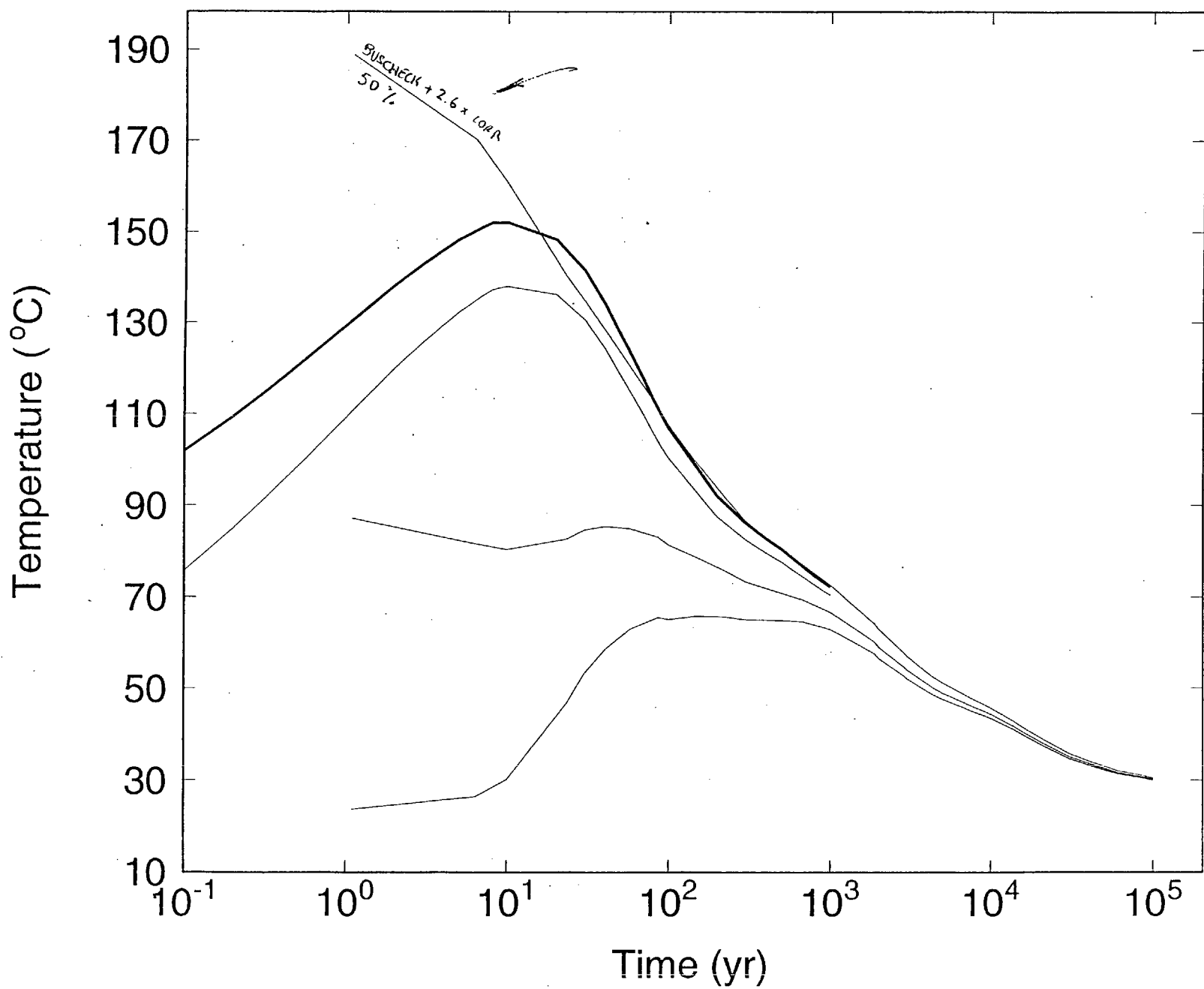
RESULTSContinuous Wetting

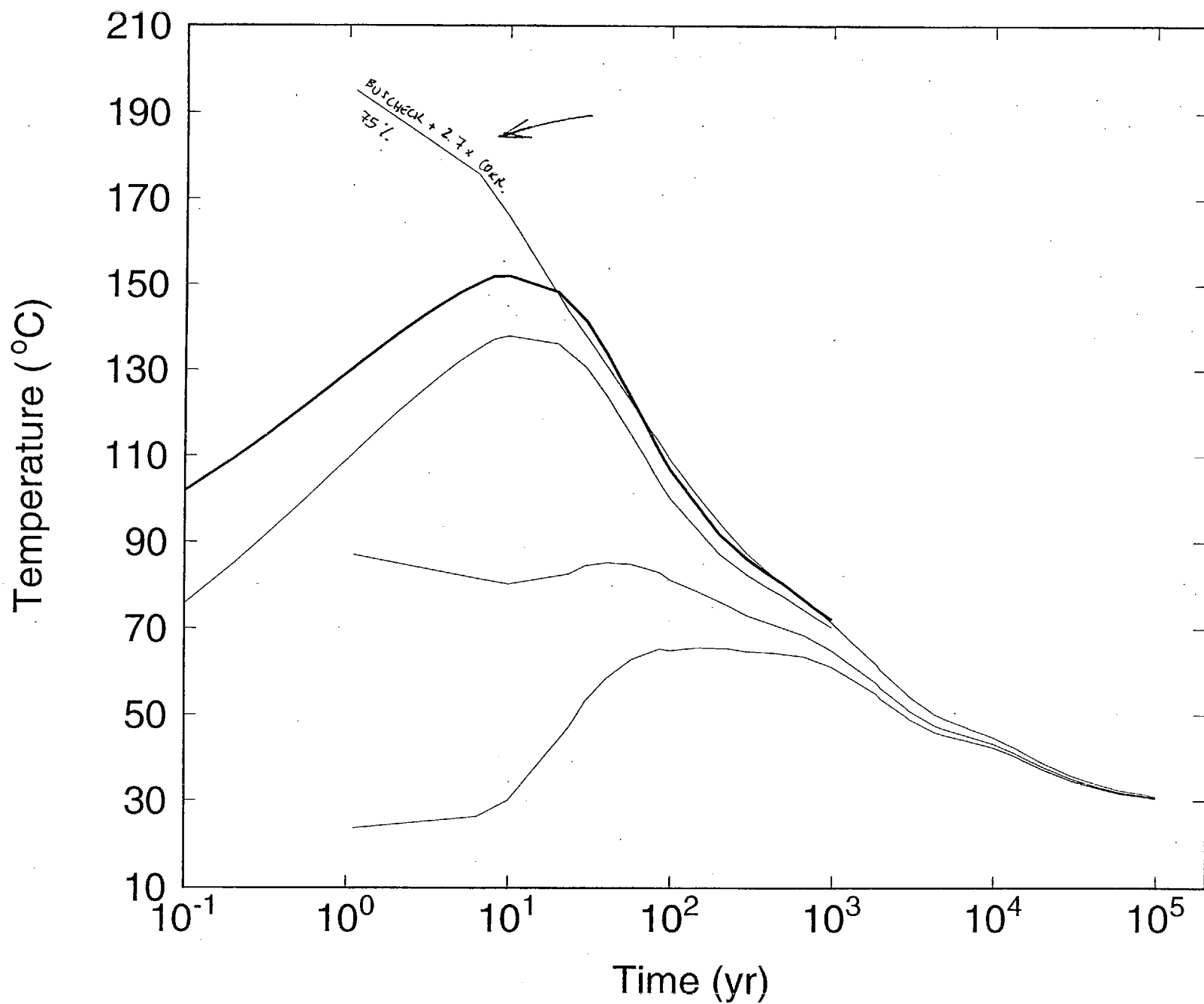
Location	CS Barrier Breach Time (years)	CS & A825 Barriers Breached Time (years)
12.5%	680.994	8188.91
50%	681.133	8250.08
75%	688.413	8594.44
90%	762.016	9348.19
97%	876.544	9960.06
99%	923.987	10174.80

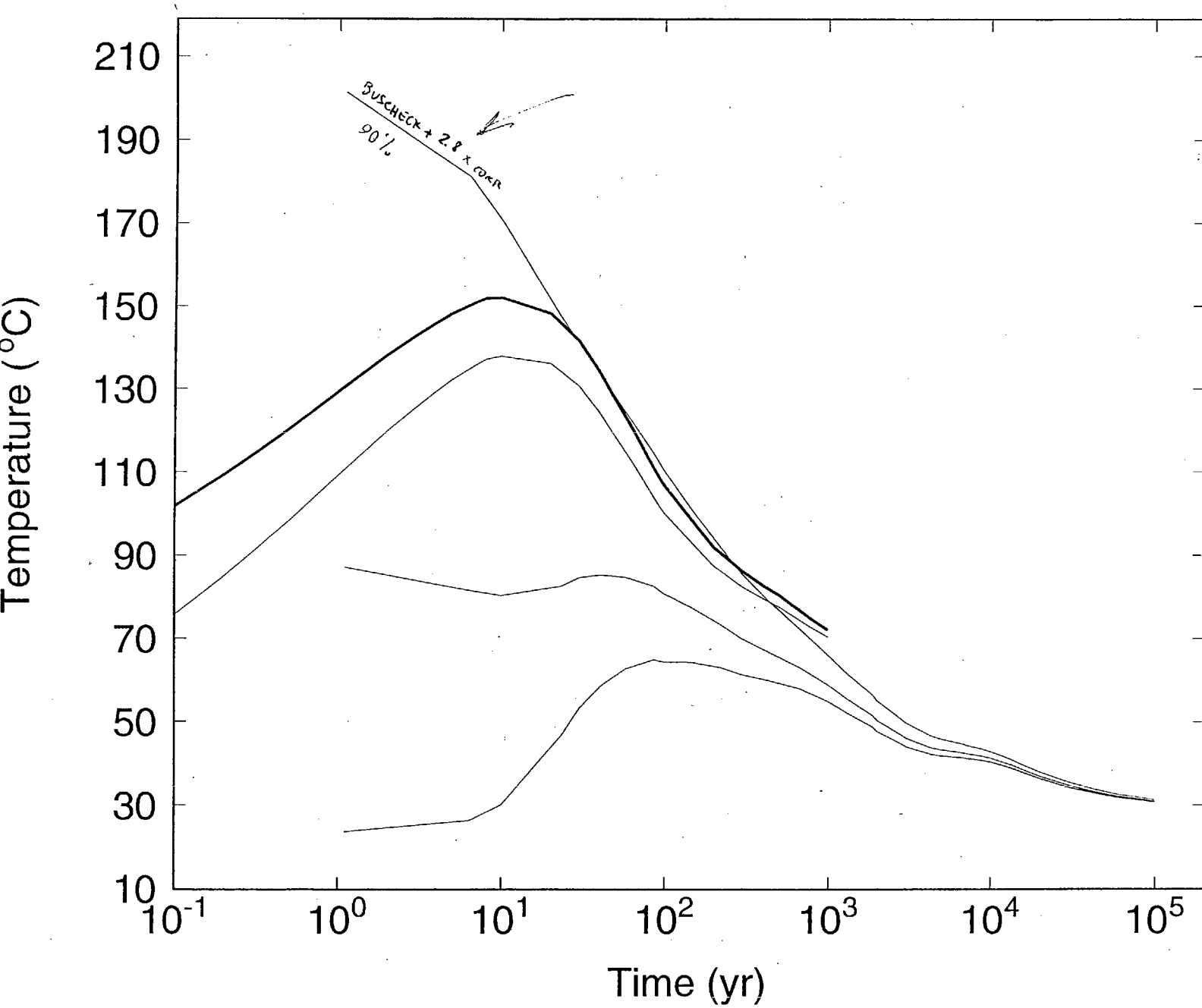
Intermittent Wetting

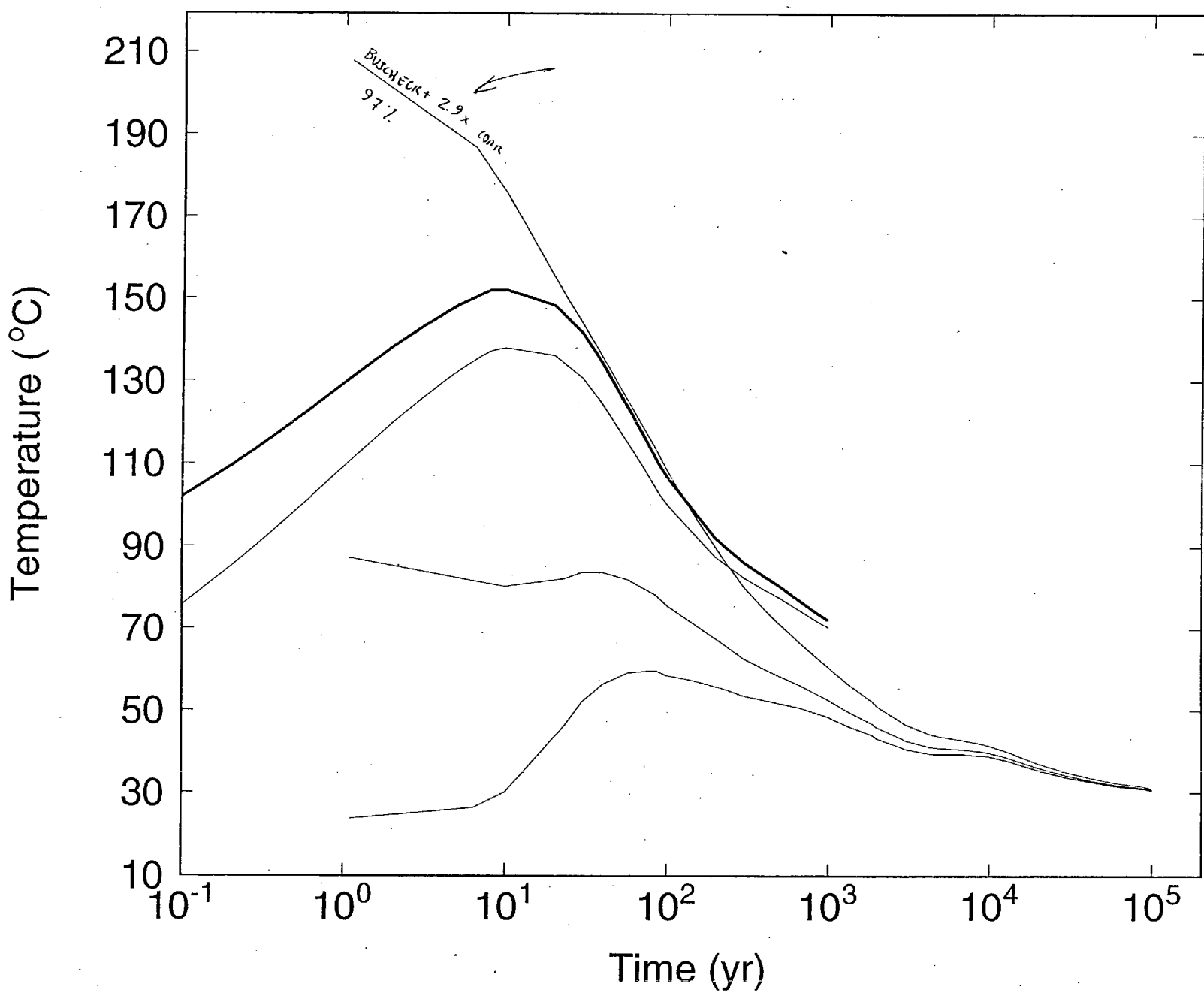
Location	CS Barrier Breach Time (years)	CS & A825 Barriers Breached Time (years)
12.5%	3150.10	34807.3
50%	3198.15	33364.5
75%	3496.40	34850.0
90%	4402.60	38286.2
97%	5279.48	40843.4
99%	5579.66	41665.6

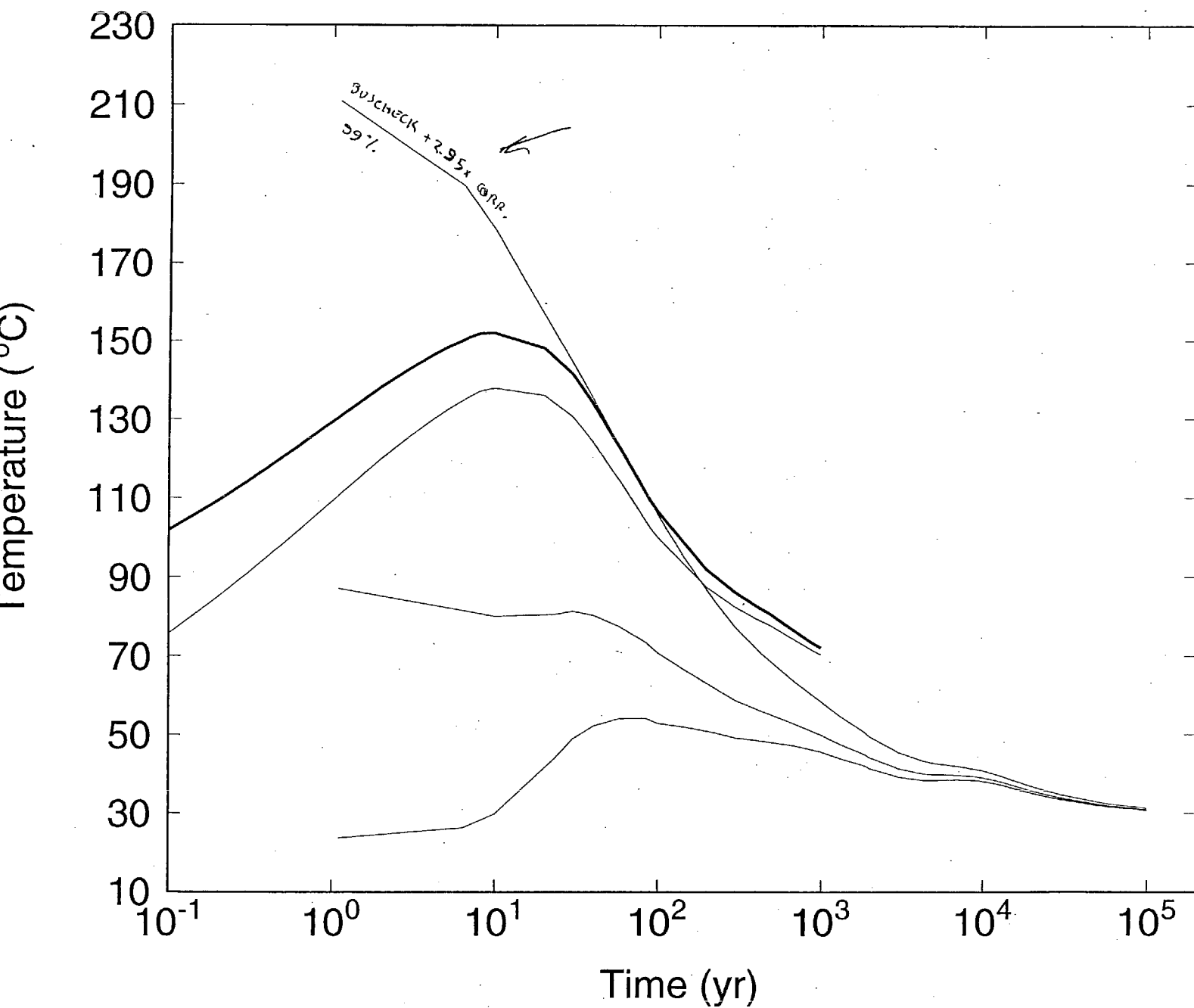












Executable corrstream. and

batch file

to run corrstream is zouter

Location	Time Temp File	CS Barrier Break Time (y)	Temp at break
12.5%	Mix_Temp_1	680.994	
50%		681.133	76.895
75%		688.413	75.952
90%		762.016	69.635
97%		876.544	62.501
99%	Mix_Temp_6	923.980	59.980

Time to fail/ice for Alloy 825 using McCoy's Model

Executables: Corr 825. and for $C = 0.75$ times < 5000 yrs 825
 Corr 825x. and for $C = 1.00$ > 5000 yrs 825
 Exposure

Batch file to run case is zsc

Time to switch $C = CS$ Barrier Break time + 5000

Location	(from zouter) Time< Temp File	CS and 825 Total Barrier Break Time(y)	825 Barrier Break
12.5%	Mix_1. and	8188.91	$- CS$ time = 1507.92
50%		8250.08	7568.95
75%		8594.44	7906.027
90%		9348.19	8586.174
97%		9960.06	9083.516
99%	Mix_6. and	10174.18	9250.813

```
#usage: zouter [data file name] [new time-temperature file]
#example: zouter mix_temp.1 mix.1e
# get wastage for outer barrier as func of time
corrsteam.aud < $1 > zzz
# use vi to dump all but lines the bracket failure time (at 100 mm)
#       echo delete all lines but the two that bracket 100 mm wastage
#       read x
vi zzz
#interpolate to get failure time
cut -f1,3 -d' ' zzz | interp -r -x100 > $2
#show failure time
cat $2
# start again for inner barrier: get copy of input file
cp $1 zzz
# use vi to throw away part of file that applies while outer barrier is intact
#       echo delete all lines but those that bracket the time displayed
#       echo previously
#       read x
vi zzz
# interpolate to get temperature at failure time for outer barrier
cut -f1,2 zzz | interp -x'cat $2'>> $2
sed '$s/$/ 1/' $2 | yoo $2
cat $1 >> $2
#       echo join first two lines, then delete starting on second line
#       echo until the times are monotonically increasing
#       read x
vi $2
```

```
#usage: zsc [data file name] [time to switch c]
#example: zsc mix.1c 5199.2
# treat corrosion of first part of inner barrier (original value of c)
corr825.aud < $1 > zzz
# use vi to grab lines that bracket time for c to switch
    echo delete all lines but the two that bracket the time you specified
    read x
vi zzz
# interpolate to get wastage at time of change...
cut -f1,3 -d' ' zzz | interp -x$2 > zfinal
# and append the time to the same line
echo $2 '\c' >> zfinal
# start again for corrosion after c changes
cp $1 zzz
# use vi to grab lines that bracket time for c to switch
    echo delete all lines but the two that bracket the time you specified
    read x
vi zzz
# and interpolate to get time and temperature at that time
cut -f1,2 zzz | interp -x$2 >> zfinal
sed '$s/$/ 1/' zfinal | yoo zfinal
cp $1 zzz
# now use vi to get rest of temperature history
    echo what should this say
    read delete all lines down to the time you specified
vi zzz
# put it together for corr825x to use
cat zzz >> zfinal
# finally, calculate wastage for second period
corr825x.aud < zfinal > zout
# now use vi to grab lines with wastages that bracket barrier thickness
    echo delete all but the two lines that bracket 20 mm of wastage
    read x
vi zout
# and use interp to calculate failure time (i.e., wastage = 20 mm)
cut -f1,3 -d' ' zout | interp -r -x20
```

```

#include <stdio.h>                                Corrsteam.c
#include <math.h>

#define c_dryox (0.33)
#define c_aqcor (0.75)

#define TEMPERATURE (params[0])
#define OLDTEMPERATURE (params[3])
#define HUMIDITY (params[1])
#define OLDHUMIDITY (params[4])
#define TIME (params[2])
#define OLDTIME (params[5])

main()
{
    double params[6];      /* temperature in K, relative humidity as fracti
    double penet_dryox = 0; /* (penetration due to dry oxidation, mm) to 1/c
    double penet_aqcor = 0; /* (penetration due to aqueous corr., mm) to 1/c

    double dryox();
    double aqcor();
    double romberg();

    scanf("%lf %lf %lf", &OLDTIME, &OLDTEMPERATURE, &OLDHUMIDITY);
    OLDTEMPERATURE += 273.15;

    while (scanf("%lf %lf %lf", &TIME, &TEMPERATURE, &HUMIDITY) == 3) {
        TEMPERATURE += 273.15;
        penet_dryox += (TIME - OLDTIME) *
            romberg(dryox, 0., 1., 5, 1.e-6, (char *)params);
        penet_aqcor += (TIME - OLDTIME) *
            romberg(aqcor, 0., 1., 5, 1.e-6, (char *)params);

        printf("%lf %lf %lf\n", TIME, pow(penet_dryox, c_dryox),
               pow(penet_aqcor, c_aqcor));

        OLDTEMPERATURE = TEMPERATURE;
        OLDHUMIDITY = HUMIDITY;
        OLDTIME = TIME;
    }
    return 0;
}

double dryox(time, argv)
    double time;
    char *argv;
{
    double A = 178.7;
    double B = 6870.0;
    double *dargv = (double *)argv;

    double temperature;

    temperature = time * dargv[0] + (1 - time) * dargv[3];

    return pow(A, 1/c_dryox) * exp(-B / (c_dryox * temperature));
}

double aqcor(time, argv)

```

```
double time;
char *argv;
{
double A = 2525.;
double B = 2850.;
double k = 19.08;
double *dargv = (double *)argv;

double temperature;
double humidity;

temperature = time * dargv[0] + (1 - time) * dargv[3];
if (temperature > 373.15)
    humidity = 95143.074 / exp(24.564 - 4888.587 / temperature);
    /* ^^^^^^^^^^ */
    /* predicted vapor pressure at 373.15 K */
else
    humidity = 1.;

return pow(A, 1/c_aqcor) *
    exp(-k * (1. - humidity) / c_aqcor - B / (c_aqcor * temperature)
}
```

```

include <stdio.h>                               Corr 825.C
include <math.h>

define c_dryox (0.33)
define c_aqcor (0.75)

define TEMPERATURE (params[0])
define OLDTEMPERATURE (params[3])
define HUMIDITY (params[1])
define OLDHUMIDITY (params[4])
define TIME (params[2])
define OLDTIME (params[5])

ain()

double params[6];      /* temperature in K, relative humidity as fracti
double penet_dryox = 0; /* (penetration due to dry oxidation, mm) to 1/c
double penet_aqcor = 0; /* (penetration due to aqueous corr., mm) to 1/c

double dryox();
double aqcor();
double romberg();

scanf("%lf %lf %lf", &OLDTIME, &OLDTEMPERATURE, &OLDHUMIDITY);
OLDTEMPERATURE += 273.15;

while (scanf("%lf %lf %lf", &TIME, &TEMPERATURE, &HUMIDITY) == 3) {
    TEMPERATURE += 273.15;
    penet_dryox += (TIME - OLDTIME) *
        romberg(dryox, 0., 1., 5, 1.e-6, (char *)params);
    penet_aqcor += (TIME - OLDTIME) *
        romberg(aqcor, 0., 1., 5, 1.e-6, (char *)params);

    printf("%.1lf %lf %lf\n", TIME, pow(penet_dryox, c_dryox),
           pow(penet_aqcor, c_aqcor));

    OLDTIME = TIME;
    OLDTIME = TEMPERATURE;
    OLDTIME = HUMIDITY;
    OLDTIME = TIME;
}
return 0;

double dryox(time, argv)
double time;
char *argv;

double A = 178.7;
double B = 6870.;
double *dargv = (double *)argv;

double temperature;

temperature = time * dargv[0] + (1 - time) * dargv[3];
return pow(A, 1/c_dryox) * exp(-B / (c_dryox * temperature));

double aqcor(time, argv)

```

```
double time;
char *argv;
{
double A = 31512.;
double B = 5000.;
double k = 19.08;
double *dargv = (double *)argv;

double temperature;
double humidity;

temperature = time * dargv[0] + (1 - time) * dargv[3];
humidity = time * dargv[1] + (1 - time) * dargv[4];

return pow(A, 1/c_aqcor) *
       exp(-k * (1. - humidity) / c_aqcor - B / (c_aqcor * temperature))
}
```

```

#include <stdio.h>                               Corr825x.c
#include <math.h>

#define c_dryox (0.33)
#define c_aqcor (1.00)

#define TEMPERATURE (params[0])
#define OLDTEMPERATURE (params[3])
#define HUMIDITY (params[1])
#define OLDHUMIDITY (params[4])
#define TIME (params[2])
#define OLDTIME (params[5])

main()
{
    double params[6];           /* temperature in K, relative humidity as fracti
    double penet_dryox = 0; /* (penetration due to dry oxidation, mm) to 1/c
    double penet_aqcor; /* (penetration due to aqueous corr., mm) to 1/c

    double dryox();
    double aqcor();
    double romberg();

    /* handle initial wastage from previous calculation */
    scanf("%lf", &penet_aqcor);
    penet_aqcor = pow(penet_aqcor, 1. / c_aqcor);

    scanf("%lf %lf %lf", &OLDTIME, &OLDTEMPERATURE, &OLDHUMIDITY);
    OLDTEMPERATURE += 273.15;

    printf("%.1lf %.1lf %.1lf\n", OLDTIME, pow(penet_dryox, c_dryox),
           pow(penet_aqcor, c_aqcor));
    while (scanf("%lf %lf %lf", &TIME, &TEMPERATURE, &HUMIDITY) == 3) {
        TEMPERATURE += 273.15;
        penet_dryox += (TIME - OLDTIME) *
            romberg(dryox, 0., 1., 5, 1.e-6, (char *)params);
        penet_aqcor += (TIME - OLDTIME) *
            romberg(aqcor, 0., 1., 5, 1.e-6, (char *)params);

        printf("%.1lf %.1lf %.1lf\n", TIME, pow(penet_dryox, c_dryox),
               pow(penet_aqcor, c_aqcor));

        OLDTEMPERATURE = TEMPERATURE;
        OLDHUMIDITY = HUMIDITY;
        OLDTIME = TIME;
    }
    return 0;
}

double dryox(time, argv)
double time;
char *argv;

double A = 178.7;
double B = 6870.;
double *dargv = (double *)argv;

double temperature;

```

```
temperature = time * dargv[0] + (1 - time) * dargv[3];
return pow(A, 1/c_dryox) * exp(-B / (c_dryox * temperature));
}

double aqcor(time, argv)
double time;
char *argv;
{
double A = 31512.;
double B = 5000.;
double k = 19.08;
double *dargv = (double *)argv;

double temperature;
double humidity;

temperature = time * dargv[0] + (1 - time) * dargv[3];
humidity = time * dargv[1] + (1 - time) * dargv[4];

return pow(A, 1/c_aqcor) *
       exp(-k * (1. - humidity) / c_aqcor - B / (c_aqcor * temperature)
}
```

WEIBULL PARAMETER ESTIMATION

$$\beta = \frac{\ln(t-\theta) \ln \ln \frac{1}{1-F} - \overline{\ln(t-\theta)} \overline{\ln \ln \frac{1}{1-F}}}{\overline{[\ln(t-\theta)]^2} - \overline{\ln(t-\theta)}^2}$$

$$\ln \alpha = \frac{\ln(t-\theta) \overline{\ln \ln \frac{1}{1-F}} \ln(t-\theta) - \overline{[\ln(t-\theta)]^2} \overline{\ln \ln \frac{1}{1-F}}}{\overline{\ln(t-\theta) \ln \ln \frac{1}{1-F}} - \overline{\ln(t-\theta)} \overline{\ln \ln \frac{1}{1-F}}}$$

WHERE

$$F = F_{\text{data}}$$

$$\ln(t-\theta) = \frac{1}{n} \sum \ln(t_i - \theta)$$

$$\overline{[\ln(t-\theta)]^2} = \frac{1}{n} \sum [\ln(t_i - \theta)]^2$$

Weibull CDF

$$F_{\text{weibull}} = 1 - \exp\left(\frac{t-\theta}{\alpha}\right)^{\beta}$$

$$\ln \ln \frac{1}{1-F} = \frac{1}{n} \sum \ln \ln \frac{1}{1-F_i}$$

$$\ln(t-\theta) \ln \ln \frac{1}{1-F} = \frac{1}{n} \sum \left(\ln \ln \frac{1}{1-F_i} \right) \ln(t_i - \theta)$$

$$MTTF = \theta + \alpha \Gamma(1 + 1/\beta)$$

$$\sigma = \alpha \sqrt{\Gamma(1+2/\beta) - [\Gamma(1+1/\beta)]^2}$$

Goodness of Fit $\Rightarrow \text{CHITEST}(F_{\text{weibull}}, F_{\text{data}})$

$$e^{-\left(\frac{t-\theta}{\alpha}\right)^B} = 1 - F$$

$$-\left(\frac{t-\theta}{\alpha}\right)^B = \ln(1 - F)$$

$$\left(\frac{t-\theta}{\alpha}\right)^B = -\ln(1 - F) = \ln \frac{1}{1 - F}$$

$$\sum (y_i - \alpha x_i - \beta)^2$$

$$\bar{y} = \alpha \bar{x} + \beta; \quad \beta = \bar{y} - \alpha \bar{x}$$

$$\sum x_i (y_i - \alpha x_i - \beta) = 0$$

$$\sum x_i y_i - \alpha \sum x_i^2 - \beta n \bar{x} = 0$$

$$\sum x_i y_i - \alpha \sum x_i^2 - n \bar{x} (\bar{y} - \alpha \bar{x}) = 0$$

$$\bar{x} \bar{y} - \bar{x}^2 \alpha - \bar{x} \bar{y} + \alpha \bar{x}^2 = 0$$

$$\alpha = \frac{\bar{x} \bar{y} - \bar{x} \bar{y}}{\bar{x}^2 - \bar{x}^2}$$

$$B \left[\ln(t-\theta) - \ln \alpha \right] = \ln \ln \frac{1}{1-F}$$

$$B \ln \left(\frac{t_i - \theta}{\alpha} \right) = \ln \ln \frac{1}{1-F_i}$$

$$\hat{\theta} = \sum_{i=1}^n \left(B \ln \left(\frac{t_i - \theta}{\alpha} \right) - \ln \ln \frac{1}{1-F_i} \right)^2$$

$$\frac{\partial \hat{\theta}}{\partial \beta} = \sum_{i=1}^n \ln \frac{t_i - \theta}{\alpha} \left(B \ln \frac{t_i - \theta}{\alpha} - \ln \ln \frac{1}{1-F_i} \right)$$

$$\frac{\partial \hat{\theta}}{\partial \alpha} = \sum_{i=1}^n -\frac{B}{2} \left(B \ln \left(\frac{t_i - \theta}{\alpha} \right) - \ln \ln \frac{1}{1-F_i} \right)$$

$$B \sum \ln(t_i - \theta) - n \beta \ln \alpha - \sum \ln \ln \frac{1}{1-F_i} = 0$$

$$\ln \alpha = \frac{\ln(t - \theta)}{B} - \frac{1}{B} \sum \ln \ln \frac{1}{1-F_i}$$

$$\begin{aligned} B \sum [\ln(t_i - \theta)]^2 - 2 \beta \ln \alpha \sum \ln(t_i - \theta) + \alpha (\ln \alpha)^2 n - \sum \ln(t_i - \theta) \ln \ln \frac{1}{1-F_i} \\ + \ln \alpha \sum \ln \ln \frac{1}{1-F_i} = 0 \end{aligned}$$

least
squares
fit
for
Weibull

$$\begin{aligned} & \overline{\beta} \left[\overline{\ln(t-\theta)} \right]^2 - 2\overline{\beta} \left(\overline{\ln(t-\theta)} - \frac{1}{\beta} \overline{\ln \ln \frac{1}{1-F}} \right) \overline{\ln(t-\theta)} \\ & + \overline{\beta} \left[\overline{\ln(t-\theta)} - \frac{1}{\beta} \overline{\ln \ln \frac{1}{1-F}} \right]^2 - \overline{\ln(t-\theta) \ln \ln \frac{1}{1-F}} \\ & + \left(\overline{\ln(t-\theta)} - \frac{1}{\beta} \overline{\ln \ln \frac{1}{1-F}} \right) \overline{\ln \ln \frac{1}{1-F}} = 0 \end{aligned}$$

$$\begin{aligned} & \left[\overline{\ln(t-\theta)} - \frac{1}{\beta} \overline{\ln \ln \frac{1}{1-F}} \right] \left\{ \overline{\beta \ln(t-\theta)} - \cancel{\overline{\ln \ln \frac{1}{1-F}}} + \cancel{\overline{\ln \ln \frac{1}{1-F}}} - 2\overline{\beta \ln(t-\theta)} \right. \\ & \left. + \overline{\beta \left[\ln(t-\theta) \right]^2} - \overline{\ln(t-\theta) \ln \ln \frac{1}{1-F}} \right\} = 0 \end{aligned}$$

$$- \overline{\beta \ln(t-\theta)} \left(\overline{\ln(t-\theta)} - \frac{1}{\beta} \overline{\ln \ln \frac{1}{1-F}} \right) + \overline{\beta \left[\ln(t-\theta) \right]^2} - \overline{\ln(t-\theta) \ln \ln \frac{1}{1-F}} = 0$$

$$\overline{\beta \left[\ln(t-\theta) \right]^2} - \overline{\ln(t-\theta)^2} = \overline{\ln(t-\theta) \ln \ln \frac{1}{1-F}} - \overline{\ln(t-\theta) \ln \ln \frac{1}{1-F}}$$

$$\beta = \frac{\overline{\ln(t-\theta) \ln \ln \frac{1}{1-F}} - \overline{\ln(t-\theta) \ln \ln \frac{1}{1-F}}}{\overline{\left[\ln(t-\theta) \right]^2} - \overline{\ln(t-\theta)^2}} \text{ sigma}$$

$$\ln \alpha = \overline{\ln(t-\theta)} + \frac{\overline{\ln(t-\theta)^2} - \overline{\left[\ln(t-\theta) \right]^2}}{\overline{\ln(t-\theta) \ln \ln \frac{1}{1-F}} - \overline{\ln(t-\theta) \ln \ln \frac{1}{1-F}}} \overline{\left(\ln \ln \frac{1}{1-F} \right)}$$

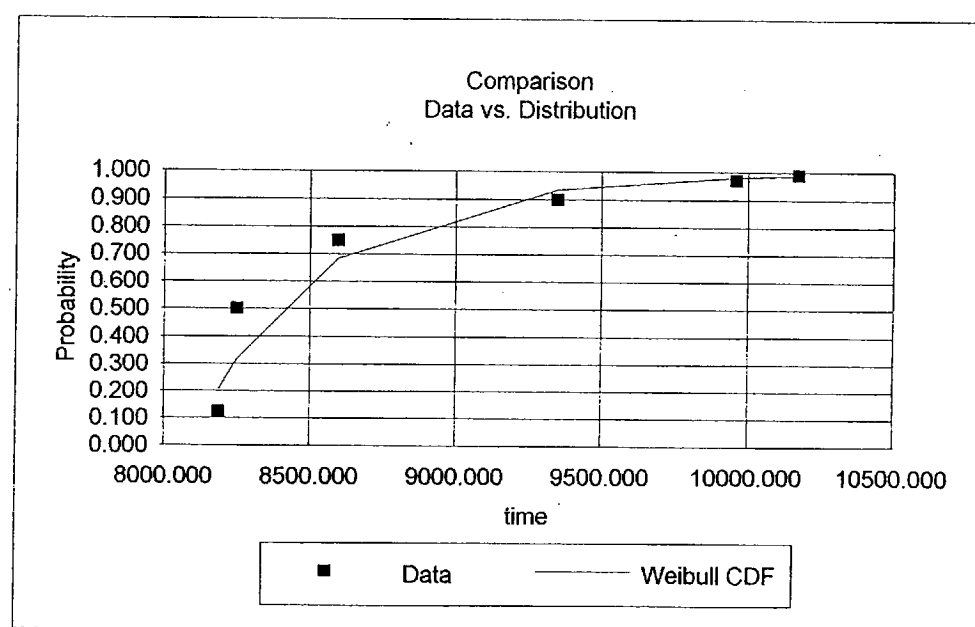
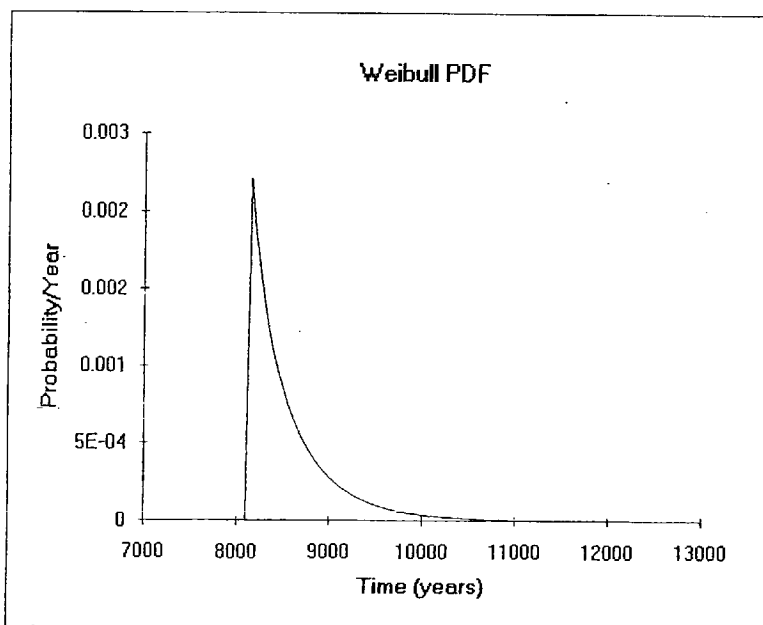
$$\ln \alpha = \frac{\overline{\ln(t-\theta)} \overline{\ln(t-\theta) \ln \ln \frac{1}{1-F}} - \overline{\left[\ln(t-\theta) \right]^2} \overline{\ln \ln \frac{1}{1-F}}}{\overline{\ln(t-\theta) \ln \ln \frac{1}{1-F}} - \overline{\ln(t-\theta) \ln \ln \frac{1}{1-F}}}$$

Computation of Weibul parameters alpha & beta

Continuous Wetting Breach

DI B00000000-01717-2200-00079 REV 01

INPUTS			CALCULATION			
theta =	8100			Ln(t-theta)	Ln(t-theta)^2	LnLn(1/(1-Fdata))
t	t-theta	Fdata	Fweibull	4.488	20.139	-2.013
8188.910	88.910	0.125	0.208	5.011	25.112	-0.367
8250.080	150.080	0.500	0.316	6.203	38.482	0.327
8594.440	494.440	0.750	0.683	7.129	50.829	0.834
9348.190	1248.190	0.900	0.934	7.528	56.676	1.255
9960.060	1860.060	0.970	0.981	7.638	58.333	1.527
10174.800	2074.800	0.990	0.987			11.664
ANSWER			Column Averages			
Alpha =	425.421	Chi Squared	1.000	A	B	C
Beta =	0.931	Goodness of Fit		6.333	41.595	0.260
Theta =	8100					3.035
MTTF =	8539.83	Used for MTTF & SD calculations		1.489	Sigma	1.386
SD =	473.04	2.075	E: $(1+\text{Beta})/\text{Beta}$	(B-A^2)	(D-C*A)	betaNum
		3.149	$1+2(E-1)$			0.931 beta (betaNum/Sigma)
						425.421 alpha (see below)
						$\text{EXP}((A*D-B*C)/\text{betaNum})$

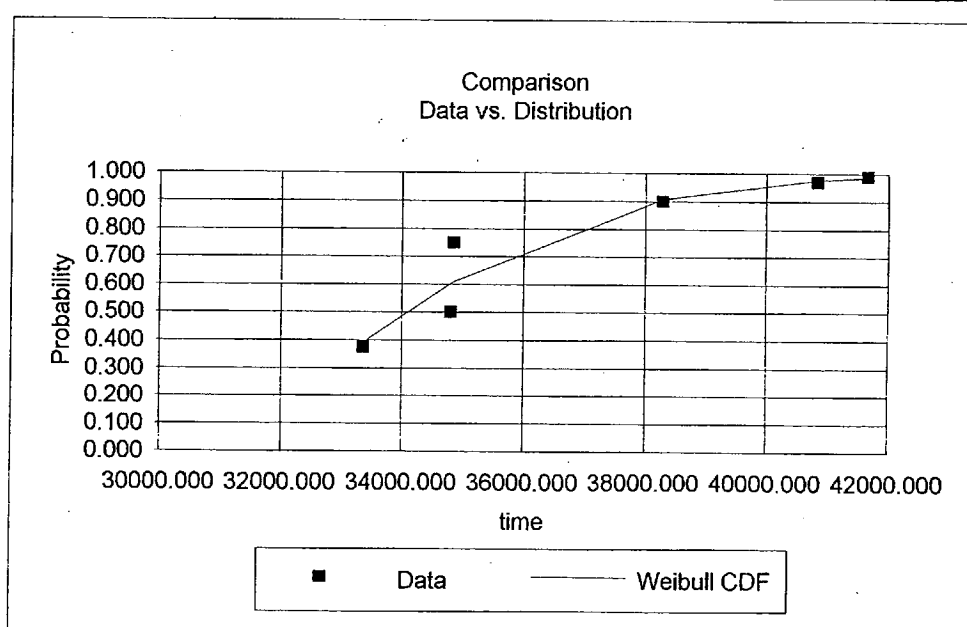
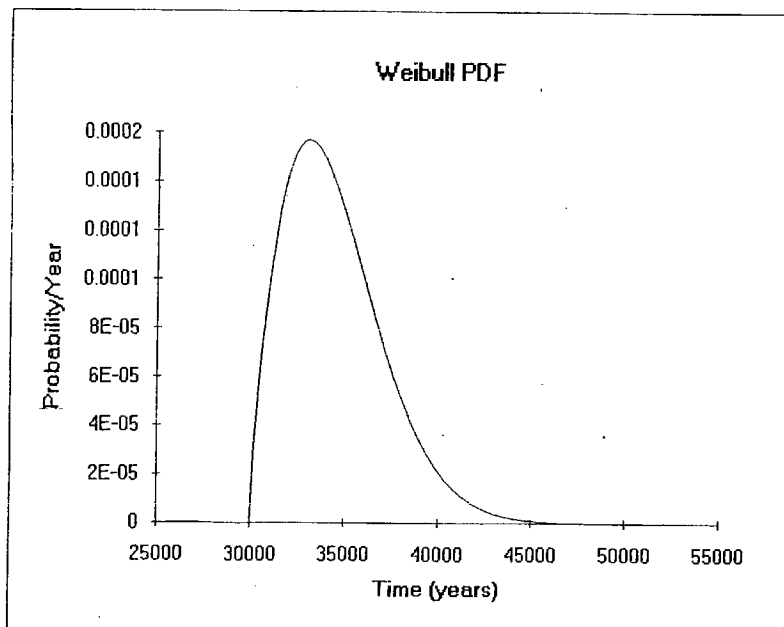


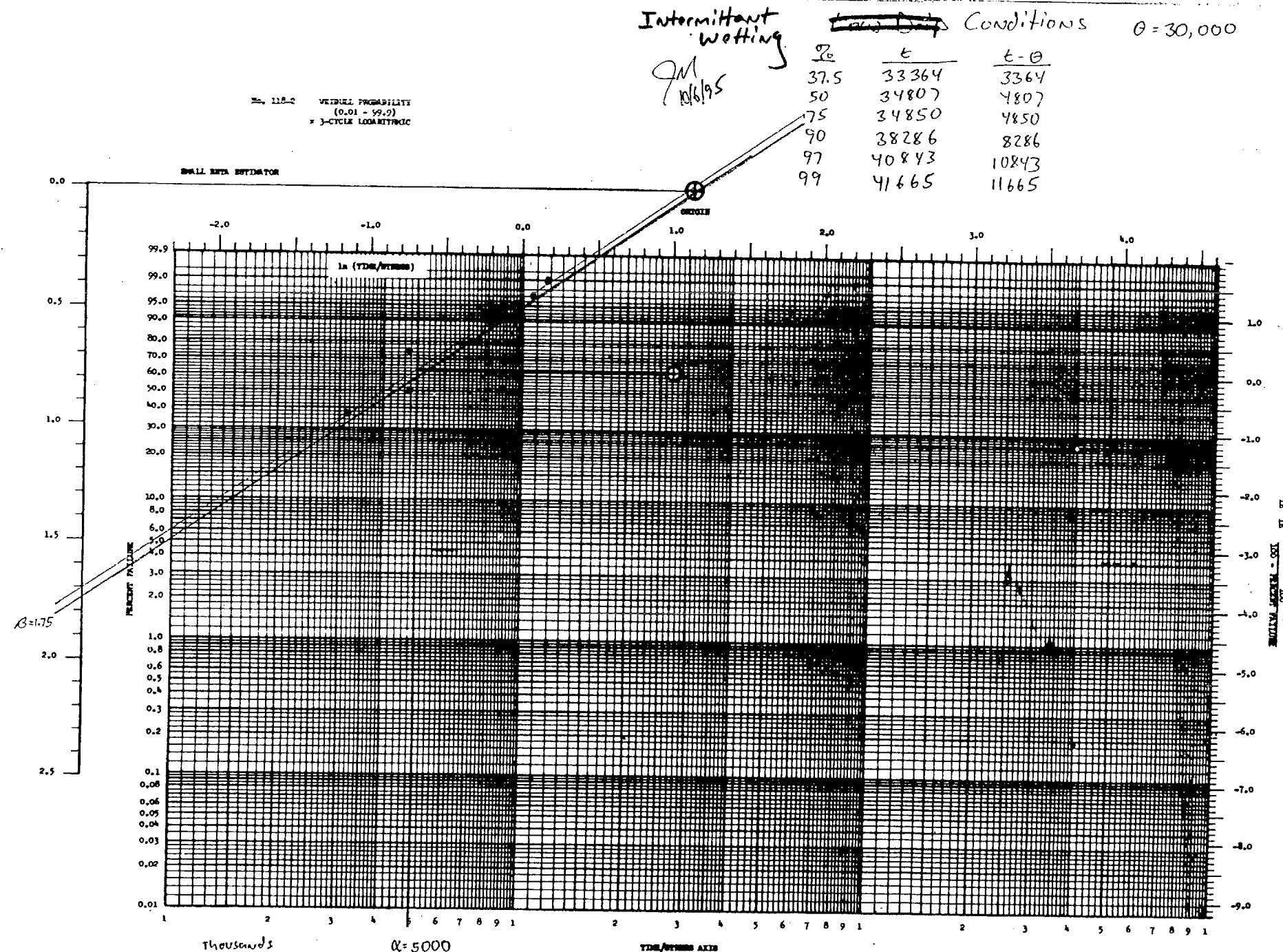
Computation of Weibul parameters alpha & beta

Intermittent Wetting Breach

DI B00000000-01717-2200-00079 REV 01

INPUTS			CALCULATION			
theta =	30000			Ln(t-theta)	Ln(t-theta)^2	LnLn(1/(1-Fdata))
t	t-theta	Fdata	Fweibull	0.392	8.121	-0.755
33364.500	3364.500	0.375		8.478	65.951	-6.132
34807.300	4807.300	0.500		8.487	71.875	-0.367
34850.000	4850.000	0.750		9.022	72.025	2.772
38286.200	8286.200	0.900		9.291	81.403	0.834
40843.400	10843.400	0.970		9.364	86.328	7.525
41665.600	11665.600	0.990				11.657
						14.301
ANSWER			Column Averages			
Alpha =	5030.338	Chi Squared	A	77.546	4.503	
Beta =	1.737	Goodness of Fit	B	0.470		
Theta =	30000	Used for MTTF & SD calculations	C	0.212 Sigma	0.368 betaNum	1.737 beta (betaNum/Sigma)
MTTF =	34481.83	1.576	D	(B-A^2)	(D-C*A)	5030.338 alpha (see below)
SD =	2661.99	2.152				EXP((A*D-B*C)/betaNum)





Probability that WP Located Under Flowing Fracture

Inputs

$$VFF := 19.64 \text{ m}^{-3} \text{ Reference 5.24}$$

$$ID := 4.27 \text{ m Drift Diameter (14 ft) Reference 5.11}$$

$$WPIL := 4.580 \text{ m UCF-WP Basket inner length Reference 5.32}$$

$$FBDL := .005 \text{ m Space between end of basket and inner lid Reference 5.32}$$

Assumptions

1. 14% of fractures are flowing.
2. 50% of fractures in cylindrical volume of tuff intersect surface of unit volume (1m of drift length).
3. STRIPA fraction reduced by a factor of 100 to account for fact that STRIPA rock is saturated while TSw2 is unsaturated.
4. Ceiling area capable of dripping on WP assumed to be top 90° arc of cylinder.

Calculation

Total number of Fractures in volume of rock that will contain drift

$$R := \frac{ID}{2} \quad L := 1 \text{ m of drift} \quad NF := VFF \cdot \pi \cdot R^2 \cdot L \quad NF = 281.246$$

Fractures intersecting surface of cylinder

$$F := 0.50 \cdot NF \quad F = 140.623$$

Total surface area of cylinder representing 1m of drift

$$\text{walls} \quad \text{ends}$$

$$TSA := 2 \cdot \pi \cdot R \cdot L + 2 \cdot \pi \cdot R^2 \quad TSA = 42.055 \text{ m}^2$$

Ceiling Surface Area

$$CSA := \frac{90}{360} \cdot 2 \cdot \pi \cdot R \cdot L \quad CSA = 3.354 \quad \text{m}^2$$

Fraction of total surface area represented by ceiling

$$C := \frac{CSA}{TSA} \quad C = 0.08$$

Fractures per 1m of drift ceiling = Fractures intersecting surface of cylinder * Fraction of surface that is ceiling

$$CF1 := C \cdot F \quad CF1 = 11.214$$

Flowing Fractures per m of Drift Ceiling

$$\lambda := (0.14) \cdot (0.01) \cdot CF1 \quad \lambda = 0.0157 \quad \text{m}^{-1}$$

Probability of no flowing fractures over package inner lid to lid length (skirts not important for filling)
Use Poisson Distribution

$$x := WPIL + FBDL$$

$$\Pr(n) := \frac{(\lambda \cdot x)^n \cdot \exp(-\lambda \cdot x)}{n!}$$

$$x = 4.585 \text{ m}$$

$$\Pr(0) = 0.931$$

Probability of at least one flowing fracture over package

$$1 - \Pr(0) = 0.0695$$

Private Communication

79 9M 06/95

w/ Larry Anna 4/10/95

Preliminary Draft

ESF Starter Tunnel Area - Tiva Canyon Stratigraphic unit

Mapped Pavement	Comparison Criteria									
	P22 m/m ²		P21 # fractures/m ²		Frequency # fractures/m		Termination Percent		Fractal dimension 2-D Box, Mass	
P100	1.95		1.35				21.3		2.0, 2.1	
P200	1.13		0.55				33.2		1.85, 1.96	
P300	2.42		2.22				32.0		NA, 1.96	
AR										
	S	M*	S	M*	S	M*	S	M*	S	M
Starter Tunnel	$\mu=1.29$ $\sigma=0.11$		$\mu=0.28$ $\sigma=0.02$				$\mu=17.8$ $\sigma=3.6$		B = 2	
Rt Wall	$\mu=1.23$ $\sigma=0.16$	1.02	$\mu=0.35$ $\sigma=0.05$	0.35	$\mu=1.36$ $\sigma=0.17$	1.16	$\mu=12.3$ $\sigma=3.2$	20.0		
Left Wall	$\mu=1.20$ $\sigma=0.14$		$\mu=0.34$ $\sigma=0.05$	0.30	$\mu=1.36$ $\sigma=0.13$	1.24	11.0			
Alcove 1	$\mu=1.29$ $\sigma=0.23$		$\mu=0.31$ $\sigma=0.05$				$\mu=15.4$ $\sigma=6.5$			
Rt Wall	$\mu=1.10$ $\sigma=0.29$	1.4	$\mu=0.59$ $\sigma=0.12$.63	$\mu=1.16$ $\sigma=0.27$	1.02	$\mu=9.9$ $\sigma=9.2$		B 1.32	
Left Wall	$\mu=1.10$ $\sigma=0.28$		$\mu=0.59$ $\sigma=0.15$.55	$\mu=1.19$ $\sigma=0.31$	1.20	$\mu=14.1$ $\sigma=10.1$		B 0.95	
Radial Boreholes					$\mu=1.10$ $\sigma=0.18$					

S = Simulated, based on 20 simulations

M = Mapped

* = does not include thin, high density, fracture/shear zones

$$P_{32} = \text{Fracture Area} / \text{Rock Volume} = 1.25$$

$$\text{m}^2/\text{m}^3$$

.97 FOR CONNECTED
 Should be less connected deeper underground.

Preliminary Draft

General Corrosion Data For 304 & 316 Stainless Steels								
SS	Material	Test Dur.(h)	Test Tem	Test Environment	Rate (um/yr)	Time To Corrode 1mm (years)	Time To Corrode 3mm (years)	
Material	Test Dur.(h)	Test Tem	Test Environment	Rate (um/yr)	Time To Corrode 1mm (years)	Time To Corrode 3mm (years)	Time To Corrode 6mm (years)	Source
316	16	27 (?)	Sea Immersion(PC)	1.25	400	1200	2400	UCID21362vol2
316	1	27 (?)	Sea Immersion(PC)	14.99	33	100	200	UCID21362vol2
316	16	27 (?)	Sea Mean Tide (PC)	0.16	3125	9375	18750	UCID21362vol2
316L	1.3	50	J-13 Immersion	0.154	3247	9740	19481	UCID21044
304L	1.3	50	J-13 Immersion	0.133	3759	11278	22556	UCID21044
304L Ann	1	28	J-13 air 6e5 rads/hr	0.0811	6165	18496	36991	UCID21044
304L Wel	1	28	J-13 air 6e5 rads/hr	0.123	4065	12195	24390	UCID21044
304L	0.23	90	J-13 Immersion	0.29	1724	5172	10345	NUREG/CR-5598
304L	0.33	90	Sol. 20 Immersion	0.2	2500	7500	15000	NUREG/CR-5598
304L	0.15	?	Tuff Grndwtr 3&6e5 r/h	0.3	1667	5000	10000	ASM Handbook vol 13
Avg Time To Corrode In J-13					3304	9912	19823	
Standard Deviation					1454	4362	8724	
Time to corrode a given thickness from both sides = Thickness (mm) / [2 * Rate (um/yr) / 1000 (um/mm)]								

DETERMINATION OF WEIBULL PARAMETERS FOR BORON LEACH (SECTION 7.4.3.2)

Continuous Wetting - Borated Stainless Steel

$1.25 \cdot 10^{-3}$ mm/year general corrosion rate of 316 SS in Panama Canal

Time to corrode 60% of 10mm thickness of 316 SS from both sides

$$\theta_C := 0.6 \cdot \frac{10}{(2 \cdot 1.25 \cdot 10^{-3})} \quad \theta_C = 2.4 \cdot 10^3$$

From corrosion data for 304 and 316 stainless steel

$$MTTFC := 19823 \quad \sigma_C := 8724$$

$$\theta := \theta_C \quad MTTF := MTTFC \quad \sigma := \sigma_C$$

Solve for α and β using Mathcad solve block to solve system of two equations

Guess

$$\alpha := 19500 \quad \beta := 2.1$$

Given

$$MTTF = \theta + \alpha \cdot \Gamma\left(1 + \frac{1}{\beta}\right)$$

$$\sigma = \alpha \cdot \sqrt{\Gamma\left(1 + \frac{2}{\beta}\right) - \left(\Gamma\left(1 + \frac{1}{\beta}\right)\right)^2}$$

$$\begin{pmatrix} \alpha C \\ \beta C \end{pmatrix} := \text{Find}(\alpha, \beta)$$

Results

$$\alpha C = 1.9671 \cdot 10^4$$

$$\beta C = 2.098$$

Intermittent Wetting - Borated Stainless Steel

For Intermittent Wetting, parameters θ , σ , and MTTF are assumed to be doubled from the Continuous Wetting case to reflect milder corrosion conditions.

$$\theta I := 2 \cdot \theta C \quad \theta I = 4.8 \cdot 10^3$$

$$MTTFI := 2 \cdot MTTFC \quad MTTFI = 3.965 \cdot 10^4$$

$$\sigma I := 2 \cdot \sigma C \quad \sigma I = 1.745 \cdot 10^4$$

$$\theta := \theta I \quad MTTF := MTTFI \quad \sigma := \sigma I$$

Solve for α and β using Mathcad solve block to solve system of two equations

Guess

$$\alpha := 19500 \quad \beta := 2.1$$

Given

$$MTTF = \theta + \alpha \cdot \Gamma \left(1 + \frac{1}{\beta} \right)$$

$$\sigma = \alpha \cdot \sqrt{\Gamma \left(1 + \frac{2}{\beta} \right) - \left(\Gamma \left(1 + \frac{1}{\beta} \right) \right)^2}$$

$$\begin{pmatrix} \alpha I \\ \beta I \end{pmatrix} := \text{Find}(\alpha, \beta)$$

Results

$$\alpha I = 3.9343 \cdot 10^4$$

$$\beta I = 2.098$$

MONTE CARLO CONVOLUTION AND CRITICALITY FAULT TREE ANALYSIS

UCF-WP with and without Barrier Credit

Model Parameters

TRIALS := 250000

i := 1.. TRIALS

*WP Barrier Breach
Intermittant Wetting
Weibull Parameters*

 $\alpha_{WPIW} := 5030.3$ $\beta_{WPIW} := 1.737$ $\theta_{WPIW} := 30000$

*WP Barrier Breach
Continuous Wetting
Weibull Parameters*

 $\alpha_{WPCW} := 425.4$ $\beta_{WPCW} := 0.93$ $\theta_{WPCW} := 8100$

*60% Boron Leach
Intermittant Wetting
Weibull Parameters*

 $\alpha_{BIW} := 39343$ $\beta_{BIW} := 2.098$ $\theta_{BIW} := 4800$

*60% Boron Leach
Continuous Wetting
Weibull Parameters*

 $\alpha_{BCW} := 19671$ $\beta_{BCW} := 2.098$ $\theta_{BCW} := 2400$ Initiating Environment Inverse CDFs for PDFs given in section 7.4.1*Time To Low Infiltration (Inverse Uniform CDF)**Time To High Infiltration (Inverse Uniform CDF)*

$$TLI_i := 1000 + \text{rnd}(1) \cdot 9000$$

$$THI_i := 2000 + \text{rnd}(1) \cdot 98000$$

Time To Flooding (Inverse Asymmetric Triangular CDF)

$$TF_i := \sqrt{\frac{2 \cdot \text{rnd}(1)}{(2 \cdot 10^{-14})} + 10000^2}$$

Inverse Weibull Distributions for WP Breach and Boron Leach for Continuous and Intermittent Wetting Conditions*Time To WP Breach (Inverse Weibull CDF)*

$$TWPIW_i := \theta_{WPIW} + \alpha_{WPIW} \cdot (-\ln(1 - \text{rnd}(1)))^{\frac{1}{\beta_{WPIW}}}$$

$$TWPCW_i := \theta_{WPCW} + \alpha_{WPCW} \cdot (-\ln(1 - \text{rnd}(1)))^{\frac{1}{\beta_{WPCW}}}$$

Time To 60% Boron Leach (Inverse Weibull CDF)

$$TBIW_i := \theta_{BIW} + \alpha_{BIW} \cdot (-\ln(1 - \text{rnd}(1)))^{\frac{1}{\beta_{BIW}}}$$

$$TBCW_i := \theta_{BCW} + \alpha_{BCW} \cdot (-\ln(1 - \text{rnd}(1)))^{\frac{1}{\beta_{BCW}}}$$

Summation of Times to Occurrence of Water Intrusion Event, WP Breaching, and Leaching 60% Boron

$$LICONV_i := TLI_i + TWPIW_i + TBIW_i$$

$$HICONV_i := THI_i + TWPCW_i + TBIW_i$$

$$FCONV_i := TF_i + TWPCW_i + TBCW_i$$

No Barrier Case (WP assumed immediately breached on occurrence of initiator)

$$LICONVNB_i := TLI_i + TBIW_i$$

$$HICONVNB_i := THI_i + TBIW_i$$

$$FCONVNB_i := TF_i + TBCW_i$$

Convolved PDF's for Time to Water, Breach, & LeachCreation of Time Intervals (250 years)

$$z := 1..1000 \quad TIME_z := z \cdot 250$$

Creation of PDFs using Mathcad histogram function (Note: first interval set to zero because Mathcad inadvertently counts zeroth row of each vector.)

*Barrier Case**Low Infiltration*

$$LIPDF := \frac{\text{hist}(TIME, LICONV)}{\text{TRIALS}}$$

$$LIPDF_0 := 0$$

High Infiltration

$$HIPDF := \frac{\text{hist}(TIME, HICONV)}{\text{TRIALS}}$$

$$HIPDF_0 := 0$$

Flooding

$$FPDF := \frac{\text{hist}(TIME, FCONV)}{\text{TRIALS}}$$

$$FPDF_0 := 0$$

No-Barrier Case

$$LIPDFNB := \frac{\text{hist}(TIME, LICONVNB)}{\text{TRIALS}}$$

$$LIPDFNB_0 := 0$$

$$HIPDFNB := \frac{\text{hist}(TIME, HICONVNB)}{\text{TRIALS}}$$

$$HIPDFNB_0 := 0$$

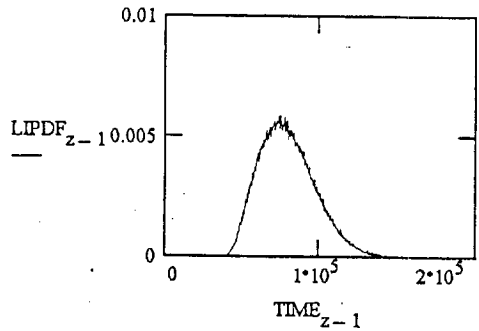
$$FPDFNB := \frac{\text{hist}(TIME, FCONVNB)}{\text{TRIALS}}$$

$$FPDFNB_0 := 0$$

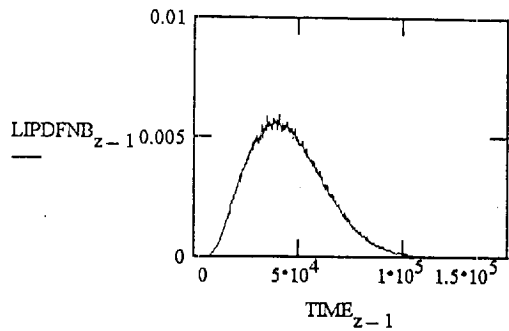
Convolved PDFs (Continued)

Barrier Case

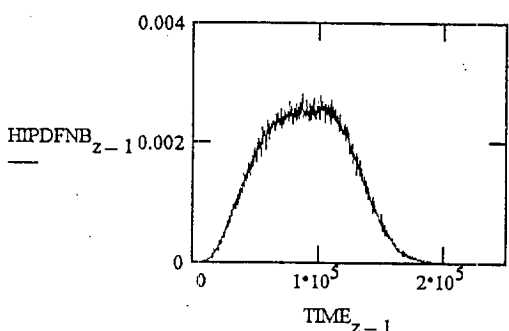
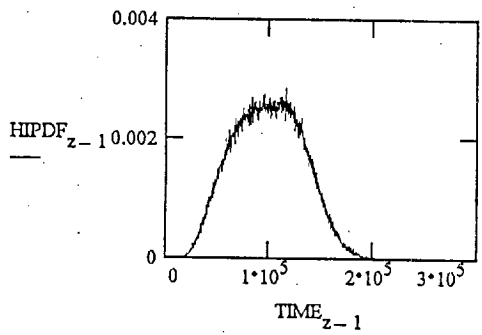
Low Infiltration



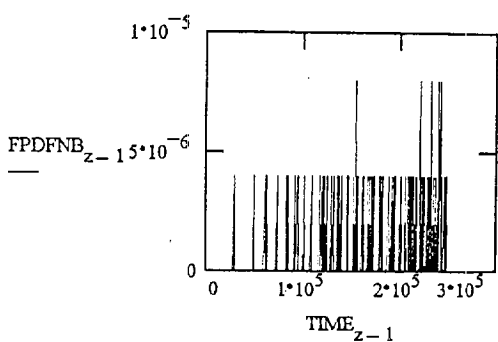
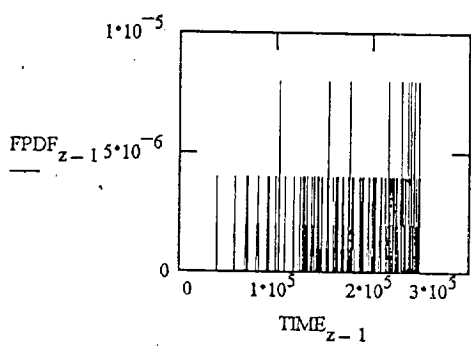
No-Barrier Case



High Infiltration



Flooding



Critical Fuel Fraction

Fit of 8th order log polynomial to data from section 7.4.4 contained in file critfuel.prn

Define polynomial

$$F(x) := \begin{bmatrix} 1 \\ \log(x) \\ \log(x)^2 \\ \log(x)^3 \\ \log(x)^4 \\ \log(x)^5 \\ \log(x)^6 \\ \log(x)^7 \\ \log(x)^8 \end{bmatrix}$$

Read File into Matrix

M := READPRN(critfuel)

time := M<sup><sub>0</sub></sup>

UCF := M<sup><sub>2</sub></sup>

Determine constants to fit polynomial to data

U := linfit(time, UCF, F)

Calculated Constants

$$U = \begin{bmatrix} 9.071 \\ -3.31 \\ -6.683 \\ 6.662 \\ -2.732 \\ 0.614 \\ -0.079 \\ 0.006 \\ -1.604 \cdot 10^{-4} \end{bmatrix}$$

CRITFUEL.PRN Input

UCF
Critical
Fraction

Time (years)

0	0
0	2 \cdot 10³
1	4 \cdot 10³
2	6 \cdot 10³
3	8 \cdot 10³
4	1 \cdot 10⁴
5	1.5 \cdot 10⁴
6	2 \cdot 10⁴
7	3 \cdot 10⁴
8	4 \cdot 10⁴
9	5 \cdot 10⁴
10	6 \cdot 10⁴
11	7 \cdot 10⁴
12	8 \cdot 10⁴
13	1 \cdot 10⁵
14	1.2 \cdot 10⁵
15	1.6 \cdot 10⁵
16	2 \cdot 10⁵
17	3 \cdot 10⁵

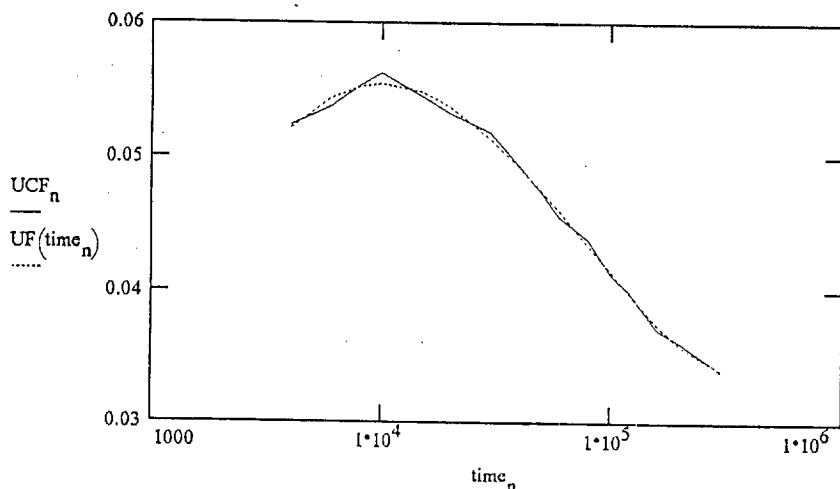
UCF =

time =

Comparison of Calculated Curve with Input

n := 1 .. 17

UF(t) := F(t) \cdot U

Multiplication of PDFs by Criticality Fraction

Barrier

No-Barrier

Low Infiltration

$$LICPDF_{z-1} := (LIPDF)_{z-1} \cdot UF(250 \cdot z)$$

$$LICPDFNB_{z-1} := (LIPDFNB)_{z-1} \cdot UF(250 \cdot z)$$

High Infiltration

$$HICPDF_{z-1} := (HIPDF)_{z-1} \cdot UF(250 \cdot z)$$

$$HICPDFNB_{z-1} := (HIPDFNB)_{z-1} \cdot UF(250 \cdot z)$$

Flooding

$$FCPDF_{z-1} := (FPDF)_{z-1} \cdot UF(250 \cdot z)$$

$$FCPDFNB_{z-1} := (FPDFNB)_{z-1} \cdot UF(250 \cdot z)$$

Determination of Cumulative Per-Package Criticality Probabilities from Critical PDFs

$$LICCDF_{z-1} := \sum_{m=0}^{z-1} LICPDF_m$$

$$LICCDFNB_{z-1} := \sum_{m=0}^{z-1} LICPDFNB_m$$

$$HICCDF_{z-1} := \sum_{m=0}^{z-1} HICPDF_m$$

$$HICCDFNB_{z-1} := \sum_{m=0}^{z-1} HICPDFNB_m$$

$$FCCDF_{z-1} := \sum_{m=0}^{z-1} FCCPDF_m$$

$$FCCDFNB_{z-1} := \sum_{m=0}^{z-1} FCCPDFNB_m$$

Quantification of algebraic form of Fault Tree

Other Fault Tree Parameters

$$CRACKSWP := 8.54 \cdot 10^{-2}$$

$$HOLES := 1 \cdot 10^{-2}$$

$$GEOMETRY := 1$$

Quantification of Fault Tree Top Event at 10000, 20000, 40000, 80000 years

$$WPCRIT10 := [((CRACKSWP \cdot LICCDF_{40}) + (CRACKSWP \cdot HICCDF_{40})) \cdot HOLES + 2 \cdot FCCDF_{40}] \cdot GEOMETRY$$

$$WPCRIT20 := [((CRACKSWP \cdot LICCDF_{80}) + (CRACKSWP \cdot HICCDF_{80})) \cdot HOLES + 2 \cdot FCCDF_{80}] \cdot GEOMETRY$$

$$WPCRIT40 := [((CRACKSWP \cdot LICCDF_{160}) + (CRACKSWP \cdot HICCDF_{160})) \cdot HOLES + 2 \cdot FCCDF_{160}] \cdot GEOMETRY$$

$$WPCRIT80 := [((CRACKSWP \cdot LICCDF_{320}) + (CRACKSWP \cdot HICCDF_{320})) \cdot HOLES + 2 \cdot FCCDF_{320}] \cdot GEOMETRY$$

$$WPCRITNB10 := [((CRACKSWP \cdot LICCDFNB_{40}) + (CRACKSWP \cdot HICCDFNB_{40})) \cdot HOLES + 2 \cdot FCCDFNB_{40}] \cdot GEOMETRY$$

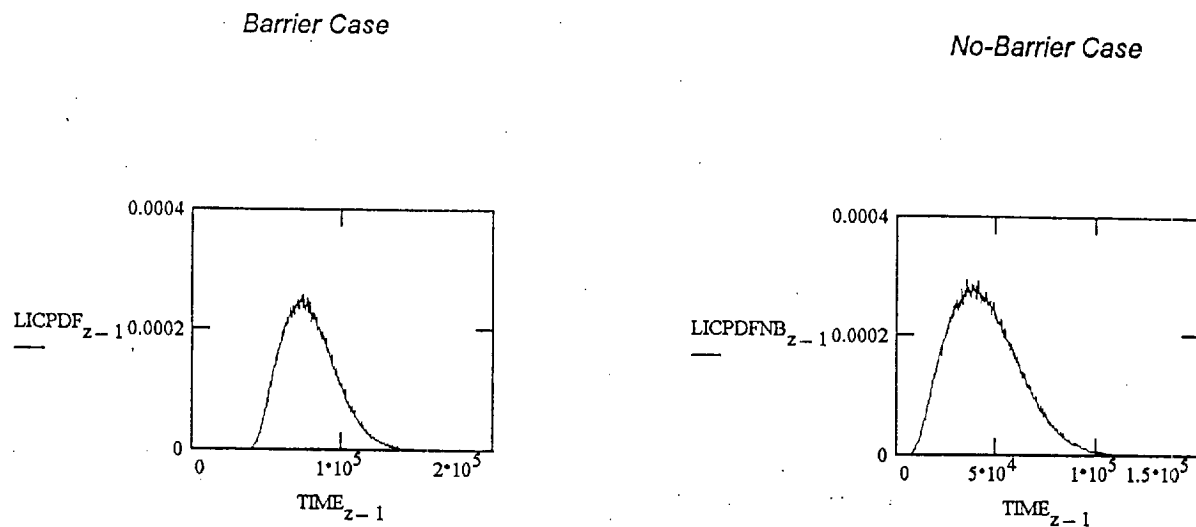
$$WPCRITNB20 := [((CRACKSWP \cdot LICCDFNB_{80}) + (CRACKSWP \cdot HICCDFNB_{80})) \cdot HOLES + 2 \cdot FCCDFNB_{80}] \cdot GEOMETRY$$

$$WPCRITNB40 := [((CRACKSWP \cdot LICCDFNB_{160}) + (CRACKSWP \cdot HICCDFNB_{160})) \cdot HOLES + 2 \cdot FCCDFNB_{160}] \cdot GEOMETRY$$

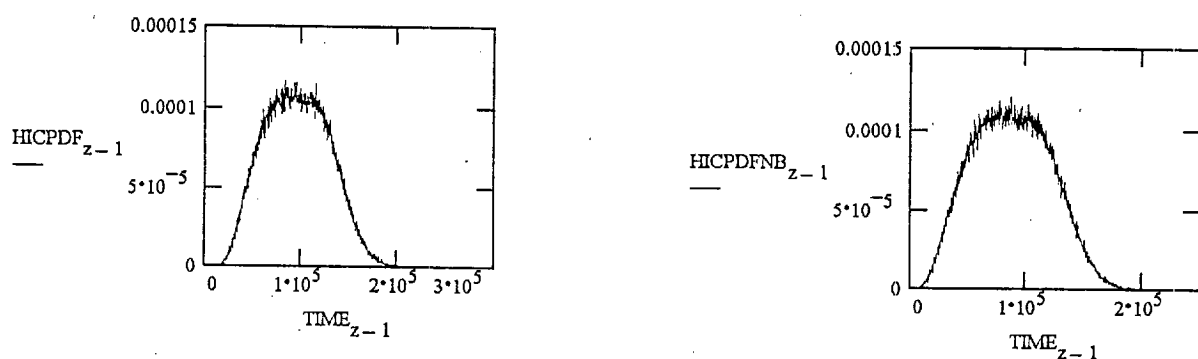
$$WPCRITNB80 := [((CRACKSWP \cdot LICCDFNB_{320}) + (CRACKSWP \cdot HICCDFNB_{320})) \cdot HOLES + 2 \cdot FCCDFNB_{320}] \cdot GEOMETRY$$

Critical PDFs for Each Sequence

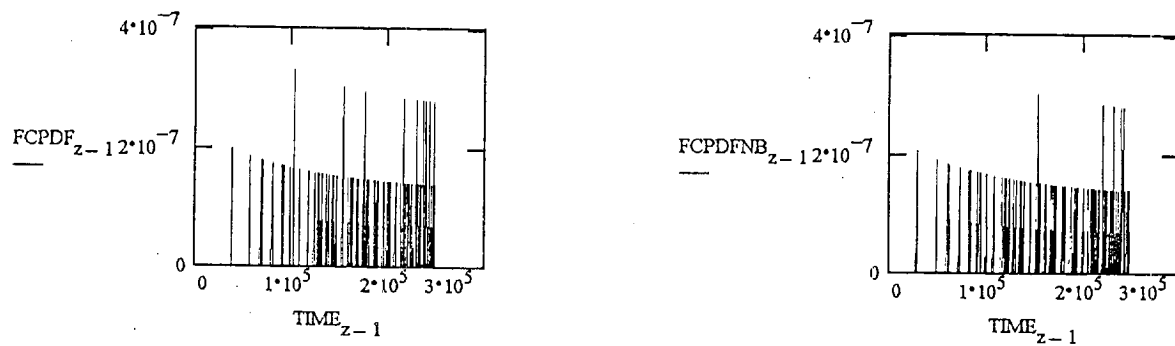
Low Infiltration



High Infiltration



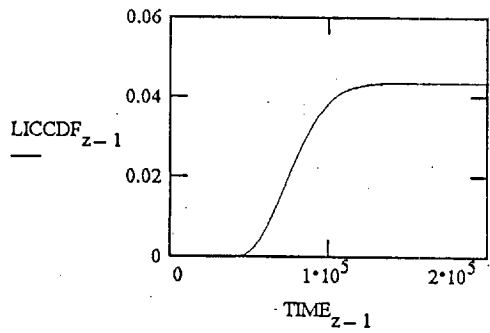
Flooding



Cummulative Per-Package Criticality Probability Plots for Each Sequence

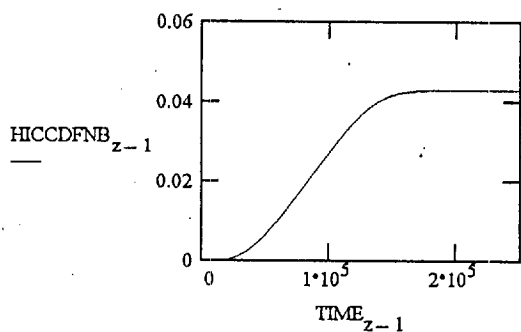
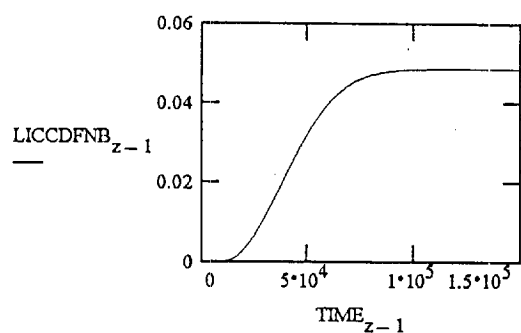
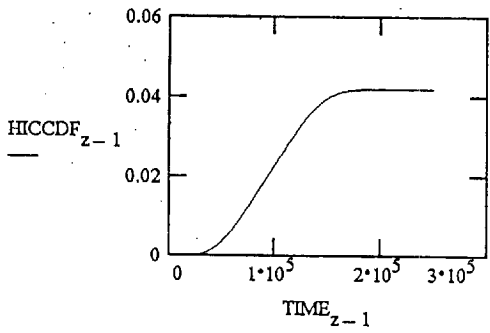
Barrier Case

Low Infiltration

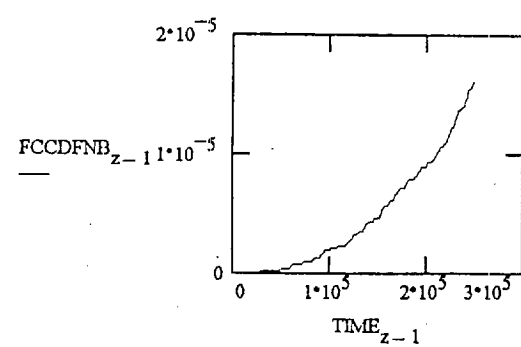
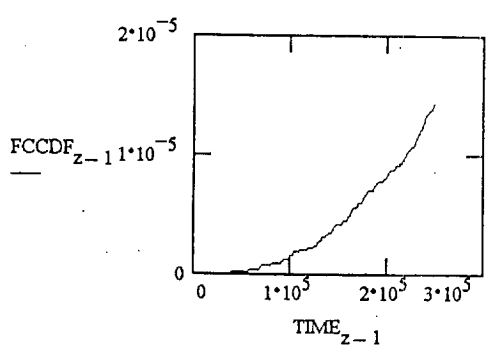


No-Barrier Case

High Infiltration



Flooding



Run #1

	10,000 years	20,000 years	40,000 years	80,000 years
Flooding w/ Barrier	$FCCDF_{40} - 0$	$FCCDF_{80} - 0$	$FCCDF_{160} - 0$	$FCCDF_{320} - 1.616 \cdot 10^{-6}$
Low Infiltration w/ Barrier	$LICCDF_{40} - 0$	$LICCDF_{80} - 0$	$LICCDF_{160} - 6.113 \cdot 10^{-6}$	$LICCDF_{320} - 2.478 \cdot 10^{-2}$
High Infiltration w/ Barrier	$HICCDF_{40} - 0$	$HICCDF_{80} - 1.1 \cdot 10^{-5}$	$HICCDF_{160} - 1.423 \cdot 10^{-3}$	$HICCDF_{320} - 1.437 \cdot 10^{-2}$
Flooding w/o Barrier	$FCCDFNB_{40} - 0$	$FCCDFNB_{80} - 0$	$FCCDFNB_{160} - 0$	$FCCDFNB_{320} - 2.011 \cdot 10^{-6}$
Low Infiltration w/o Barrier	$LICCDFNB_{40} - 8.993 \cdot 10^{-5}$	$LICCDFNB_{80} - 3.103 \cdot 10^{-3}$	$LICCDFNB_{160} - 2.218 \cdot 10^{-2}$	$LICCDFNB_{320} - 4.706 \cdot 10^{-2}$
High Infiltration w/o Barrier	$HICCDFNB_{40} - 3.99 \cdot 10^{-6}$	$HICCDFNB_{80} - 2.475 \cdot 10^{-4}$	$HICCDFNB_{160} - 3.289 \cdot 10^{-3}$	$HICCDFNB_{320} - 1.841 \cdot 10^{-2}$

Note: $FCCDF$ = climate & tectonic, $LICCDF$ = $wpb\&ldl$, $HICCDF$ = $wpb\&ldh$

Run #2

	10,000 years	20,000 years	40,000 years	80,000 years
Flooding w/ Barrier	$FCCDF_{40} = 0$	$FCCDF_{80} = 0$	$FCCDF_{160} = 1.974 \cdot 10^{-7}$	$FCCDF_{320} = 7.267 \cdot 10^{-7}$
Low Infiltration w/ Barrier	$LICCDF_{40} = 0$	$LICCDF_{80} = 0$	$LICCDF_{160} = 6.307 \cdot 10^{-6}$	$LICCDF_{320} = 2.475 \cdot 10^{-2}$
High Infiltration w/ Barrier	$HICCDF_{40} = 0$	$HICCDF_{80} = 1.292 \cdot 10^{-5}$	$HICCDF_{160} = 1.423 \cdot 10^{-3}$	$HICCDF_{320} = 1.447 \cdot 10^{-2}$
Flooding w/o Barrier	$FCCDFNB_{40} = 0$	$FCCDFNB_{80} = 0$	$FCCDFNB_{160} = 2.052 \cdot 10^{-7}$	$FCCDFNB_{320} = 9.233 \cdot 10^{-7}$
Low Infiltration w/o Barrier	$LICCDFNB_{40} = 8.637 \cdot 10^{-5}$	$LICCDFNB_{80} = 3.144 \cdot 10^{-3}$	$LICCDFNB_{160} = 2.216 \cdot 10^{-2}$	$LICCDFNB_{320} = 4.709 \cdot 10^{-2}$
High Infiltration w/o Barrier	$HICCDFNB_{40} = 3.991 \cdot 10^{-6}$	$HICCDFNB_{80} = 2.413 \cdot 10^{-4}$	$HICCDFNB_{160} = 3.288 \cdot 10^{-3}$	$HICCDFNB_{320} = 1.857 \cdot 10^{-2}$

Note: $FCCDF$ = climate & tectonic, $LICCDF$ = wpb&ldl, $HICCDF$ = wpb&ldh

Run #3

	10,000 years	20,000 years	40,000 years	80,000 years
Flooding w/ Barrier	$FCCDF_{40} = 0$	$FCCDF_{80} = 0$	$FCCDF_{160} = 0$	$FCCDF_{320} = 8.964 \cdot 10^{-7}$
Low Infiltration w/ Barrier	$LICCDF_{40} = 0$	$LICCDF_{80} = 0$	$LICCDF_{160} = 6.903 \cdot 10^{-6}$	$LICCDF_{320} = 2.477 \cdot 10^{-2}$
High Infiltration w/ Barrier	$HICCDF_{40} = 0$	$HICCDF_{80} = 1.078 \cdot 10^{-5}$	$HICCDF_{160} = 1.412 \cdot 10^{-3}$	$HICCDF_{320} = 1.437 \cdot 10^{-2}$
Flooding w/o Barrier	$FCCDFNB_{40} = 0$	$FCCDFNB_{80} = 0$	$FCCDFNB_{160} = 0$	$FCCDFNB_{320} = 1.096 \cdot 10^{-6}$
Low Infiltration w/o Barrier	$LICCDFNB_{40} = 8.505 \cdot 10^{-5}$	$LICCDFNB_{80} = 3.15 \cdot 10^{-3}$	$LICCDFNB_{160} = 2.221 \cdot 10^{-2}$	$LICCDFNB_{320} = 4.707 \cdot 10^{-2}$
High Infiltration w/o Barrier	$HICCDFNB_{40} = 4.433 \cdot 10^{-6}$	$HICCDFNB_{80} = 2.29 \cdot 10^{-4}$	$HICCDFNB_{160} = 3.256 \cdot 10^{-3}$	$HICCDFNB_{320} = 1.843 \cdot 10^{-2}$

Run #4

	10,000 years	20,000 years	40,000 years	80,000 years
Flooding w/ Barrier	$FCCDF_{40} = 0$	$FCCDF_{80} = 0$	$FCCDF_{160} = 0$	$FCCDF_{320} = 9.116 \cdot 10^{-7}$
Low Infiltration w/ Barrier	$LICCDF_{40} = 0$	$LICCDF_{80} = 0$	$LICCDF_{160} = 7.492 \cdot 10^{-6}$	$LICCDF_{320} = 2.475 \cdot 10^{-2}$
High Infiltration w/ Barrier	$HICCDF_{40} = 0$	$HICCDF_{80} = 9.907 \cdot 10^{-6}$	$HICCDF_{160} = 1.432 \cdot 10^{-3}$	$HICCDF_{320} = 1.433 \cdot 10^{-2}$
Flooding w/o Barrier	$FCCDFNB_{40} = 0$	$FCCDFNB_{80} = 0$	$FCCDFNB_{160} = 0$	$FCCDFNB_{320} = 1.638 \cdot 10^{-6}$
Low Infiltration w/o Barrier	$LICCDFNB_{40} = 9.703 \cdot 10^{-5}$	$LICCDFNB_{80} = 3.1 \cdot 10^{-3}$	$LICCDFNB_{160} = 2.215 \cdot 10^{-2}$	$LICCDFNB_{320} = 4.704 \cdot 10^{-2}$
High Infiltration w/o Barrier	$HICCDFNB_{40} = 2.659 \cdot 10^{-6}$	$HICCDFNB_{80} = 2.555 \cdot 10^{-4}$	$HICCDFNB_{160} = 3.277 \cdot 10^{-3}$	$HICCDFNB_{320} = 1.841 \cdot 10^{-2}$

Run #5

	10,000 years	20,000 years	40,000 years	80,000 years
Flooding w/ Barrier	$FCCDF_{40} = 0$	$FCCDF_{80} = 0$	$FCCDF_{160} = 1.969 \cdot 10^{-7}$	$FCCDF_{320} = 1.836 \cdot 10^{-6}$
Low Infiltration w/ Barrier	$LICCDF_{40} = 0$	$LICCDF_{80} = 0$	$LICCDF_{160} = 7.696 \cdot 10^{-6}$	$LICCDF_{320} = 2.48 \cdot 10^{-2}$
High Infiltration w/ Barrier	$HICCDF_{40} = 0$	$HICCDF_{80} = 1.335 \cdot 10^{-5}$	$HICCDF_{160} = 1.448 \cdot 10^{-3}$	$HICCDF_{320} = 1.441 \cdot 10^{-2}$
Flooding w/o Barrier	$FCCDFNB_{40} = 0$	$FCCDFNB_{80} = 0$	$FCCDFNB_{160} = 6.066 \cdot 10^{-7}$	$FCCDFNB_{320} = 2.068 \cdot 10^{-6}$
Low Infiltration w/o Barrier	$LICCDFNB_{40} = 9.17 \cdot 10^{-5}$	$LICCDFNB_{80} = 3.13 \cdot 10^{-3}$	$LICCDFNB_{160} = 2.224 \cdot 10^{-2}$	$LICCDFNB_{320} = 4.71 \cdot 10^{-2}$
High Infiltration w/o Barrier	$HICCDFNB_{40} = 3.323 \cdot 10^{-6}$	$HICCDFNB_{80} = 2.533 \cdot 10^{-4}$	$HICCDFNB_{160} = 3.319 \cdot 10^{-3}$	$HICCDFNB_{320} = 1.844 \cdot 10^{-2}$

TOPEVENT.XLS

Page 1

Sequence Cumulative Probabilities For Each Monte-Carlo Run							
		climate & tectonc	wpb&ldl	wpb&ldh	climate tectonc	wpb&ldl	wpb&ldh
Time (yrs)	Run #	F w/ B	LI w/ B	HI w/ B	F w/o B	LI w/o B	HI w/o B
10,000	1	0	0	0	0	8.99E-05	3.99E-06
	2	0	0	0	0	8.64E-05	3.99E-06
	3	0	0	0	0	8.51E-05	4.43E-06
	4	0	0	0	0	9.70E-05	2.66E-06
	5	0	0	0	0	9.17E-05	3.32E-06
	Mean	0	0	0	0	9E-05	3.68E-06
	SD	0	0	0	0	4.74E-06	6.95E-07
20,000	1	0	0	1.11E-05	0	3.10E-03	2.48E-04
	2	0	0	1.29E-05	0	3.14E-03	2.41E-04
	3	0	0	1.08E-05	0	3.15E-03	2.29E-04
	4	0	0	9.91E-06	0	3.10E-03	2.56E-04
	5	0	0	1.34E-05	0	3.13E-03	2.53E-04
	Mean	0	0	1.16E-05	0	3.13E-03	2.45E-04
	SD	0	0	1.47E-06	0	2.3E-05	1.07E-05
40,000	1	0.00E+00	6.11E-06	1.42E-03	0.00E+00	2.22E-02	3.29E-03
	2	1.97E-07	6.31E-06	1.42E-03	2.05E-07	2.22E-02	3.29E-03
	3	0	6.90E-06	1.41E-03	0.00E+00	2.22E-02	3.26E-03
	4	0	7.49E-06	1.43E-03	0	2.22E-02	3.28E-03
	5	1.97E-07	7.70E-06	0.001	6.07E-07	2.22E-02	3.32E-03
	Mean	7.89E-08	6.9E-06	1.43E-03	1.62E-07	2.22E-02	3.29E-03
	SD	1.08E-07	6.99E-07	1.34E-05	2.64E-07	3.7E-05	2.28E-05
80,000	1	1.62E-06	2.48E-02	1.44E-02	2.01E-06	4.71E-02	1.84E-02
	2	7.27E-07	2.48E-02	1.45E-02	9.23E-07	4.71E-02	1.86E-02
	3	8.96E-07	2.48E-02	1.44E-02	1.10E-06	4.71E-02	1.84E-02
	4	9.12E-07	2.48E-02	1.43E-02	1.64E-06	4.70E-02	1.84E-02
	5	1.84E-06	2.48E-02	1.44E-02	2.07E-06	4.71E-02	1.84E-02
	Mean	1.2E-06	2.48E-02	1.44E-02	1.55E-06	4.71E-02	1.85E-02
	SD	4.94E-07	2.12E-05	5.29E-05	5.21E-07	2.39E-05	6.72E-05
crackswp	6.95E-02						
holes	1.00E-02						
geometry	1						
CUTSETS							
W/ Barrier Credit				10,000	20,000	40,000	80,000
crackswp geometry holes wpb&ldh				0	8.07E-09	9.92E-07	1.00E-05
crackswp geometry holes wpb&ldl				0	0	4.8E-09	1.72E-05
tectonc geometry				0	0	7.89E-08	1.20E-06
climate geometry				0	0	7.89E-08	1.20E-06
TOP EVENT				0	8.07E-09	1.15E-06	2.96E-05
W/O Barrier Credit				10,000	20,000	40,000	80,000
crackswp geometry holes wpb&ldh				2.56E-09	1.7E-07	2.28E-06	1.28E-05
crackswp geometry holes wpb&ldl				6.26E-08	2.17E-06	1.54E-05	3.27E-05
tectonc geometry				0	0	1.62E-07	1.55E-06
climate geometry				0	0	1.62E-07	1.55E-06
TOP EVENT				6.51E-08	2.34E-06	1.8E-05	4.86E-05

Cumulative Per-Package Probability Plot Of Means

	Time (y)	Barrier Credit	No Barrier Credit
<i>Note: 1E-11 Probability Added</i>	10,000	1.00E-11	6.51182E-08
<i>for 10,000 year barrier case</i>	20,000	8.07E-09	2.34265E-06
<i>for graphing purposes</i>	40,000	1.1547E-06	1.8029E-05
	80,000	2.9611E-05	4.8634E-05

